7-16-2021

Modeling Cyanotoxin Production, Fate and Transport in Surface Waterbodies

Bernadel Rose Hintz Garstecki
Portland State University

Recommended Citation

Garstecki, Bernadel Rose Hintz, "Modeling Cyanotoxin Production, Fate and Transport in Surface Waterbodies" (2021). *Dissertations and Theses.* Paper 5774.
https://doi.org/10.15760/etd.7645

Modeling Cyanotoxin Production, Fate and Transport in Surface Waterbodies

by

Bernadel Rose Hintz Garstecki

A thesis submitted in partial fulfillment of the
requirements for the degree of

Master of Science
in
Civil and Environmental Engineering

Thesis Committee:
Scott Wells, Chair
Chris Berger
Zhonglong Zhang

Portland State University
2021

Abstract

Cyanobacteria exist throughout the world and are frequently associated with forming toxic blooms. The toxins produced by cyanobacteria, cyanotoxins, are harmful to both humans and animals. Rising temperatures due to global climate change, increased nutrient loading, and other anthropogenic impacts on waterbodies are expected to increase the prevalence of cyanobacteria. It is vital that we protect our drinking water supplies and natural water resources. Modeling the production and movement of these toxins is an important step in limiting exposure to them and evaluating management strategies to mitigate their impact. Cyanotoxins are diverse and the conditions under which they are formed are variable and depend on species, strain, and environmental factors. The research provided here offers an overview of some of the environmental factors and cyanobacteria species that are associated with toxin production, and the research also presents preliminary models for the transport and fate of cyanotoxins. Cyanotoxins can be either intracellular or extracellular and a model for each was developed. The models were first tested using published data from laboratory experiments, and then the models were incorporated into the two-dimensional (longitudinal and vertical) hydrodynamic and water quality model CE-QUAL-W2. The toxin models were tested using a model of Henry Hagg Lake (Oregon). Additional research was done to improve the water quality predictions of the CE-QUAL-W2 model of Henry Hagg Lake that had previously been developed. This involved updating the model simulation period through the end of 2020 and calibrating the model to better match field data through the new simulation period. The preliminary models were able to capture similar dynamics as the published data from the laboratory experiments, but the

toxin data available at Henry Hagg Lake was minimal so it was difficult to compare the model results to the field data using the CE-QUAL-W2 model. Four scenarios were conducted to test the functionality of the toxin models in CE-QUAL-W2. The predicted results from each test scenario matched expected outcomes based on the parameters used in each scenario. Further applications of the toxin models to other waterbodies with more consistent toxin data will help verify the accuracy of the preliminary models. In addition, further research of the environmental factors that affect toxin production is necessary to incorporate variable rates of toxin dynamics. While the simulations of the Henry Hagg Lake CE-QUAL-W2 model closely match the field data for many water quality parameters, additional calibration of the model is required to refine the results. The preliminary models should provide a framework to develop more specific models through continued research of cyanotoxins.

Acknowledgements

I would like to extend my gratitude to my thesis committee chair, Dr. Scott Wells, for all his support and encouragement. I would also like to thank my thesis committee members, Dr. Chris Berger and Dr. Zhonglong Zhang, for their time and assistance. I would like to extend additional acknowledgements to Scott Mansell and the staff at Clean Water Services, the Joint Water Commission, Tualatin Valley Water District, and the City of Hillsboro for providing toxin and water quality data for Henry Hagg Lake and expertise on the model.

Table of Contents

List of Tables

List of Figures

Chapter 1: Introduction

1.1 Objective

Cyanobacteria have been increasing in prevalence in the U.S. and across the world (Antoniou, de la Cruz and Dionysiou, 2005). Since warmer temperatures have been shown to increase algal and bacterial growth, this increase in prevalence may be correlated with global climate change (Graham *et al.*, 2018). While all bacterial and algal blooms can have harmful effects on the environment by reducing the availability of oxygen in waterbodies, cyanobacterial blooms are particularly harmful due to their ability to produce cyanotoxins (U.S. EPA, 2014b). Human effects from exposure to the cyanotoxins can include headaches, vomiting, ulcers, seizures, liver failure, and, in severe cases, death (U.S. EPA, 2014b). The toxins can bioaccumulate in the tissues of other animals such as fish and shellfish, and then cause affects later down the food chain (Antoniou, de la Cruz and Dionysiou, 2005).

Rising temperatures brought about by global climate change, increased nutrient loading due to agricultural runoff or sewage treatment plants, and other anthropogenic impacts on waterbodies are expected to increase the frequency, magnitude, and toxicity of harmful algal blooms (HABs) caused by cyanobacteria (Corbel, Mougin and Bouaïcha, 2014; Ralston and Moore, 2020). One of the difficulties with modeling HAB development is that HABs vary greatly by region and species, and the processes that influence HABs are very complex (Ralston and Moore, 2020). The uncertainty associated with climate change will make modeling the formation and spread of HABs that much more difficult, but it is crucial for the health of humans and the environment that we mitigate and prevent these blooms. Many waterbodies in Oregon including

Klamath Lake, South Tenmile Lake, Lake Billy Chinook, and Detroit Lake have recently experienced blooms to an extent that has caused the Oregon Health Authority to limit human exposure to cyanobacteria (OHA, 2020a).

Since the toxins that cyanobacteria produce can have harmful effects on plants and animals, protecting our drinking water supplies and our natural water resources is vital. According to the Oregon Health Authority, people should avoid swimming or other recreational water activities in waterbodies that have cyanobacteria blooms present (OHA, 2020b). Since the toxins cannot be removed by boiling, filtering, or treating water with camping filters, people may become infected by the toxin even when they think that they are treating their water (OHA, 2020b). When the toxins are released from cyanobacteria, they become dissolved in the water and can accumulate in drinking water plants (Almuhtaram *et al.*, 2018). By modeling the production and movement of these toxins, we can evaluate management strategies to mitigate their impact.

According to the Environmental Protection Agency (EPA), factors that impact cyanobacteria blooms include water temperature, pH, nutrient availability, and sunlight duration (U.S. EPA, 2014b). Under certain favorable conditions such as warmer temperatures and increased nutrient availability the algae may produce cyanotoxins (U.S. EPA, 2014b). The 2016 EPA Contaminant Candidate List (CCL) lists cyanotoxins as contaminants in drinking water that may require future regulation (U.S. EPA, 2014a). Different cyanobacteria strains appear to have different responses to environmental conditions; one strain may be impacted more by temperature while another strain might depend on nutrient availability and not all toxin producing algae will produce the toxins under all conditions (U.S. EPA, 2014b; Shan *et al.*, 2019). In addition to different strains

of cyanobacteria having different responses, a given species of toxigenic cyanobacteria can produce both toxic and nontoxic strains and some species can produce multiple types and variants of toxins (Fristachi *et al.*, 2008; U.S. EPA, 2014b).

As climate change continues, the favorable conditions for cyanobacteria to produce toxins might become more common leading to an increase in HABs. To predict the fate and transport of cyanotoxins, it is necessary to model the production, distribution, and degradation of the toxins in a surface waterbody. CE-QUAL-W2 (Wells, 2020b), a two-dimensional (longitudinal and vertical) hydraulic and water quality model of rivers, lakes/reservoirs, and estuaries was used to model these processes. This model is currently capable of modeling eutrophication processes such as temperature, dissolved oxygen, organic matter, pH, nutrients, and algae.

The objectives of this research were to develop a framework for modeling cyanobacteria and their toxins by determining the answers to the following questions: (1) What species produce the toxins? (2) Under what conditions do cyanobacteria produce toxins either as intracellular or extracellular toxins? (3) How much toxin is released to the waterbody under different environmental conditions? (4) What is the persistence of the cyanotoxins in the water and what are the pathways of transport and degradation? The preliminary models developed were integrated into CE-QUAL-W2 and tested to field data acquired at Henry Hagg Lake in Oregon. An additional objective of this research was to calibrate and improve the water quality predictions of the model for Henry Hagg Lake that had previously been developed in CE-QUAL-W2.

Chapter 2: Literature Review of Cyanotoxins

2.1 Cyanobacteria and Cyanotoxin Overview

Cyanobacteria are prokaryotes (as opposed to algae which are eukaryotes) and can be either planktonic (floating near the water surface) or benthic (forming mats on the floor of the waterbody) (O'Neil *et al.*, 2012; Bouma-Gregson, Power and Bormans, 2017). Huang and Zimba (2019) report that there are more than 270 cyanobacteria genera with over 3000 species. There are several competitive advantages that cyanobacteria possess over eukaryotic algae such as higher surface to volume ratio allowing for more efficient nutrient uptake, the ability of cyanobacteria to form colonies providing for protection from grazing, and nitrogen fixing abilities, in addition to other advantages that help cyanobacteria proliferate over other organisms in the same waterbody (Huang and Zimba, 2019). Previous research conducted at Portland State University studied how some cyanobacteria species are able to migrate vertically in a water column enabling them to travel between layers of a waterbody to more favorable growing conditions (Overman, 2019).

Temperature, stratification, precipitation, nutrients, carbon dioxide, pH, and biogeochemistry are some of the main drivers that affect cyanobacteria growth (O'Neil *et al.*, 2012; Glibert, 2020). Of these drivers, nutrient availability has been given the most attention on the size of cyanobacteria populations especially phosphorus (P) and nitrogen (N) concentrations (Falconer, 2005; O'Neil *et al.*, 2012). While both P and N may affect HAB size, the addition of P (such as through agricultural runoff) may play a larger role due to the ability of many cyanobacteria species to fix nitrogen from the air in cells called heterocysts thereby not requiring a supply of N in the water (Falconer, 2005; O'Neil *et*

al., 2012). The addition of nutrients in a waterbody often leads to eutrophication (high in nutrients) where algae and cyanobacteria grow excessively and form blooms. Algal or bacterial blooms are defined as large amounts of biomass and cell concentrations that often create surface scum (Smith, 2018). During blooms, as the large amount of biomass dies and drops to the bottom of the waterbody, dissolved oxygen is used up to decompose the biomass leading to hypoxic or anoxic (partial or complete lack of oxygen) conditions regardless of whether there are toxins present or not (Fristachi *et al.*, 2008; Heisler *et al.*, 2008). In addition, as the blooms die, they may release nutrients back into the waterbody which can further promote the growth of photosynthetic organisms. However, even though many cyanobacteria species are associated with eutrophication, there are several species that can form blooms with low concentrations of N and P making cyanobacteria that much more diverse and able to grow in a wide range of habitats (O'Neil *et al.*, 2012).

Cyanobacteria are also photosynthetic and can grow at low light levels which allow them to grow at depth in clear lakes (Falconer, 2005). Blooms can occur in both freshwater and marine environments allowing for widespread distribution of the bacteria and toxins which is due largely to the fact that there are so many different types of cyanobacteria (Fristachi *et al.*, 2008). Warmer temperatures affect cyanobacteria growth as it has been shown that most cyanobacteria grow the fastest at temperatures greater than 25 degrees Celsius, and cyanobacteria are able to grow better under these warmer conditions than eukaryotic algae (Paerl *et al.*, 2016). As global temperatures rise with global warming, it could be expected that cyanobacteria populations will grow and become more persistent. One aspect that makes the management of cyanobacteria difficult is the wide range of conditions under which they can grow; they have been

recorded at sites across the world in Africa, Asia, North and South America, Europe, Australia, and in both fresh and marine water (Fristachi *et al.*, 2008).

In addition to forming blooms, cyanobacteria blooms are harmful due to their ability to produce cyanotoxins, harmful metabolites produced through biosynthesis (Carmichael, 1992; Merel *et al.*, 2013). Various factors have been studied as possible causes of cyanotoxin production such as nutrients, pH, and temperature (Facey, Apte and Mitrovic, 2019). Not all cyanobacteria will produce toxins and not all species will produce toxins under the same conditions (Smith, 2018; Shan *et al.*, 2019). The harmful cyanotoxins that can be produced have been reported to cause sickness and death in animals that have ingested contaminated water (either through ingestion of intracellular toxins still within the bacteria cells or through ingestion of extracellular toxins that have been released from the cells) including gastrointestinal illness, swimmers itch, and skin rashes (Carmichael, 1992; Fristachi *et al.*, 2008). In addition, the toxins can also bioaccumulate in food and animals such as shellfish posing threats to humans through the food chain (Corbel, Mougin and Bouaïcha, 2014).

Cyanotoxins are divided into four main classes depending on the organs they affect: hepatotoxins (liver), cytotoxins (several organs), neurotoxins (nervous system) and dermatotoxins (irritant toxins) (Carmichael, 1992; Corbel, Mougin and Bouaïcha, 2014). Hepatotoxins are the most common type of cyanotoxin followed by neurotoxins (O'Neil *et al.*, 2012). Table 2-1 lists the most common cyanotoxins and the species that produce them.

Table 2-1 Main toxins from cyanobacteria, including genera of main producers, type, and health effects (Fristachi* et al.*, 2008; Lopez* et al.*, 2008; Chorus and Welker, 2021).

Cyanotoxins	Genera of main producers	Type	Health Effects
Hepatotoxins (liver)			
Microcystins	*Microcystis, Planktothrix, Dolichospermum (Anabaena), Nostoc*	Cyclic heptapeptide	Gastrointestinal, liver inflammation and hemorrhage, liver failure, pneumonia, dermatitis, tumor promoter
Nodularins	*Nodularia*	Cyclic pentapeptide	Similar to microcystins
Cytotoxins (several organs: liver, kidneys, adrenal glands, small intestine)			
Cylindrospermopsins	*Cylindrospermopsis (Raphidiopsis), Aphanizomenon (Chrysosporum), Anabaena (Chrysosporum)*	Alkaloid	Gastrointestinal, liver inflammation and hemorrhage, pneumonia, dermatitis, malaise, anorexia, liver failure
Neurotoxins (nervous system)			
Anatoxins			
Anatoxin-a	*Dolichospermum (Anabaena), Aphanizomenon (Chrysosporum), Cylindrospermopsis (Raphidiopsis)*	Alkaloid	Tingling, burning, numbness, drowsiness, incoherent speech, respiratory paralysis, cardiac arrhythmia
Anatoxin-a(s)	*Dolichospermum (Anabaena)*	Organophosphate	
Homoanatoxin-a	*Raphidiopsis, Oscillatoria*	Alkaloid	
Saxitoxins	***Dinoflagellates:*** *Alexandrium, Pyrodinium, Gymnodinium* ***Cyanobacteria:*** *Dolichospermum (Anabaena), Aphanizomenon, Cylindrospermopsis (Raphidiopsis)*	Alkaloid	Tingling, burning, numbness, drowsiness, incoherent speech, respiratory paralysis
BMAA (neurotoxic amino acid)	Most cyanobacteria	Modified amino acid	Potential link to neurodegenerative diseases
Dermatotoxins (irritant toxins)			
Lyngbyatoxin-a	*Lyngbya*	Alkaloid	Dermatitis, skin tumors
Aplysiatoxin	*Lyngbya, Schizothrix*	Alkaloid	
Lipopolysaccharides (LPS)	*Aphanizomenon, Oscillatoria*	Lipopolysaccharides	Gastrointestinal, dermatitis
Taste and Odor Compounds			
Geosmin	*Dolichospermum (Anabaena), Oscillatoria, Phormidium, Lyngbya*	Tertiary alcohol	Not considered health hazards, but make water unacceptable for consumption

Microcystins (MCs) are considered to be the most common of the cyanotoxins worldwide with more than 80 variants reported, and both microcystin and cylindrospermopsin are the two main toxins of concern in drinking water (Falconer, 2005; Corbel, Mougin and Bouaïcha, 2014). Classifying and identifying cyanotoxins is difficult due to the quantity of toxins and strains present as well as new discoveries being made that identify both new toxins being produced and new genera of cyanobacteria producing toxins (O'Neil *et al.*, 2012). According to the USGS, studies of Oregon drinking water sources such as the Clackamas, North Santiam, McKenzie, and Tualatin Rivers have revealed the presence of cyanotoxins including microcystin, anatoxin-a, saxitoxin, and cylindrospermopsin (USGS, 2015). Table 2-2 shows the Oregon Health Authority's advisory levels for these four toxins for recreational activities and drinking water.

Table 2-2 Oregon Health Authority Advisory Toxin Levels (OHA, 2018, 2019b).

	MC	CYN	ATX-a	STX	Units	Notes
OHA Recreational Use Values	4	8	8	4	$\mu g\ L^{-1}$	Everyone
OHA Drinking Water Guidance Values	1.6	3	3	1.6	$\mu g\ L^{-1}$	Adults
	0.3	0.7	0.7	0.3	$\mu g\ L^{-1}$	Ages 5 years and younger

1. Units for STX are in saxitoxin equivalents: μg STX-eq L^{-1}
2. Advisory levels were provided for all four toxins in 2018, but only MC and CYN in drinking water are regulated under current rules.

In addition to harmful human health effects from exposure to cyanotoxins there are also harmful effects on plants (phytotoxicity). Studies have shown that exposure to cyanobacterial neurotoxins have decreased photosynthetic oxygen production in some aquatic plants (Corbel, Mougin and Bouaïcha, 2014). The majority of the research on cyanotoxin phytotoxicity has been associated with microcystins. Studies showed that

MCs have allelopathic interactions with algae thereby inhibiting the growth of the algae and outcompeting the algae for resources and nutrients (Corbel, Mougin and Bouaïcha, 2014).

2.2 Management of Cyanobacteria and Cyanotoxins

Cyanotoxins can pose serious health threats to humans, animals, and wildlife. While it is difficult to fully prevent toxic blooms due to the knowledge gaps surrounding cyanobacteria and toxin production, there are still efforts being taking in the management of cyanobacteria and cyanotoxins such as prevention, removal, and monitoring. The most ideal scenario in toxin management is to prevent the blooms and toxins from being produced. A primary mitigation effort has been to decrease nutrient loads into waterbodies since there has been shown to be significant correlation between increased levels of nutrients and increases in cyanobacteria growth (Merel *et al.*, 2013). Decreasing nutrient loads to waterbodies was first achieved in the 1970s after the Clean Water Act was enacted and widespread wastewater treatment facilities were built significantly reducing bloom occurrences across the US such as in Lake Washington and the Potomac River (Merel *et al.*, 2013). However, controlling point source pollutants is relatively easy and only a portion of the problem. Most of the nutrients that affect cyanobacteria growth currently are from agricultural runoff, and diffuse pollution is much harder to control (Paerl *et al.*, 2016). It is necessary to enact more stringent rules on fertilizer application to reduce nutrient runoff, but it is also important to note that these management strategies will not be immediately noticeable as the amount of nutrients already in waterbodies may affect cyanobacteria populations for years into the future (Merel *et al.*, 2013).

If prevention is not possible or cyanobacterial blooms have already occurred, another management option that has been practiced is to remove the cyanobacterial blooms or toxins. One removal method that has been used is to apply algaecides, such as copper sulfate, that are effective at killing cyanobacteria, however, these chemicals can induce cell lysis that may release intracellular toxins into the waterbody potentially increasing toxin concentrations (Merel *et al.*, 2013). Due to the possibility of increasing toxin concentrations, algaecides should be avoided as a management technique (Merel *et al.*, 2013). Other removal methods include skimming or collecting blooms from the surface, inducing mixing in the waterbody to encourage more competition from other phytoplankton and algae, or flushing the waterbody by diverting upstream waters through a lake or reservoir to make bloom formation more difficult (Paerl *et al.*, 2016).

Another important management step is to monitor bloom formation and toxin production. Monitoring and modeling cyanobacteria movement and toxin production will help reduce the risk of exposure to harmful toxins by notifying people of potential upcoming bloom occurrences. While prevention of blooms might not always be possible, preventing human exposure to cyanobacteria and cyanotoxins is imperative to prevent ingestion.

2.3 Selected Toxin Production, Persistence, and Degradation

The following section outlines more in depth the reported conditions under which various cyanotoxins are produced, the quantity of toxin produced, and the persistence and degradation of the toxins for four of the main cyanotoxins of most concern to humans: microcystin (MC), cylindrospermopsin (CYN), anatoxin (ATX), and saxitoxin (STX). As shown in Table 2-1, cyanobacterial toxins cover a range of chemical compounds,

predominantly alkaloids and peptides for those currently identified (Falconer, 2005). The alkaloid toxins are more likely to be present separated from the cyanobacteria cells, whereas the peptide toxins remain with the cells and are only separated from the cells upon cell damage or death or through some water treatment processes (Falconer, 2005; Corbel, Mougin and Bouaïcha, 2014). Some of the factors that affect toxin production include light, water movement, allelopathic interactions (inhibition of one organism by another), competition for resources, grazing, nutrients, temperature, salinity, and cell division and growth rates (Merel *et al.*, 2013). While the ability of cyanobacterial blooms to form toxins depends on their gene pool (i.e., if the bloom contains any of the species that have the required genes to form toxins), the activation of these genes to form toxins depends on specific combinations of environmental conditions and these combinations are not well understood (Merel *et al.*, 2013).

In a 2013 publication on the state of knowledge on cyanobacterial blooms and toxins, a summary of the current analytical methods used for detection of the cyanotoxins was presented and is reproduced below in Figure 2-1 (Merel *et al.*, 2013). Due to the various detection methods available, differences in reporting may occur.

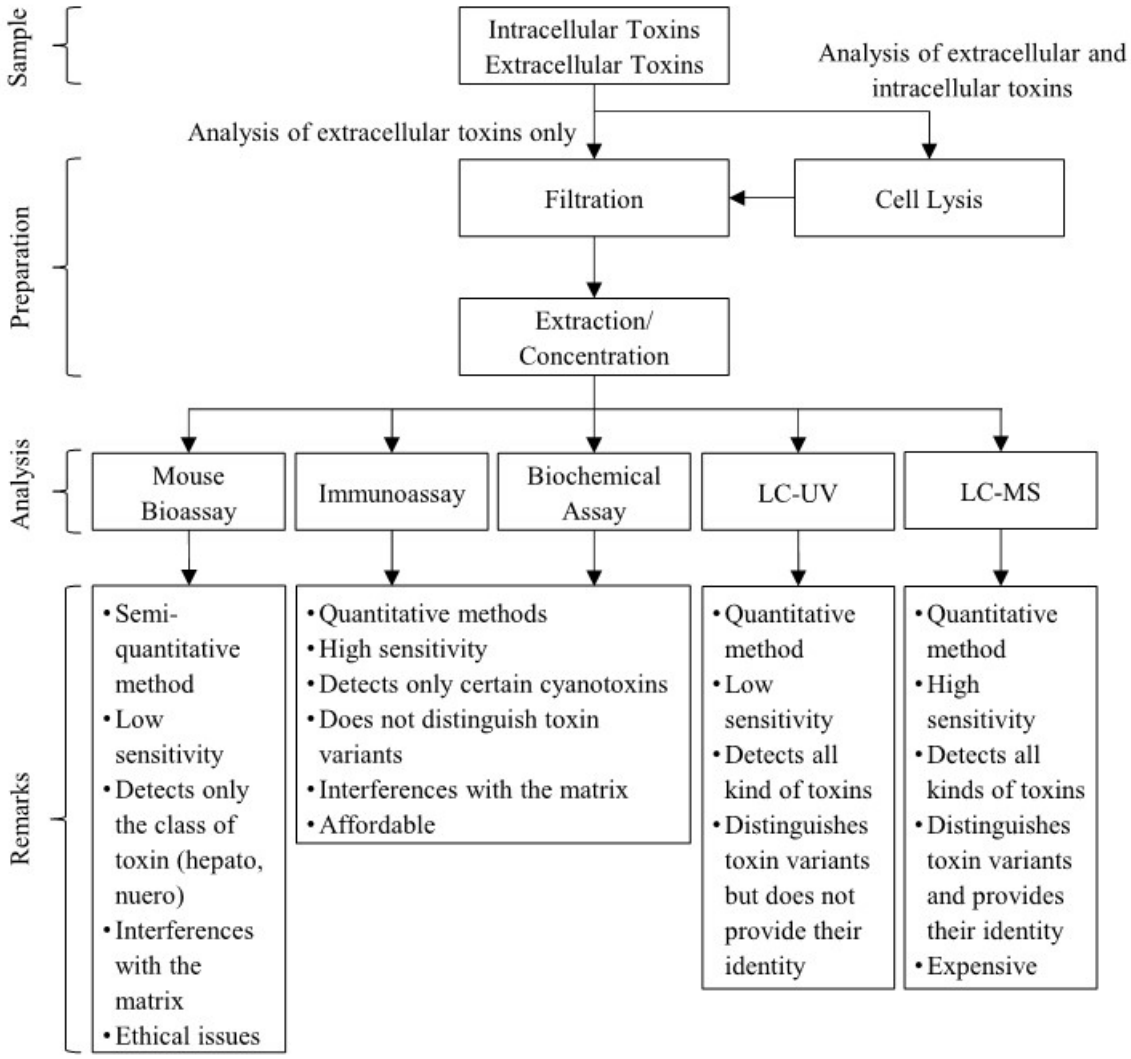

Figure 2-1 Overview of sample preparation and analytical methods for the detection of cyanotoxins, reproduced after Merel et al. (2013).

2.3.1 Microcystins

Microcystins (MC) are the most studied of cyanotoxins and one of the most widespread, therefore creating significant threats to humans worldwide (Merel *et al.*, 2013). Microcystins are classified as hepatotoxins that affect the liver and have health effects that can lead to death.

2.3.1.1 Production

Microcystins mostly exist as intracellular toxins, but can also be present as extracellular toxins that are water-soluble and stable molecules (Merel *et al.*, 2013). There are many microcystin variants of which the three most common are MC-LR, MC-RR, and MC-YR resulting from the presence of the amino acids leucine (L), arginine (R), or tyrosine (Y) in positions 2 and 4 (Buratti *et al.*, 2017). MC-LR is the most studied of the individual variants, but many studies will combine all variants together and report total microcystin content. The generic chemical structure of MC is shown in Figure 2-2.

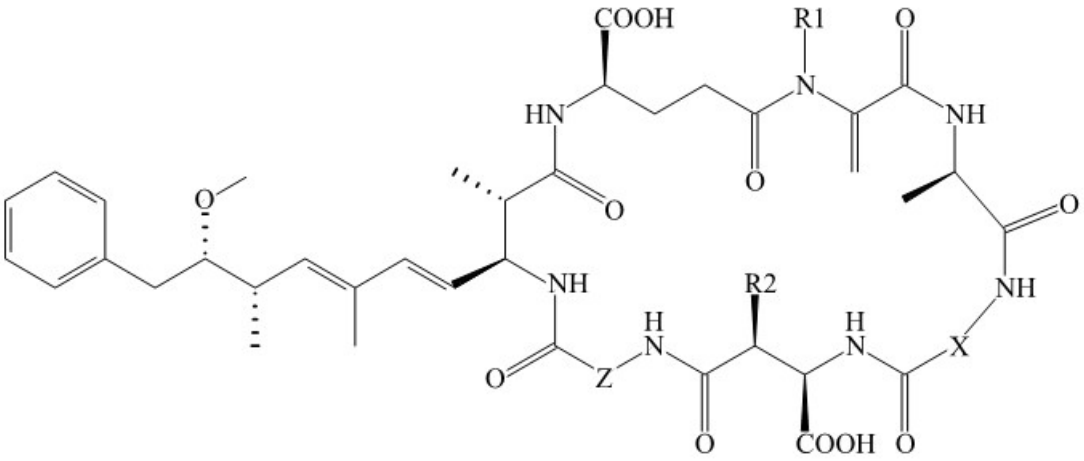

Figure 2-2 Generic chemical structure of MC reproduced after Chorus and Welker (2021). Amino acid positions 2 and 4 are indicated by X and Z, and R1 and R2 are either H or CH_3.

Extracellular MC, either dissolved in water or bound to other materials, typically make up less than 30 percent of the total MC concentrations found in water (Buratti *et al.*, 2017). A gene for microcystin export (mcyH) has been discovered in some MC producing strains, but it is commonly hypothesized that MC become extracellular toxins primarily through cell lysis (Rohrlack and Hyenstrand, 2007; Gouvêa, Boyer and Twiss, 2008). Microcystins are synthesized non-ribosomally by nonribosomal peptide

synthetase (NRPS) and polyketide synthase (PKS) domains that are encoded by the *mcy* gene cluster (Tillett *et al.*, 2000; Christiansen *et al.*, 2003; Rouhiainen *et al.*, 2004).

MC concentrations can vary considerably across different blooms and over the course of a single bloom likely due to changes in how much toxin is produced by cells and how many toxin producing cells there are (Buratti *et al.*, 2017). It has also been observed that during the sudden formation of scum or foam (which can occur over a few hours), cells in Microcystis species can be induced to produce more toxins making exposure to water during this time more dangerous to humans (Buratti *et al.*, 2017). In select studies, microcystin concentrations have been found at levels up to 10,000 micrograms per liter in surface water in the USA and 103,000 micrograms per liter in bloom and scum in South Africa (Buratti *et al.*, 2017). Table 2-3 shows literature values for MC occurrence in surface water, bloom and scum.

Table 2-3 MC occurrence in surface water, bloom and scum (Buratti* et al.*, 2017).

Organism	Type of Waterbody	Toxin	Surface water (μg L^{-1})	Bloom and Scum (μg g^{-1} DW)
Anabaena	Gulf	MC	ND-0.05	
Anabaena spp., Microcystis spp	Lake/Reservoir	MC	2700	
Anabaenopsis arnoldi	Lake/Reservoir	MC	1.6-8.3	Up to 364
Arthrospira fusiformis, Anabaenopsis abijatae, Spirulina subsalsa, Phormidium terebriformis	Lake/Reservoir	MC		16-4593
Cylindrospermopsis raciborskii, Aphanizomenon flos-aquae	Lake/Reservoir	MC	3.9-108	
Chroococcales, Microcoleus	Water impoundment	MC	ND-0.8902	
Lyngbya wollei	Stream/River	MC		ND
Microcystis aeruginosa	Lake/Reservoir	MC	2.9-13.5	320
Microcystis Microcystis flosaquae, Anabaena crassa, Aphanizomenon flosaquae	Unknown	MC	0.025-82.3	

Organism	Type of Waterbody	Toxin	Surface water (μg L^{-1})	Bloom and Scum (μg g^{-1} DW)
Microcystis aeruginosa, Planktothrix rubescens, Dolichospermum flos-aquae	Lagoon	MC		Up to 153.6 μg L^{-1}
Microcystis aeruginosa, Planktothrix rubescens	Lake/Reservoir	MC	ND-18	
Microcystis ichthyoblabe, Microcystis wesenbergii, Oscillatoria tenuis, Dolichospermum planctonicum, Dolichospermum spiroides	Lake/Reservoir	MC	ND-0.246	
Microcystis	Lake/Reservoir	MC	ND-1.9	
Microcystis	Lake/Reservoir	MC	1931 (intracellular), 90 (extracellular)	
Microcystis aeruginosa	Lagoon	MC		Up to 11400 μg L^{-1}
Microcystis flos-aquae	Stream/River	MC		16.86-484.48
Microcystis sp.	Lake/Reservoir	MC		1120
Microcystis sp.	Lake/Reservoir	MC		62
Microcystis spp.	Pond	MC	7.5-126.42	
Microcystis spp., Anabaena spp.	Lake/Reservoir	MC	Up to 1600	
Microcystis, Dolicospermum	Lake/Reservoir	MC	0.28-8.86	
Microcystis, Oscillatoria, Anabaena	Rivers and reservoirs	MC	0.057-19.1	133-2612
Microcystis, Pseudanabaena, Oscillatoria, Anabaena	Lake/Reservoir	MC	ND-119	
Nodularia spp., Microcystis spp.	Lake/Reservoir	MC	0.08-3.38	
Nostoc sp.	Pond	MC		25.2
Planktothrix rubescens	Lake/Reservoir	MC	ND-5	Up to 46 μg L^{-1}
Scytonema cf. crispum	Lake/Reservoir	MC		ND
Tychonema bourrelly	Lake/Reservoir	MC	ND	
Tychonema bourrellyi, Planktothrix rubescens	Lake/Reservoir	MC	ND	
Unknown	Lake/Reservoir	MC	Up to 10000	
Unknown	Stream/River	MC	Up to 3.2	
Unknown	Water impoundment	MC		Up to 103000 μg L^{-1}

ND, no detect

Several studies have been conducted on the effects of various environmental factors on the production of microcystin from various MC producing strains. Some studies have suggested that environmental conditions affect cyanobacteria growth, which in turn indirectly affects toxin production. Orr and Jones (1998) hypothesized from studies of nitrogen limitation on MC production that there is a direct linear correlation between cell growth rates and MC production rates. Polyak *et al.* (2013) noted in their study that there was a positive correlation between biomass and MC concentrations, for which they hypothesized that the toxin concentrations were controlled by phosphorus on the cell growth rates and not directly on the metabolic pathways of toxin production. However, other studies have hypothesized that environmental factors may have a direct effect on MC production independent of the influences on growth rate (Jähnichen, Long and Petzoldt, 2011). In addition, environmental factors have shown to only affect the toxin quota of the cells by a factor of 2-4 (Long, Jones and Orr, 2001; Preußel *et al.*, 2009). The main cause for differences in MC concentration across blooms or occurrences is most likely due to the species (and strain) composition producing MC as the MC content of different strains and species vary significantly (Preußel *et al.*, 2009). Table 2-4 shows literature values for various species producing microcystin, and Table 2-5 summarizes the influence of environmental factors on microcystin production.

Table 2-4 Literature Values for Species Producing Microcystin in Laboratory and Field Conditions.

Species	Cell Growth (day-1)	Dry Weight Ratio (µg toxin g-1 DW)	Quota (pg toxin cell-1)	Extracellular Percent of Total Toxin (intra+extra)	Ratio of Intracellular Toxin to Chl a	References
Microcystis sp.			0.2 (NS)		0.4 (NS)	(World Health Organization, 2003)
Microcystis aeruginosa	0.1-1.08	710-7600 (intra)	Up to 0.073 (intra)	0.21-0.47	0.59-0.81 (intra) Up to 2.5 in N limiting conditions*	(Long, Jones and Orr, 2001; Jähnichen *et al.*, 2007)
Microcystis aeruginosa	0.1-0.8	555-1113 (NS)				(Oh *et al.*, 2000)
Microcystis aeruginosa		1000-9000 (NS)	0.05-0.16 (intra)			(Orr and Jones, 1998)
Planktothrix agardhii					1-2 (NS)	(World Health Organization, 2003)
Anabaena, Dolichospermum		760-24000 (NS)				(Buratti *et al.*, 2017)

DW, dry weight; intra, intracellular toxin; extra, extracellular toxin; total, intracellular and extracellular; NS, toxin type (intra, extra, or total) not specified

* Value obtained by dividing toxin quota by chlorophyll a quota

Table 2-5 Influence of Environmental Factors on Species Producing Microcystin in Laboratory and Field Conditions.

Species	Environmental Factor	Effect on Cell Growth Rate	Effect on Dry Weight Ratio	Effect on Cell Quota	Effect on Percent Extracellular Toxin	References
Microcystis aeruginosa	Intracellular inorganic carbon				Highest with low availability of inorganic carbon	(Jähnichen *et al.*, 2007)
Microcystis aeruginosa	NO3			Highest at 0.01 mmol L^{-1} NO3 Lowest at 0.1 and 1 mmol L^{-1} NO3		(Pimentel and Giani, 2014)
Microcystis aeruginosa	NH4			Highest at 0.002 mmol L^{-1} NH4 Lowest at 0.02 and 0.2 mmol L^{-1} NH4		(Pimentel and Giani, 2014)
Microcystis aeruginosa	PO4			Highest at 0.0005 mmol L^{-1} PO4 Lowest at 0.005 and 0.05 mmol L^{-1} PO4		(Pimentel and Giani, 2014)

2.3.1.2 Degradation

Microcystins can remain in the water for weeks after being released from the cells, and some studies have even claimed that these toxins could remain in the water for months (Corbel, Mougin and Bouaïcha, 2014). However, degradation by sunlight (photodegradation) and bacteria can increase the rate at which the toxins are removed from the water; for example, photodegradation can take as little as two weeks (Corbel, Mougin and Bouaïcha, 2014). MCs can also be removed from the water by adsorption onto sediment particles where the toxins are exposed to microbes and bacteria that biodegrade the toxins (Corbel, Mougin and Bouaïcha, 2014). Degradation rates for various environmental conditions are shown in Table 2-6.

Table 2-6 Influence of Environmental Factors on Microcystin Degradation.

Degradation Type	Environmental Quantity	Effect on Toxin Degradation*	References
Light	Artificial equivalence to approximately 20 days of natural sunlight	0.071 day^{-1} (24% left after 144 hours of light, equivalent to 20 days of natural sunlight)	(León *et al.*, 2019)
Light & cell pigments	Full sunlight in the presence of cell pigments	0.055-0.164 day^{-1} (90 % breakdown in 2 to 6 weeks)	(Chorus and Welker, 2021)
UV	254 nm UV light at 250 W m^{-2}	1326 day^{-1} (1% left after 5 minutes)	(León *et al.*, 2019)

* Decay rate calculated using the first-order decay reaction $c = c_0 e^{-kt}$, where c is the final toxin concentration, c_0 is the initial toxin concentration, t is time, and k is the decay rate (Chapra, 2008).

2.3.2 Cylindrospermopsins

Cylindrospermopsin (CYN) is one of the two main toxins of concern for drinking water along with microcystins. Cylindrospermopsins are cytotoxins that affect multiple organs and have the ability to cause liver failure that can lead to death.

2.3.2.1 Production

Cylindrospermopsin is a guanidine alkaloid, of which there are two known variants: 7-deoxy-cylindrospermopsin (relatively less toxic) and 7-epi-cylindrospermopsin (relatively more toxic) (Norris *et al.*, 1999; Banker *et al.*, 2000). 7-epi-cylindrospermopsin has been reported as a minor component of the overall CYN population and is not often included in studies (Pierangelini *et al.*, 2015). Not all studies distinguish between cylindrospermopsin and the two variants and it is sometimes unclear if only CYN is being studied or if the other two variants are being included in the total CYN amount. Cylindrospermopsin is the most commonly studied toxin and will be the primary focus of this section. The chemical structure of CYN is shown in Figure 2-3

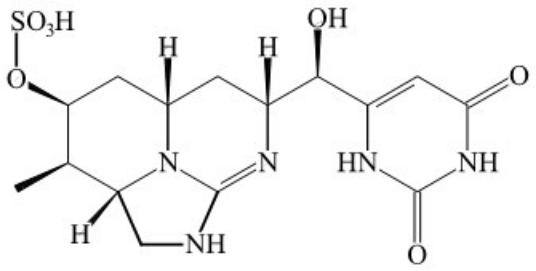

Figure 2-3 Chemical structure of CYN reproduced after Chorus and Welker (2021).

Cylindrospermopsin was originally thought to only occur in tropical environments until its presence was discovered in more temperate areas including Germany and France, likely due to increasing temperatures (Merel *et al.*, 2013; Buratti *et al.*, 2017). CYN is highly water-soluble and has a half-life of more than ten days in high purity water (Merel

et al., 2013; Buratti *et al.*, 2017). Similar to MC, a main cause of the variation in CYN across blooms is likely due to variations in bloom composition as different species and strains produce different amounts of CYN (Preußel *et al.*, 2009). In select studies, CYN concentrations have been found at levels up to 36 micrograms per liter in surface water in Taiwan and 568 micrograms per gram dry weight in bloom and scum in Saudi Arabia (Buratti *et al.*, 2017). The *cyr* gene cluster has been found to synthesize CYN (Mihali *et al.*, 2008). Table 2-7 shows literature values for CYN occurrence in surface water, bloom and scum.

Table 2-7 CYN and deoxy-CYN occurrence in surface water, bloom and scum (Buratti* et al.*, 2017).

Organism	Type of Waterbody	Toxin	Surface water (µg L^{-1})	Bloom and Scum (µg g^{-1} DW)
Cylindrospermopsis raciborskii	Lake/Reservoir	CYN	0.03-23.3	568
Cylindrospermopsis raciborskii, Aphanizomenon flos-aquae	Lake/Reservoir	CYN	0.3-2.8	
Cylindrospermopsis raciborskii, Aphanizomenon gracile	Lake/Reservoir	CYN	ND-3	
Lyngbya wollei	Dam and creek	CYN		ND-2.9
Lyngbya wollei	Dam and creek	Deoxy-CYN		3-86
Microcystis aeruginosa, Planktothrix rubescens, Dolichospermum flos-aquae	Lagoon	CYN		ND
Nodularia spp., Microcystis spp.	Lake/Reservoir	CYN	ND-36	
Scytonema cf. crispum	Lake/Reservoir	CYN		ND
Unknown	Lake/Reservoir	CYN	ND-4.4	
Unknown	Lake/Reservoir	CYN	0.002-0.484 (intracellular), 0.08-11.75 (extracellular)	

ND, no detect

In contrast to microcystin production, CYN concentrations are often higher as extracellular toxins (dissolved) than as intracellular toxins (Buratti *et al.*, 2017). The

processes by which cylindrospermopsin is released to the water column (either actively or through cell lysis) is not well understood, and it seems that different species may release CYN through different means. One study of a CYN producing species (*Aphanizomenon flos-aquae*) hypothesized that main source of the extracellular content of CYN is due to active release from the cells, and another study of a different species (*Cylindrospermopsis raciborskii*) claimed that while active release and leaking may occur, the accumulation of dissolved CYN is due primarily to cell lysis or another environmental stressor (Preußel *et al.*, 2009; Davis *et al.*, 2014). A study by Pierangelini *et al.* (2015) observed that cell quotas of CYN are fixed for *Cylindrospermopsis raciborskii* under different experimental conditions of light and CO2. They suggested that CYN production may be constitutive and not affected by these environmental conditions, and so the toxicity of a waterbody is due to the absolute abundance of toxic *C. raciborskii* cells in the water column. Carneiro *et al.* (2013) also concluded in their research that the production of CYN by *C. raciborskii* is not affected by light intensity. Other studies have shown that cell quota changes by a factor of 2-6 in response to nutrient limitation (Preußel, Chorus and Fastner, 2014).

Cylindrospermopsis raciborskii is able to fix nitrogen and can adapt to changing habitat conditions such as nutrient availability and light (Buratti *et al.*, 2017). Nitrogen limitation has been shown to cause an increase in the intracellular fraction of the toxin, where the extracellular fraction is likely due to only the release from dead cells (Preußel, Chorus and Fastner, 2014; Buratti *et al.*, 2017). Phosphorus limitation and nitrogen availability have been shown to cause an increase in the extracellular fraction through active release of CYN from intact cells (Preußel, Chorus and Fastner, 2014; Buratti *et al.*,

2017). The extracellular fraction of CYN from the *Aphanizomenon* species may be related to environmental factors that cause stress to the bacteria such as temperature and nutrient levels and in turn promote active transport of CYN from the cells (Preußel *et al.*, 2009; Preußel, Chorus and Fastner, 2014). In one study there were higher shares of extracellular toxins at lower growth rates and in another study the observed extracellular concentrations exceeded the estimated maximum release possible for dead cells (Preußel *et al.*, 2009; Preußel, Chorus and Fastner, 2014). Both studies indicate active release of CYN. While the extracellular share increased at lower growth rates for *Aphanizomenon flos-aquae*, there wasn't a very strong relation between growth rate and total CYN production (Preußel *et al.*, 2009). In addition to active release of CYN, another possible reason that extracellular CYN concentrations are higher than MC concentrations may be due to the slower degradation of CYN than MC and so more CYN can accumulate in the water column (Chiswell *et al.*, 1999; Rücker *et al.*, 2007). Table 2-8 shows literature values for various species producing cylindrospermopsin, and Table 2-9 summarizes the influence of environmental factors on cylindrospermopsin production.

Table 2-8 Literature Values for Species Producing Cylindrospermopsin in Laboratory and Field Conditions.

Species	Cell Growth (day-1)	Dry Weight Ratio (µg toxin g-1 DW)	Quota (pg toxin cell-1)	Extracellular Percent of Total Toxin (intra+extra)	Ratio of Intracellular Toxin to Chl a	References
Aphanizomenon flos-aquae	0.1-0.2	2300-6600 (total)		8-58		(Preußel *et al.*, 2006, 2009)
Aphanizomenon ovalisporum	0.08-0.35	Up to 6400 (total) Up to 4800 (intra)*	Up to 0.191 (total) Up to 0.143 (intra)*	23-64	Up to 0.5 (total) Up to 0.4 (intra)*	(Cirés *et al.*, 2011)
Aphanizomenon sp.				8-96		(Preußel, Chorus and Fastner, 2014)
Cylindrospermopsis raciborskii	0.313-0.524	568 (NS)	0.003-0.025 (intra)	79	0.021-0.094 (intra)	(Chiswell *et al.*, 1999; Carneiro *et al.*, 2013; Davis *et al.*, 2014; Buratti *et al.*, 2017)

DW, dry weight; intra, intracellular toxin; extra, extracellular toxin; total, intracellular and extracellular; NS, toxin type (intra, extra, or total) not specified

* Intracellular value obtained by multiplying value in text for total toxins by percent of intracellular toxin

Table 2-9 Influence of Environmental Factors on Species Producing Cylindrospermopsin in Laboratory and Field Conditions.

Species	Environmental Factor	Effect on Cell Growth Rate	Effect on Dry Weight Ratio	Effect on Cell Quota	Effect on Percent Extracellular Toxin	References
Aphanizomenon sp.	Nitrogen			Highest in low N culture Lowest in high N culture*	Highest in high N culture Lowest in low N culture*	(Preußel, Chorus and Fastner, 2014)
Aphanizomenon sp.	Phosphorus			Typically higher in high P culture than low P culture*	Highest in low P culture Lowest in high P culture*	(Preußel, Chorus and Fastner, 2014)
Cylindrospermopsis raciborskii	Light	Highest at 100 µmol photons m^{-2} s^{-1} Lowest at 40 µmol photons m^{-2} s^{-1}		Highest at 40 µmol photons m^{-2} s^{-1} Lowest at 100 and 348 µmol photons m^{-2} s^{-1}		(Carneiro *et al.*, 2013)
Aphanizomenon ovalisporum	Temperature	Highest at 35 C Lowest at 15 C	Highest at 20-30 C Lowest at 35 C	Highest at 20-30 C Lowest at 35 C	Highest at 15 C and 35 C Lowest at 20-30 C	(Cirés *et al.*, 2011)
Aphanizomenon ovalisporum	Light	Highest at 60 µE m^{-2} s^{-1} Lowest at 340 µE m^{-2} s^{-1}	Highest at 60 µE m^{-2} s^{-1} Lowest at 340 µE m^{-2} s^{-1}	Highest at 60 µE m^{-2} s^{-1} Lowest at 340 µE m^{-2} s^{-1}	No statistical difference	(Cirés *et al.*, 2011)

* units of ng CYN per cubic mm biovolume

2.3.2.2 Degradation

The dissolved toxins can remain in a waterbody for longer than a month even as the concentrations become diluted through mixing, sediment adsorption, and degradation (Buratti *et al.*, 2017). Cylindrospermopsin seems to be affected by photodegradation but biodegradation by microbes does not seem to affect toxin concentrations significantly (Buratti *et al.*, 2017). While CYN is fairly stable at low light levels, it is very sensitive to photodegradation as it has been shown that 90 percent of the toxin concentration can degrade in as little as two to three days (Corbel, Mougin and Bouaïcha, 2014). In addition to photodegradation, CYN has also been shown to be susceptible to biodegradation due to bacteria and microbes (Cruz *et al.*, 2013; Corbel, Mougin and Bouaïcha, 2014). Degradation rates for various environmental conditions are shown in Table 2-10.

Table 2-10 Influence of Environmental Factors on Cylindrospermopsin Degradation.

Degradation Type	Environmental Quantity	Effect on Toxin Degradation*	References
Light	Natural sunlight	4.16-11.09 day^{-1} (half-lives of 1.5 and 4 hours for extracts) 0.046-0.063 day^{-1} (half-lives of 11 and 15 days for natural water samples)	(Chiswell *et al.*, 1999)
UV	257 nm UV light at 300 mW m^{-2}	10.3 day^{-1} (decrease from 1.5 to 1.3 mg L^{-1} after 20 minutes)	(Chiswell *et al.*, 1999)
UV	257 nm UV light at 400 mW m^{-2}	0.924 day^{-1} (half-life of 18 hours)	(Chiswell *et al.*, 1999)
Temperature	Range of temperatures from 4 C-35 C	0.010-0.015 day^{-1} (80-86% of initial concentration left after 14 days)	(Chiswell *et al.*, 1999)
pH	Range of pH values from 4-10	0.004-0.005 day^{-1} (75-81% of initial concentration left after 8 weeks)	(Chiswell *et al.*, 1999)
Light	Range of artificial light from 9 µE m^{-2} s^{-1} to 42 µE m^{-2} s^{-1}	0.005-0.025 day^{-1} (62-84% of initial concentration left after 35 days)	(Chiswell *et al.*, 1999)
Light	Artificial equivalence to approximately 20 days of natural sunlight	0.0317 day^{-1} (53% left after 144 hours of light, equivalent to 20 days of natural sunlight)	(León *et al.*, 2019)
UV	254 nm UV light at 250 W m^{-2}	26.5 day^{-1} (1% left after 250 minutes)	(León *et al.*, 2019)

* Decay rate calculated using the first-order decay reaction $c = c_0 e^{-k}$, where c is the final toxin concentration, c_0 is the initial toxin concentration, t is time, and k is the decay rate (Chapra, 2008).

2.3.3 Anatoxins

As mentioned previously, anatoxins are neurotoxins that affect the nervous system and can cause cardiac arrhythmia leading to death.

2.3.3.1 Production

While anatoxin-a (ATX-a), homoanatoxin-a, and anatoxin-a(s) are all neurotoxins and often grouped together as anatoxins, homoanatoxin-a is a structural analogue of anatoxin-a where anatoxin-a(s) is not structurally related to the other two (Corbel, Mougin and Bouaïcha, 2014). There are other analogues of anatoxin-a, but homoanatoxin-a is one of the most commonly found and of a similar toxic potency to ATX-a (Méjean *et al.*, 2014). Anatoxin-a is the most studied of the anatoxins and will be the primary focus of this section. The chemical structure of ATX-a is shown in Figure 2-4.

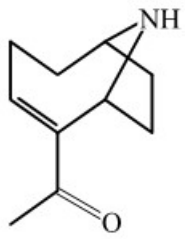

Figure 2-4 Chemical structure of ATX-a reproduced after Chorus and Welker (2021).

Anatoxin-a is highly water-soluble but unstable at pH values higher than 10 and they are also transformed into a non-toxic form from sunlight exposure (Merel *et al.*, 2013). Extracellular anatoxin-a is likely largely produced by cell lysis, but there may also be leakage from cells during the growth phase (Christensen and Khan, 2020). In select studies, anatoxin concentrations have been found at levels up to 1170 micrograms per liter in surface water in Washington State and 8000 micrograms per gram dry weight

in bloom and scum in France (Buratti *et al.*, 2017). There are six gene clusters that have been identified that synthesize ATX-a (Méjean *et al.*, 2009, 2014; Rantala-Ylinen *et al.*, 2011; Shih *et al.*, 2013; Jiang *et al.*, 2015). Table 2-11 shows literature values for ATX-a occurrence in surface water, bloom and scum.

Table 2-11 ATX-a occurrence in surface water, bloom and scum (Buratti* et al.*, 2017).

Organism	Type of Waterbody	Toxin	Surface water (μg L^{-1})	Bloom and Scum (μg g^{-1} DW)
Arthrospira fusiformis, Anabaenopsis abijatae, Spirulina subsalsa, Phormidium terebriformis	Lake/Reservoir	ATX-a		0.3-223
Lyngbya wollei	Stream/River	ATX-a		ND
Microcystis aeruginosa, Planktothrix rubescens, Dolichospermum flos-aquae	Lagoon	ATX-a		ND
Microcystis, Oscillatoria, Anabaena	Rivers and reservoirs	ATX-a	0.01-0.08	
Microcystis, Pseudanabaena, Oscillatoria, Anabaena	Lake/Reservoir	ATX-a	ND-0.006	
Phormidium favosum	Stream/River	ATX-a		8000
Tychonema bourrelly	Lake/Reservoir	ATX-a	ND-11.32	
Tychonema bourrellyi, Planktothrix rubescens	Lake/Reservoir	ATX-a	1.42-154.23	
Unknown	Lake/Reservoir	ATX-a	Up to 1170	
Unknown	Stream/River	ATX-a	ND-0.007	

ND, no detect

Whereas microcystin production is based primarily on cellular growth rates, a study of the effect of nitrogen on ATX-a production showed that the cultures with the highest growth rates (highest nitrogen concentration) did not have the highest toxin production (Gagnon and Pick, 2012). The highest ATX-a production corresponded with a lower nitrogen concentration indicating that increased toxin production may be related to moderate nitrogen limitation or subsequently moderate nutrient stress (Gagnon and

Pick, 2012). For studies of some ATX-a producing species, environmental factors such as light and temperature showed a variation in ATX-a content of around 2-4 fold (Chorus and Welker, 2021). Table 2-12 shows literature values for various species producing anatoxin-a, and Table 2-13 summarizes the influence of environmental factors on anatoxin-a production.

Table 2-12 Literature Values for Species Producing Anatoxin-a in Laboratory and Field Conditions.

Species	Cell Growth (day-1)	Dry Weight Ratio (µg toxin g-1 DW)	Quota (pg toxin cell-1)	Extracellular Percent of Total Toxin (intra+extra)	Ratio of Intracellular Toxin to Chl a	References
Anabaena circinalis		1396-8200 (NS)				(Testai *et al.*, 2016)
Anabaena flos-aquae		1017-13013 (NS)				(Testai *et al.*, 2016)
Aphanizomenon issatschenkoi	0.03-0.07	Up to 1408 (intra)	0.1-0.4 (total)	3-47	0.103-0.339* (intra)	(Wood *et al.*, 2007; Ballot *et al.*, 2010; Gagnon and Pick, 2012)
Aphanizomenon sp.		1562-6700 (NS)		3.6-19		(Cires and Ballot, 2016; Testai *et al.*, 2016)
Cylindrospermopsis raciborskii	0.15-0.47		0.016 (intra)	26		(Pierangelini *et al.*, 2015)
Phormidium autumnale			Up to 0.1 (intra)			(Heath *et al.*, 2014)

DW, dry weight; intra, intracellular toxin; extra, extracellular toxin; total, intracellular and extracellular; NS, toxin type (intra, extra, or total) not specified

* Value obtained by dividing toxin concentration by chlorophyll a concentration

Table 2-13 Influence of Environmental Factors on Species Producing Anatoxin-a in Laboratory and Field Conditions

Species	Environmental Factor	Effect on Cell Growth Rate	Effect on Dry Weight Ratio	Effect on Cell Quota	Effect on Percent Extracellular Toxin	References
Aphanizomenon issatschenkoi	Nitrogen	Highest at 1500 mg L^{-1} NaNO3 Lowest at 15 mg L^{-1} NaNO3	Highest at 75 mg L^{-1} NaNO3 Lowest at 1500 mg L^{-1} NaNO3	Highest at 75 mg L^{-1} NaNO3 Lowest at 1500 mg L^{-1} NaNO3	Highest at 15 mg L^{-1} NaNO3 Lowest at 1500 mg L^{-1} NaNO3	(Gagnon and Pick, 2012)
Aphanizomenon sp.	Temperature		Highest at 20 C Lowest at 30 C			(Rapala *et al.*, 1993)
Aphanizomenon sp.	Light		Highest at 128 µmol photons m^{-2} s^{-1} Lowest at 2 µmol photons m^{-2} s^{-1}			(Rapala *et al.*, 1993)
Aphanizomenon sp.	Nitrogen		Highest at 0 mg L^{-1} N Lowest at 84 mg L^{-1} N			(Rapala *et al.*, 1993)

2.3.3.2 Degradation

Anatoxin-a degrades quickly in water due to photolysis and chemical instability and therefore the amount that can bioaccumulate in organisms is likely low (Buratti *et al.*, 2017). Similar to Cylindrospermopsin, anatoxin-a is also a stable toxin at low light levels but will degrade quickly in the presence of light (photodegradation) especially in alkaline environments (Corbel, Mougin and Bouaïcha, 2014). Studies have also shown that anatoxin-a is also susceptible to rapid biodegradation by bacteria in the waterbody (Corbel, Mougin and Bouaïcha, 2014). Degradation rates for various environmental conditions are shown in Table 2-14.

Table 2-14 Influence of Environmental Factors on Anatoxin-a Degradation.

Degradation Type	Environmental Quantity	Effect on Toxin Degradation*	References
Bacteria	Microbial populations from bed sediment	0.14 day^{-1} (half-life of 5 days)	(Smith and Sutton, 1993)
pH	pH 8 and 10	0.21 day^{-1} (less than 5% left after 14 days)	(Smith and Sutton, 1993)
pH	basic pH	0.05 day^{-1} (half-life of 14 days)	(Testai *et al.*, 2016)
Light	normal environmental levels	8.32 day^{-1} (half-life of 1-2 hours)	(Stevens and Krieger, 1991)

* Decay rate calculated using the first-order decay reaction $c = c_0 e^{-kt}$, where c is the final toxin concentration, c_0 is the initial toxin concentration, t is time, and k is the decay rate (Chapra, 2008).

2.3.4 Saxitoxins

As mentioned previously, like anatoxins, saxitoxins are also neurotoxins that affect the nervous system and can cause respiratory paralysis leading to death.

2.3.4.1 Production

Saxitoxins are also classified as paralytic shellfish toxins (PSTs) which can accumulate in shellfish and cause food poisoning in humans (Indrasena and Gill, 2000). PSTs are a family of structurally related toxins divided into carbamate, sulfomate, and decarbamoyl toxins (Indrasena and Gill, 2000). Some research uses the terms saxitoxins (STXs) and PSTs interchangeably to refer to all the toxins of which saxitoxin (STX) is the most studied. Individual STXs vary in toxicity and so toxin concentrations are often expressed as saxitoxin equivalents (STX-eq) to consider all the toxin variants present using toxic equivalency factors (TEFs) (OHA, 2019a). Saxitoxin has the highest acute toxicity in mice and is set as the reference compound (Testai *et al.*, 2016). It is not always clear in the literature whether values are reported as STX-eq, total STXs, or are reported only considering the single STX toxin. Where possible, these values will be distinguished in this research. The chemical structure of STX is shown in Figure 2-5.

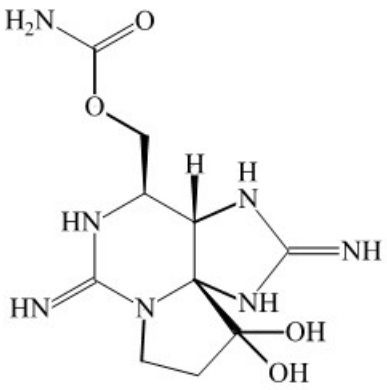

Figure 2-5 Chemical structure of STX reproduced after Chorus and Welker (2021).

Whether the concentrations of STXs are intracellular or extracellular in the species of *Anabaena* or *Cylindrospermopsis* depends on environmental factors that cause stress for the bacteria mostly due to ionic stress such as pH and sodium concentrations (Buratti *et al.*, 2017). In an experiment of saxitoxin production by *Cylindrospermopsis*, no measurable extracellular concentration was detected (Carneiro, Pacheco and De Oliveira e Azevedo, 2013). Table 2-15 shows literature values for STX occurrence in surface water, bloom and scum.

Table 2-15 STX occurrence in surface water, bloom and scum (Buratti* et al.*, 2017).

Organism	Type of Waterbody	Toxin	Surface water ($\mu g\ L^{-1}$)	Bloom and Scum ($\mu g\ g^{-1}$ DW)
Cylindrospermopsis raciborskii, A. flos-aquae	Lake/Reservoir	STX	0.4-1.2	
Lyngbya wollei	Stream/River	STX		ND
Microcystis aeruginosa, Planktothrix rubescens, Dolichospermum flos-aquae	Lagoon	STX		ND
Scytonema cf. crispum	Lake/Reservoir	STX		65.6
Unknown	Lake/Reservoir	STX	ND-193	

ND, no detect

Like anatoxin-a, saxitoxins also do not appear to be dependent on cellular growth rates. A study by Castro *et al.* (2004) showed that the maximum growth rate did not correspond with the maximum toxin production. A study by Ongley *et al.* (2016) showed that as sodium concentrations increased, the production of STX decreased in *Anabaena* and increased in *Cylindrospermopsis*, but the intracellular and extracellular ratios were relatively constant as compared to the control experiment for each species. The same study showed that changes in pH also had different effects on each species. An increase in pH caused a reduction in STX production in *Anabaena* and an increase in production for *Cylindrospermopsis*, but the extracellular ratios increased for both species (Ongley,

Pengelly and Neilan, 2016). Another study by Carneiro *et al.* (2013) looked at the effect of water hardness on STXs production from *Cylindrospermopsis raciborskii*. The authors observed that in most of the tested conditions the STXs quota was larger than the control group after six days, but after 12 days the quotas reached levels similar to the control group indicating an adaptation of this species to the environmental change. Environmental factors have shown to affect the quota of STX by a factor of about 2-4 (Chorus and Welker, 2021).

In select studies, saxitoxin concentrations have been reported at levels up to 193 micrograms per liter in surface water in Washington State and 0.29 micrograms per gram dry weight in bloom and scum in Russia (Buratti *et al.*, 2017). Saxitoxin has been found to be synthesized by the *sxt* gene cluster (Kellmann *et al.*, 2008; Mihali, Kellmann and Neilan, 2009; Stucken *et al.*, 2010; Mihali, Carmichael and Neilan, 2011). Table 2-16 shows literature values for various species producing saxitoxins, and Table 2-17 summarizes the influence of environmental factors on saxitoxins production.

Table 2-16 Literature Values for Species Producing Saxitoxins in Laboratory and Field Conditions.

Species	Cell Growth (day-1)	Dry Weight Ratio (µg toxin g-1 DW)	Quota (pg toxin cell-1)	Extracellular Percent of Total Toxin (intra+extra)	Ratio of Intracellular Toxin to Chl a	References
Anabaena circinalis		1580-4466 (STXs, intra) Up to 169 (STX, intra)	0.12-0.45 (STX, NS)	29-83 (STX)		(Negri and Jones, 1995; Velzeboer *et al.*, 2000; Ongley, Pengelly and Neilan, 2016; Testai *et al.*, 2016)
Cylindrospermopsis raciborskii	0.029-0.238		Up to 0.025 (STXs, intra)	53-95 (STX)		(Carneiro, Pacheco and De Oliveira e Azevedo, 2013; Ongley, Pengelly and Neilan, 2016)

DW, dry weight; intra, intracellular toxin; extra, extracellular toxin; total, intracellular and extracellular; NS, toxin type (intra, extra, or total) not specified

Table 2-17 Influence of Environmental Factors on Species Producing Saxitoxins in Laboratory and Field Conditions.

Species	Environmental Factor	Effect on Cell Growth Rate	Effect on Dry Weight Ratio	Effect on Cell Quota	Effect on Percent Extracellular Toxin	References
Anabaena circinalis	Osmotic stress			Decrease in STX concentration with 20 mM sorbitol compared to sterile MilliQ water	Increase with 20 mM sorbitol compared to sterile MilliQ water (STX)	(Ongley, Pengelly and Neilan, 2016)
Anabaena circinalis	Ionic stress			Decrease in STX concentration with 10 mM NaCl compared to sterile MilliQ water	Increase with 10 mM NaCl compared to sterile MilliQ water (STX)	(Ongley, Pengelly and Neilan, 2016)
Anabaena circinalis	pH stress			Decrease in STX concentration at pH 9 compared to sterile MilliQ water	Increase with pH 9 compared to sterile MilliQ water (STX)	(Ongley, Pengelly and Neilan, 2016)
Cylindrospermopsis raciborskii	Osmotic stress			Approximately no change in STX concentration with 20 mM sorbitol compared to sterile MilliQ water	Decrease with 20 mM sorbitol compared to sterile MilliQ water (STX)	(Ongley, Pengelly and Neilan, 2016)
Cylindrospermopsis raciborskii	Hardness	Magnesium promoted growth Sodium slowed growth Calcium inhibited growth		Initial increase in STXs cell quota with addition of hardness compared to control followed by return to original toxin quota for MgCO3 and Na2CO3	Approximately no change with 10 mM NaCl compared to sterile MilliQ water (STX)	(Carneiro, Pacheco and De Oliveira e Azevedo, 2013; Ongley, Pengelly and Neilan, 2016)
Cylindrospermopsis raciborskii	pH stress			Approximately no change in STX concentration with pH 9 compared to sterile MilliQ water	Increase with pH 9 compared to sterile MilliQ water (STX)	(Ongley, Pengelly and Neilan, 2016)

STX, saxitoxin; STXs, total saxitoxins

2.3.4.2 Degradation

Saxitoxins are water soluble and can persist in freshwater for over 90 days, but they are affected by high temperatures and can be degraded into more toxic variants (Merel *et al.*, 2013). The pH level has also been shown to have an effect on saxitoxin degradation where faster degradation has occurred at higher pH levels (Indrasena and Gill, 2000). Some studies have shown that saxitoxins can biodegrade quickly due to bacterial activity (Corbel, Mougin and Bouaïcha, 2014). One study showed that bacteria in biological treatment processes may cause structural modifications of the toxins that lead to an increase in toxin variants that are more toxic than the original variants (Kayal, Newcombe and Ho, 2008). Degradation rates for various environmental conditions are shown in Table 2-18.

Table 2-18 Influence of Environmental Factors on Saxitoxins Degradation.

Degradation Type	Environmental Quantity	Effect on Toxin Degradation*	References
Temperature and pH	5 C - 25 C, pH 3-7	0.0012 day^{-1} (87% STX left after 4 months at pH7 at both 5 C and 25 C) No significant STX degradation at pH 3-5	(Indrasena and Gill, 2000)
Temperature and pH	Natural waters at 25 C with high DOC and TSS	0.025-0.077 day^{-1} (half-lives for STXs of 9-28 days)	(Jones and Negri, 1997)
Temperature	20 C - 30 C	0.0107-0.0218 (Half-lives for STXs increased when temp was decreased from 30 C to 20 C at neutral pH)	(Pereira, Dias and Franca, 2002)

* Decay rate calculated using the first-order decay reaction $c = c_0 e^{-k}$, where c is the final toxin concentration, c_0 is the initial toxin concentration, t is time, and k is the decay rate (Chapra, 2008).
STX, saxitoxin; STXs, total saxitoxins

2.4 Models in Literature

Long *et al.* (2001) proposed a linear model of microcystin production in a batch culture from *Microcystis aeruginosa* as follows

$$Q_{MCYST} = \mu * \left(\frac{Q_{MCYSTmax} - Q_{MCYSTmin}}{\mu_{max}}\right) + Q_{MCYSTmin} \quad \textbf{(2-1)}$$

where Q_{MCYST}, microcystin cell quota in units of fmol cell^{-1}, and μ, specific growth rate in units of day^{-1}, have a linear relationship that can be described in terms of the maximum and minimum cell quotas ($Q_{MCYSTmax}, Q_{MCYSTmin}$) and the maximum specific growth rate (μ_{max}). They demonstrated that under nitrogen-limited growth, the microcystin cell quota in *M. aeruginosa* was a function of specific growth rate. This model shows that microcystin cell quota is indirectly affected by environmental variables through growth rate.

Jähnichen *et al.* (2011) proposed a dynamic model of microcystin production in a batch culture from *M. aeruginosa* using two differential equations describing cell growth and microcystin production separately as follows

$$\frac{dX}{dt} = \mu * X * \left(1 - \frac{X}{K}\right) \quad \textbf{(2-2)}$$

$$\frac{dM}{dt} = p * \frac{dX}{dt} - d_M * M \quad \textbf{(2-3)}$$

where X is cell abundance in units of cell mL^{-1}, μ is intrinsic growth rate in units of day^{-1}, K is carrying capacity in units of cell mL^{-1}, M is microcystin concentration in units of fg mL^{-1}, p is the microcystin production coefficient that describes a constant amount of MC passed to every new cell during division in units of fg cell^{-1}, and d_M is a first-order MC depletion rate in units of day^{-1}. The MC depletion rate describes a decrease in MC cell

quota over time as the culture ages, and it accounts for deviation of the ratio of rates of cell division and MC production from unity (Jähnichen, Long and Petzoldt, 2011). This model was developed to identify the effect of environmental factors on MC production both indirectly (through growth rate) and directly (through the production coefficient p that modifies the growth rate in the MC production rate equation). Different environmental conditions were tested, and the resulting model parameters (μ, K, p, and d_M) were estimated by fitting the differential equations to the experimental data. The control group of this study had the following conditions: temperature of 26 °C, irradiance of 40 μmol photons m^2 s^{-1}, SO_4^{2-} molar concentration of 200 μM, P molar concentration of 20 μM, and Fe^{3+} molar concentration of 6 μM (Jähnichen, Long and Petzoldt, 2011). The estimated model parameters based off these conditions were 0.54 day^{-1} for intrinsic growth, 2.68e7 cells ml^{-1} for carrying capacity, 87.7 for MC production coefficient, and 0.009 for the MC depletion rate (Jähnichen, Long and Petzoldt, 2011). The cell concentration predicted by these model parameters is shown in Figure 2-6. The microcystin concentration predicted by the dynamic model is shown in Figure 2-7.

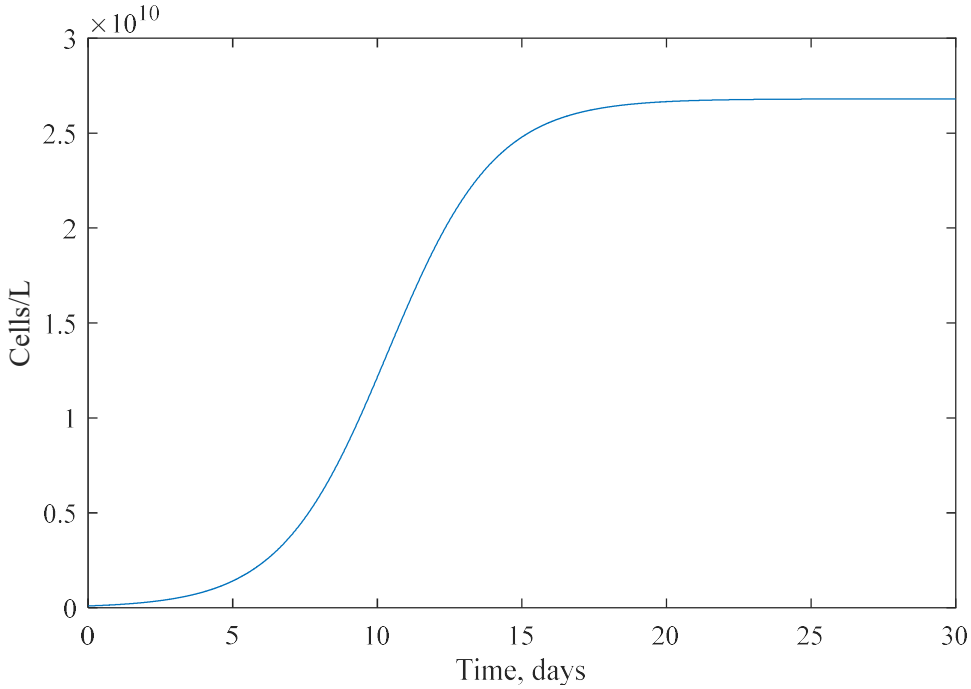

Figure 2-6 Dynamic model time series of* M. aeruginosa *cell concentrations.

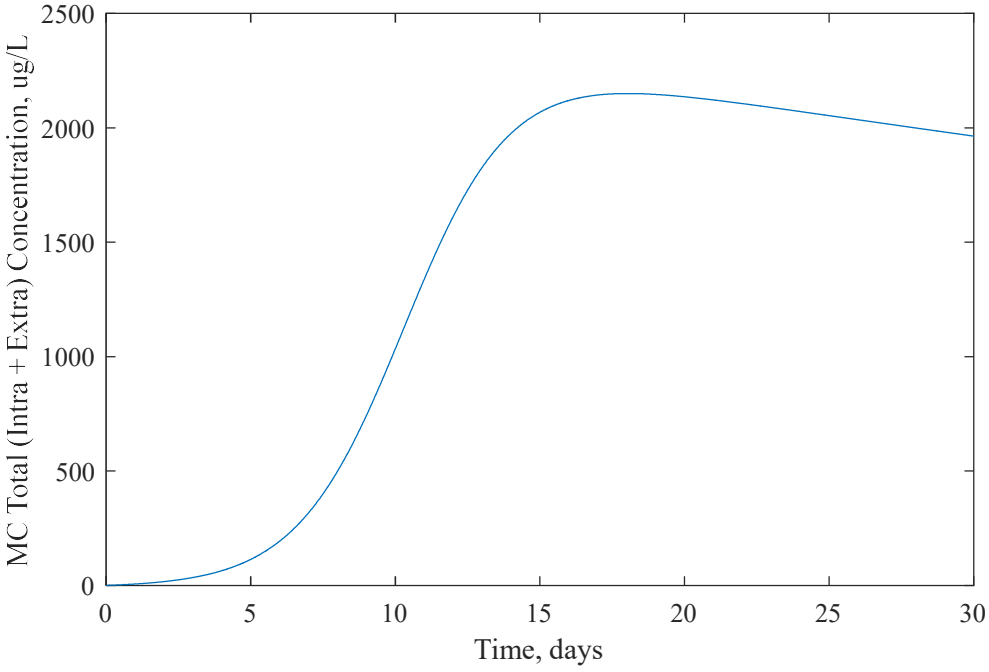

Figure 2-7 Dynamic model time series of microcystin concentrations.

Chapter 3: Model Development

3.1 Overview

The objectives of this research are to develop a framework for modeling cyanobacteria and their toxins. The literature review helped to answer the following questions: (1) What species produce the toxins? (2) Under what conditions do cyanobacteria produce toxins either as intracellular or extracellular toxins? (3) How much toxin is released to the waterbody under different environmental conditions? (4) What is the persistence of the cyanotoxins in the water and what are the pathways of transport and degradation? This information was put into a modeling framework so that a predictive model could answer questions about toxic algae blooms and their impact on water quality. Once the algorithms were developed and tested, they were added, tested and evaluated in the model CE-QUAL-W2, a two-dimensional (longitudinal and vertical) hydraulic and water quality model of rivers, lakes/reservoirs, and estuaries (Wells, 2020b).

3.2 Cyanobacteria and Toxin Governing Equations for Preliminary Model

3.2.1 Cyanobacteria Mass Balance

Figure 3-1 shows the sources and sinks of cyanobacteria in the preliminary model. The CE-QUAL-W2 model uses a more detailed approach to model algae and cyanobacteria, but for preliminary testing of the cyanotoxin equations, a simplified batch reactor model was used. The methods used in the CE-QUAL-W2 model are described in more detail following this section.

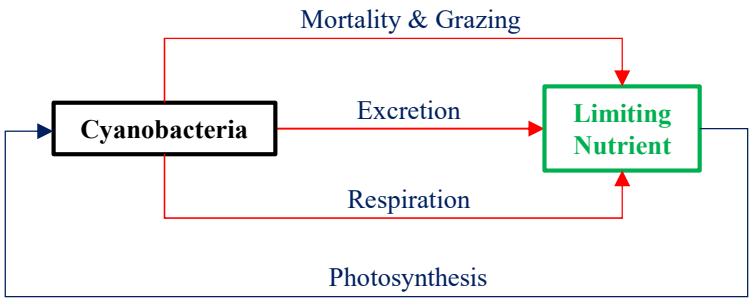

Figure 3-1 Sources and sinks of cyanobacteria as described by the preliminary model.

Referring to Figure 3-1, the sources and sinks of cyanobacteria mass concentration in a batch reactor of constant solution volume over time is predicted by Equation (3-1):

$$\frac{da}{dt} = \left(k_g - k_r - k_e - k_d\right) * a \qquad \textbf{(3-1)}$$

where k_g is first-order cell growth (a function of temperature, light, and nutrients) in units of inverse time, k_r is cell respiration in units of inverse time, k_e is cell excretion in units of inverse time, k_d is cell death which also includes losses to grazing in units of inverse time, and a is cyanobacteria concentration (in units of mass of dry weight organic matter per volume) (Chapra, 2008).

The cell growth rate, k_g, is given by Equation (3-2):

$$k_g(T, N, I) = k_{g,T} * \phi_N * \phi_L \qquad \textbf{(3-2)}$$

where $k_g(T, N, I)$ is growth rate as a function of temperature, nutrients, and light, $k_{g,T}$ is the maximum growth rate at a particular temperature, and ϕ_N and ϕ_L are attenuation factors for nutrient and light limitation, respectively (Chapra, 2008). The attenuation factors can have values from 0 to 1, representing complete limitation (0) or no limitation (1) on the maximum growth rate.

The maximum growth rate at a given temperature is commonly given by the theta model (Equation (3-3)):

$$k_{g,T} = k_{g,20}\theta^{T-20} \tag{3-3}$$

where $k_{g,20}$ is the maximum growth rate at a reference temperature of 20 degrees Celsius, θ is a temperature correct coefficient (1.066 is often used based off a large number of growth studies), and *T* is the temperature of interest in degrees Celsius (Chapra, 2008). A different approach for calculating the maximum growth rate at a given temperature is used in CE-QUAL-W2 that is more precise, but for preliminary model testing before incorporation into CE-QUAL-W2 the above equation will be used.

The Michaelis-Menten equation is commonly used to model nutrient limitation and is given by Equation (3-4):

$$\phi_N = \frac{N}{k_{sN} + N} \tag{3-4}$$

where *N* is the available concentration of the limiting nutrient and k_{sN} is the half-saturation constant for the nutrient (Chapra, 2008). The half-saturation constant is the nutrient concentration at which growth is half of the maximum growth rate and describes at what point nutrients become limiting. The limiting nutrient (nitrogen, phosphorus, silica, or carbon) often varies between species of algae or cyanobacteria depending on environmental factors. The equation to model the limiting nutrient as a function of algal concentration for a batch reactor is given by Equation (3-5):

$$\frac{dN}{dt} = -\left(k_g - k_r - k_e - k_d\right) * a * a_{Na} \tag{3-5}$$

where N represents the concentration of the limiting nutrient and a_{Na} is the ratio of the limiting nutrient to dry weight biomass of the algae in units of mass of nutrient per mass of dry weight organic matter.

Light limitation is modeled taking into consideration multiple factors including diurnal light variation, depth, and growth dependence on light. The Steele (1962) equation is a function of light that takes into account that growth is limited at high light levels and is given by Equation (3-6):

$$F(I) = \frac{I}{I_s} e^{-\frac{I}{I_s}+1} \tag{3-6}$$

where I is light intensity and I_s is the optimal light level for growth (saturating light intensity at maximum photosynthetic rate) (Chapra, 2008; Wells, 2020a). For average light over 12 daylight hours, I_a (average light intensity over daylight hours) can replace I. The variation of light with depth in the water column is given by the Beer-Lambert law (Equation (3-7)):

$$I(z) = I_0 e^{-k_e z} \tag{3-7}$$

where I_0 is the light intensity at the surface and k_e is the extinction coefficient. The extinction coefficient can be related to other variables as developed by Riley (1956) and shown in Equation (3-8):

$$k_e = k'_e + 0.0088a + 0.054a^{2/3} \tag{3-8}$$

where k'_e is the light extinction due to factors other than phytoplankton (Chapra, 2008). Equations 7 and 8 can be substituted into Equation 6 and then integrated over depth and time to develop the mean value of light limitation over depth resulting in Equation (3-9):

$$\phi_L = \frac{2.718f}{k_e H}(e^{-\alpha_1} - e^{-\alpha_0}) \quad \textbf{(3-9)}$$

where f is the photoperiod (fraction of day with daylight hours), H is the water layer thickness from H_1 (top of layer) to H_2 (bottom of layer) where $H_1 = 0$ is the surface, and α_1 and α_0 relate light variation in the water column to optimal light conditions for growth (Chapra, 2008). The coefficients α_0 and α_1 are given by Equations (3-10) and (3-11):

$$\alpha_0 = \frac{I_a}{I_s} e^{-k_e H_1} \quad \textbf{(3-10)}$$

$$\alpha_1 = \frac{I_a}{I_s} e^{-k_e H_2} \quad \textbf{(3-11)}$$

Equation 9 can be rewritten so as to model light limitation on a fractional day basis over the course of the daylight period instead of averaging growth over a day as given by Equation (3-12):

$$\phi_L = \frac{2.718}{k_e H}(e^{-\alpha_1} - e^{-\alpha_0}) \quad \textbf{(3-12)}$$

where the photoperiod has been removed and I_a (average light intensity) in the α_1 and α_0 terms has been replaced with I (light intensity at each fractional day timestep). The light intensity is given by Equation (3-13) for different time (t) periods:

$$\begin{aligned} &\text{0.25 days (6AM) < t < 0.75 days (6PM)}, \quad I = I_{max} \sin\left(\frac{\pi(t - 0.25)}{0.5day}\right) \\ &\text{0.75 days (6PM) < t < 0.25 days (6AM)}, \quad I = 0 \end{aligned} \quad \textbf{(3-13)}$$

where there is no growth in the absence of light and I_{max} is the maximum light intensity.

3.2.2 Cyanotoxin Mass Balances

Figure 3-2 shows the sources and sinks of the intracellular and extracellular toxins as described by the cyanotoxin mass balances.

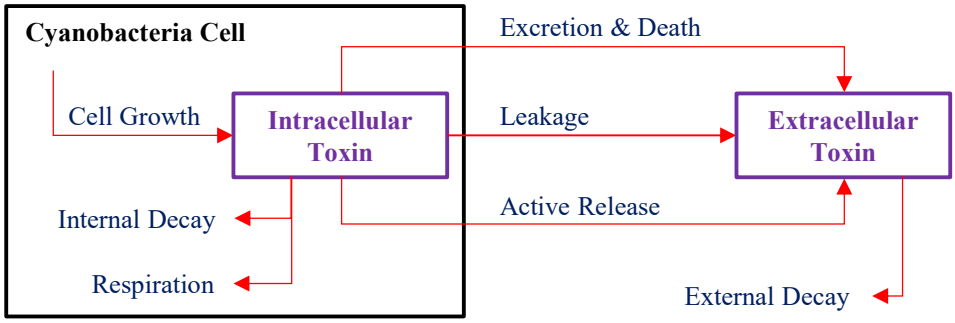

Figure 3-2 Sources and sinks of the intracellular and extracellular toxins as described by the preliminary model.

Referring to Figure 3-2, it is predicted that for a specific toxin in a batch reactor, the sources and sinks of intracellular toxin concentration can be modeled by Equation (3-14) and the sources and sinks of extracellular toxin concentration can be modeled by Equation (3-15):

$$\frac{dC_{intra}}{dt} = \left(k_g - k_r - k_e - k_d\right) * a * \beta - k_{leak} * C_{intra} - k_{decay\_intra} * C_{intra} - k_{active} * C_{intra} \quad \textbf{(3-14)}$$

$$\frac{dC_{extra}}{dt} = (k_e + k_d) * a * \beta + k_{leak} * C_{intra} - k_{decay\_extra} * C_{extra} + k_{active} * C_{intra} \quad \textbf{(3-15)}$$

where C_{intra} is intracellular toxin concentration, $k_g * a * \beta$ is the increase of intracellular toxin during growth, $-k_r * a * \beta$ is the loss of intracellular toxin during respiration, $\pm k_e * a * \beta$ is the loss of intracellular toxin (increase of extracellular toxin) to cell excretion, $\pm k_d * a * \beta$ is the loss of intracellular toxin (increase of extracellular toxin) to death, β is the ratio of intracellular toxin mass to mass of dry weight organic matter, $\pm k_{leak} * C_{intra}$ is the loss of intracellular toxin (increase of extracellular toxin) due to leakage from the cell, $-k_{decay\_intra} * C_{intra}$ is the loss of intracellular toxin to internal

decay, $\pm k_{active} * C_{intra}$ is the loss of intracellular toxin (increase of extracellular toxin) due to active toxin release from the cell, C_{extra} is the extracellular toxin concentration, and $-k_{decay\_extra} * C_{extra}$ is the loss of extracellular toxin to extracellular decay (a function of temperature, light, pH, and other water quality parameters). Research has shown that exposure to light increases the degradation of cyanotoxins, and so the preliminary model will look at how light affects the extracellular decay rate by using two different decay rates, a decay rate during the day ($k_{decay\_extra\_day}$) and a decay rate at night ($k_{decay\_extra\_nigh}$).

Separate toxin mass balances are used for each toxin of interest. Literature values for extracellular decay rates for each toxin under different environmental parameters are listed previously in Chapter 2. Literature values of β are also listed previously in Chapter 2. It is assumed that the value of β represents the intracellular toxin production rate (100 percent of the production rate), and that the extracellular toxin is only released from the intracellular toxin produced. The toxins are primarily peptides and alkaloids as shown previously in Chapter 2, and it is predicted that during cellular respiration, when the cell releases carbon dioxide, the cells may use the toxin for cell processes thereby decreasing the amount of intracellular toxin while not adding to the amount of extracellular toxin (Chapra, 2008). It is also predicted that during excretion, when the cells release nutrients and organic carbon, the cells may also release toxins as extracellular byproducts (Chapra, 2008). The pathways of toxin production and release are not well known, and so the toxin mass balance includes production and decay rates to account for predicted pathways that toxins may take. The leakage, active release, and internal decay rates can either be

given values or set to zero for each toxin depending on the likelihood that the toxin of interest undergoes that process.

3.3 Description of Algae Equations Used in CE-QUAL-W2

CE-QUAL-W2 is currently capable of modeling any number of algae groups. While cyanobacteria are not algae, they follow similar growth and death kinetics as algae and can be modeled as an algal group in CE-QUAL-W2. Cyanobacteria are photosynthetic (contain chlorophyll) and share many similar properties to algae such as their response to environmental properties like light and nutrients (Merel *et al.*, 2013; U.S. EPA, 2014b). The following section details the equations and methods used for modeling algal sources and sinks. Cyanobacteria are also modeled using these same equations. Equations (3-14) and (3-15) for toxin sources and sinks were coupled with these CE-QUAL-W2 algal equations as described in following sections. The internal flux between algae and other water quality state variables as modeled in CE-QUAL-W2 is shown in Figure 3-3.

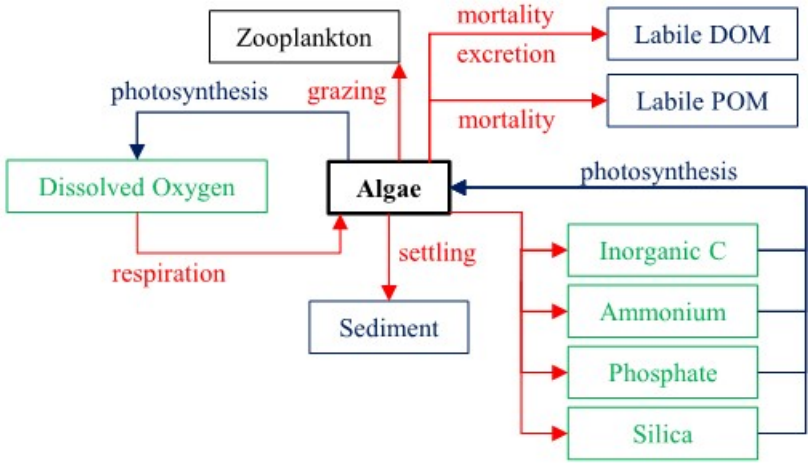

Figure 3-3 Internal flux between algae and other water quality state variables, reproduced after Wells (2020b).

Referring to Figure 3-3, the rate equation for the sources and sinks of mass concentration of each algal group is similar to Equation (3-1) and is given by Equation (3-16):

$$S_a = K_{ag}\Phi_a - K_{ar}\Phi_a - K_{ae}\Phi_a - K_{am}\Phi_a - \omega_a \frac{\delta \Phi_a}{\delta z} - \sum \left(Z_\mu \Phi_{zoo} \frac{\sigma_{alg}\Phi_a}{\sum \sigma_{alg}\Phi_a + \sigma_{pom}\Phi_{lpom} + \sum \sigma_{zoo}\Phi_{zoo}} \right) \quad \textbf{(3-16)}$$

where z is cell height in meters, Z_μ is net growth rate of a zooplankton species in sec^{-1}, σ_{alg} and σ_{zoo} are zooplankton grazing preference factors for algae (alg) or zooplankton (zoo), K_{ag} is algal growth rate in sec^{-1}, K_{ar} is algal dark respiration rate in sec^{-1}, K_{ae} is algal excretion rate in sec^{-1}, K_{am} is algal mortality rate in sec^{-1}, ω_a is algal settling rate in m sec^{-1}, and Φ_a is algal concentration in g m^{-3} (Wells, 2020a). The first term represents increase in algal concentration due to growth, the second term represents loss due to respiration, the third term represents loss due to excretion, the fourth term represents loss due to mortality, the fifth term represents loss due to settling, and the sixth term represents the net loss due to grazing.

CE-QUAL-W2 computes growth rate based on temperature, light, and nutrient availability as shown in Equation (3-17):

$$K_{ag} = \gamma_{ar}\gamma_{af}\lambda_{min}K_{ag\,max} \quad \textbf{(3-17)}$$

where γ_{ar} is the temperature rate multiplier for rising limb of curve, γ_{af} is the temperature rate multiplier for the falling limb of curve, λ_{min} is the multiplier for limiting growth factor (minimum of light, phosphorus, silica, and nitrogen) between 0 and 1, K_{ag}

is the algal growth rate in units of sec^{-1}, and $K_{ag\ max}$ is the maximum algal growth rate in units of sec^{-1} (Wells, 2020a).

The rate multiplier for light limitation, λ_l, is based on the Steele function as previously shown in Equation (3-6) above where λ_l is equal to $F(I)$. The decrease of light penetration with depth is modeled similarly to Equation (3-7) above and is shown in Equation (3-18):

$$I(z) = (1-\beta)I_0 e^{-\alpha z} \tag{3-18}$$

where I_0 is the solar radiation at the water surface in W m^{-2}, α is the attenuation coefficient in m^{-2}, z is depth in meters, and $(1-\beta)$ is the fraction of solar radiation absorbed at the water surface (Wells, 2020a). The average effect of light on algal growth in a model cell can be obtained by combining $F(I)$ and $I(z)$ and integrating over cell depth which results in Equations (3-19), (3-20), and (3-21):

$$\lambda_l = \frac{e}{\alpha \Delta z}[e^{-\gamma_2} - e^{-\gamma_1}] \tag{3-19}$$

$$\gamma_1 = \frac{(1-\beta)I_0}{I_s} e^{-\alpha d} \tag{3-20}$$

$$\gamma_2 = \frac{(1-\beta)I_0}{I_s} e^{-\alpha(d+\Delta z)} \tag{3-21}$$

where d is the depth at the top of the model cell in meters (Wells, 2020a). The attenuation coefficient, α, consists of a baseline value to which the effects of other material in the water column are added (organic and inorganic suspended solids and algae).

The rate multiplier for nutrient limitation, λ_i, is based on the Monod relationship as shown in Equation (3-22) (same as Equation (3-4) above):

$$\lambda_i = \frac{\Phi_i}{P_i + \Phi_i} \quad \textbf{(3-22)}$$

where Φ_i is the phosphorus or nitrate and ammonium concentration in g m^{-3} and P_i is the half-saturation coefficient for phosphorus or nitrate and ammonium in g m^{-3}. The algal nitrogen preference for ammonium is shown in Equation (3-23) which allows algae to use ammonium when available and then switch to nitrate as ammonium concentrations decrease:

$$P_{NH4} = \Phi_{NH4} \frac{\Phi_{NOx}}{(K_{NH4} + \Phi_{NH4})(K_{NH4} + \Phi_{NOx})} + \Phi_{NH4} \frac{K_{NH4}}{(\Phi_{NH4} + \Phi_{NOx})(K_{NH4} + \Phi_{NOx})} \quad \textbf{(3-23)}$$

where P_{NH4} is the ammonium preference factor, K_{NH4} is the ammonia preference half-saturation coefficient in g m^{-3}, Φ_{NH4} is the ammonium concentration in g m^{-3}, and Φ_{NOx} is the nitrate-nitrite concentration in g m^{-3} (Thomann and Fitzpatrick, 1982; Wells, 2020a).

Algal dark respiration, photorespiration (excretion) and mortality rates are computed using Equations (3-24), (3-25), and (3-26):

$$K_{ar} = \gamma_{ar}\gamma_{af}K_{ar\,max} \quad \textbf{(3-24)}$$

$$K_{ae} = (1 - \lambda_l)\gamma_{ar}\gamma_{af}K_{ae\,max} \quad \textbf{(3-25)}$$

$$K_{am} = \gamma_{ar}\gamma_{af}K_{am\,max} \quad \textbf{(3-26)}$$

where $K_{ar\,max}$, $K_{ae\,max}$, $K_{am\,max}$ are the maximum rates for dark respiration, excretion, and mortality in sec^{-1}, respectively.

The temperature rate multipliers for the rising limb of curve and the falling limb of the curve are computed using Equations (3-27) and (3-28):

$$\gamma_{ar} = \frac{1}{T_2 - T_1} \ln \frac{K_2(1 - K_1)}{K_1(1 - K_2)} \quad \textbf{(3-27)}$$

$$\gamma_{af} = \frac{1}{T_4 - T_3} \ln \frac{K_3(1 - K_4)}{K_4(1 - K_3)} \quad \textbf{(3-28)}$$

where T_1 and T_4 represent mortality limit temperatures and T_2 and T_3 define the lower and upper limit temperatures of the optimum range for the rate to occur, respectively. K_1 to K_4 are multiplier factors applied to each temperature T_1 to T_4, respectively, and define the fraction of the maximum growth that occurs at that temperature.

Settling rates are constant for each algae species except cyanobacteria when using model enhancements from Overman (2019). Cyanobacteria are able to migrate vertically in the water column through a process called buoyancy regulation which utilizes carbohydrate gas vesicles. Model updates from Overman capture this process to allow for variable settling rates of cyanobacteria within CE-QUAL-W2.

Chapter 4: Comparison of Preliminary Model to Experimental Data

4.1 Overview

The equations outlined in Chapter 3 for the preliminary model development were used to develop curves for algae, nutrient, and toxin concentrations. Once the model was developed, results from the model were compared to published data on toxins. Figure 4-1 and Figure 4-2 illustrate the functionality of the preliminary model. The growth of the cyanobacteria in the preliminary model is a function of temperature, light, and nutrients. As shown in Figure 4-1, the cyanobacteria concentration increases while the nutrient concentration decreases until steady-state is achieved. The oscillations shown in Figure 4-1 are the result of a light and dark cycle where there is no growth (only excretion, respiration, and death) in the absence of light.

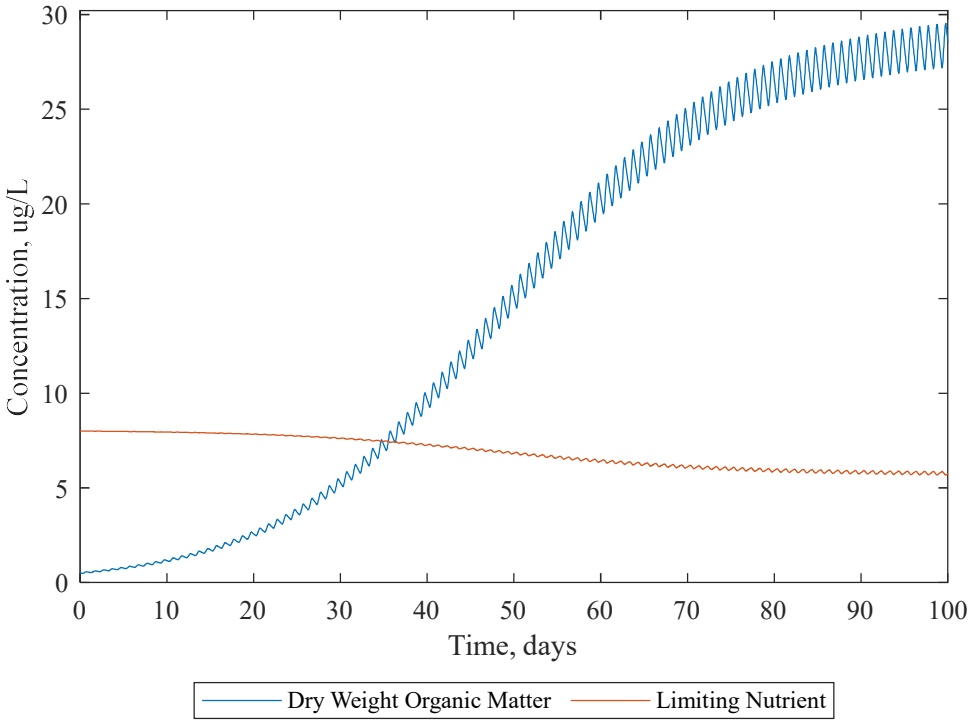

Figure 4-1 Change in concentration over time of cyanobacteria and limiting nutrient using preliminary model.

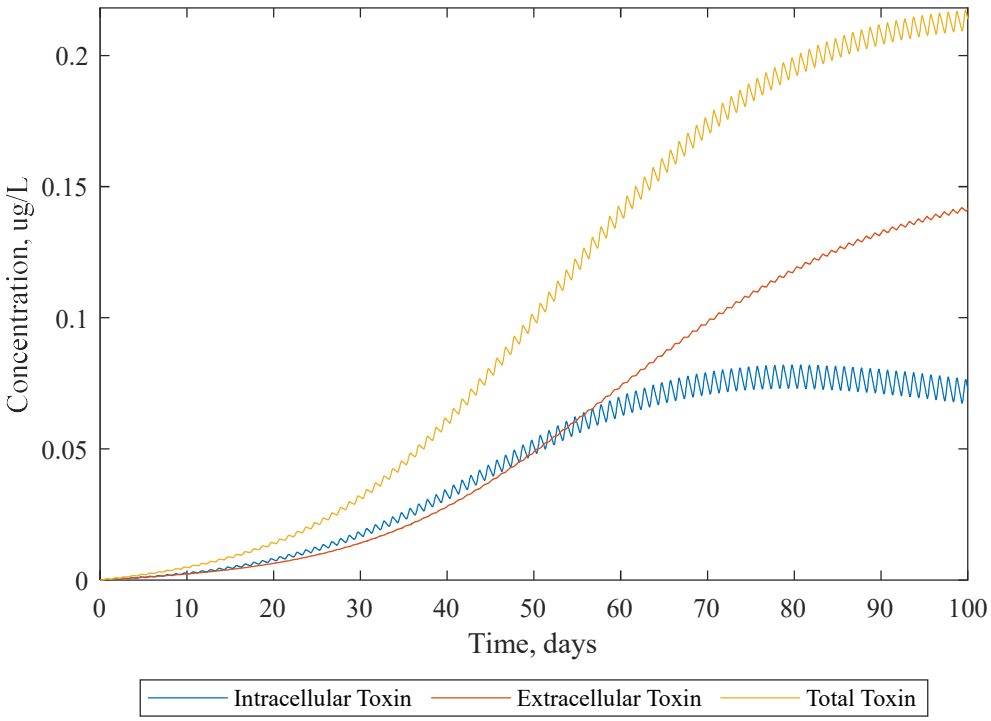

Figure 4-2 Change in concentration over time of cyanotoxin producing cyanobacteria and limiting nutrient using preliminary model.

4.2 Comparison of Preliminary Model to Published Data: Microcystin

A model for microcystin production was developed by Jähnichen *et al.* (2011) as described previously in Chapter 2. Their model was developed using values obtained experimentally from Jähnichen *et al.* (2011) and Long (2001) for microcystin content of *M. aeruginosa*. Microcystin concentration was modeled using the preliminary model and compared to results from Long (2001) and the control group of Jähnichen *et al.* (2011) for their batch reactor experiments. Table 4-1 shows the inputs that were used in the preliminary model to model microcystin production and degradation.

Table 4-1 Input values used in preliminary model for microcystin production and degradation.

Microcystin			
Variable	**Abbreviation**	**Units**	**Value**
Initial cyanobacteria concentration, dry weight organic matter (OM)	a_0	mg m^{-3}	1800
Initial limiting nutrient concentration	N_0	mg m^{-3}	620

Microcystin			
Variable	**Abbreviation**	**Units**	**Value**
Initial intracellular toxin concentration	Cin_0	mg m^{-3}	0
Initial extracellular toxin concentration	Cex_0	mg m^{-3}	0
Ratio of the limiting nutrient to dry weight organic matter (OM)	a_{Na}	mgNutrient $mgOM^{-1}$	0.0013-0.002*
Nutrient half-saturation constant	k_{sN}	mg m^{-3}	3
Maximum growth rate at 20 °C	$k_{g,20}$	day^{-1}	0.82
Temperature correction coefficient	θ	unitless	1.066
Temperature	T	°C	26
Light extinction due to factors other than phytoplankton	k'_e	m^{-1}	0
Bottom layer elevation	H_2	m	0.005-0.01*
Top layer elevation	H_1	m	0
Layer depth	H	m	0.005-0.01*
Optimal light level for growth	I_s	µmol photons m^{-2} s^{-1}	50
Maximum light level	I_{max}	µmol photons m^{-2} s^{-1}	40
Ratio of intracellular toxin to dry weight organic matter (OM)	β	mgToxin $mgOM^{-1}$	0.004-0.006*
Rate of cell respiration	k_r	day^{-1}	0
Rate of cell excretion	k_e	day^{-1}	0.03
Rate of cell death	k_d	day^{-1}	0.01
Rate of intracellular toxin release from cell due to leakage	k_{leak}	day^{-1}	0
Rate of intracellular toxin decay inside the cell	k_{decay_intra}	day^{-1}	0.009
Rate of intracellular toxin release from cell due to active release	k_{active}	day^{-1}	0
Rate of extracellular toxin decay during the day	$k_{decay\_extra\_day}$	day^{-1}	0.1
Rate of extracellular toxin decay during the night	$k_{decay\_extra\_night}$	day^{-1}	0

*Range of values modeled

The initial cyanobacteria concentration (a_0) was obtained from the control group of Jähnichen *et al.* (2011) by converting cells per liter to dry weight organic matter using a value of 18E-12 g $cell^{-1}$ based on the values reported by Long *et al* (2001) for *Microcystis aeruginosa*. The initial nutrient concentrations were 0.02 mM for phosphorus and 2 mM for nitrogen in the modified MLA medium used in the experiment

(Long, 2001). The limiting nutrient for the control group was estimated to be phosphorus as described by Long (2001). The initial limiting nutrient concentration (N_0) was estimated from the molar concentration. The initial intracellular and extracellular concentrations (Cin_0, Cex_0) were assumed to be zero. The limiting nutrient parameters (a_{Na} and k_{sN}) were estimated from the CE-QUAL-W2 manual (Wells, 2020a). A minimum value of 0.0013 and a maximum value of 0.002 for the ratio of the limiting nutrient to dry weight organic matter (a_{Na}) were chosen to compare the sensitivity of the model to this parameter.

The maximum growth rate at 20 degrees Celsius ($k_{g,20}$) used in the model was back-calculated from the maximum growth of 1.2 day^{-1} observed at 26 degrees Celsius in Long *et al* (2001), and the temperature of the model (T) was obtained from the experiments of Jähnichen *et al.* (2011) and Long (2001). The temperature correction coefficient (θ) value was obtained from Chapra (2008). It was assumed that there was no light extinction due to factors other than the growth of the cyanobacteria ($k'_e = 0$). The layer depth and bottom layer elevation (H, H_2) were estimated from the approximate height of 250 mL in a 500 mL flask as was used in the experiment by Jähnichen *et al.* (2011) and Long (2001). A minimum of 0.005 meters and a maximum of 0.01 meters were chosen for depth estimates. The optimal light level for growth (I_s) of *M. aeruginosa* was estimated from experiments done by Hesse *et al.* (2001). The maximum light level was obtained from the experiment of Jähnichen *et al.* (2011) and Long (2001) and constant light was applied during the experiments. The model sensitivity to light limitation was also tested by setting the light attenuation factor to 1.0 (no light limitation) to compare to the results with light limitation.

The ratio of intracellular toxin to dry weight organic matter (β) was estimated from the range of values provided by Long *et al* (2001). A minimum value of 0.004 and a maximum value of 0.006 for the ratio of toxin to dry weight organic matter were chosen to compare the sensitivity of the model to this parameter. It was assumed that there was no cell respiration (k_r) due to the constant application of light. The rate of cell excretion (k_e) and rate of cell death (k_d) were estimated based on values provided in the CE-QUAL-W2 manual. The rate of cell death was assumed to be small since there would be no grazing losses. The rate of toxin leakage from cells (k_{leak}) and the rate of active release of toxins from cells (k_{active}) were assumed to be zero based on the low values of extracellular toxin observed in laboratory and field studies. The rate of intracellular toxin decay inside the cell (k_{decay_intra}) was estimated from the values obtained by Jähnichen *et al.* (2011) for microcystin depletion rate. The rate of extracellular toxin decay during the day ($k_{decay\_extra\_day}$) was estimated from the decay rate due to light exposure observed by León *et al.* (2019). The rate of extracellular decay during the night ($k_{decay\_extra\_night}$) was assumed to not be applicable since constant light was applied.

4.2.1 Results

The results obtained from the preliminary model were compared to model results from Jähnichen *et al.* (2011) and experimental data from Long (2001) as estimated from figures. Figure 4-3 through Figure 4-6 show the change in concentration over time of cyanobacteria (Microcystis aeruginosa) in dry weight organic matter. The results are shown with and without light limitation, with a ratio of limiting nutrient to dry weight organic matter of 0.0013 or 0.002, and with a depth of 0.005 or 0.01 as indicated on each

figure. The mean error between the preliminary model and the experimental data is shown on each figure.

Figure 4-7 and Figure 4-8 show the change in concentration over time of intracellular toxin, extracellular toxin, and total toxin (combination of intracellular and extracellular toxins) for the preliminary model and the total toxin concentration of the model by Jähnichen *et al.* (2011) and total toxin concentration from experimental data from Long (2001) as estimated from figures. The toxin results are shown with light limitation and with a ratio of toxin to dry weight organic matter of 0.004 or 0.006 as indicated on each figure. The depth is 0.005 meters and the value of a_{Na} is 0.0013 for all toxin results. The mean error between the preliminary model total toxin concentration and the experimental data is shown on each figure.

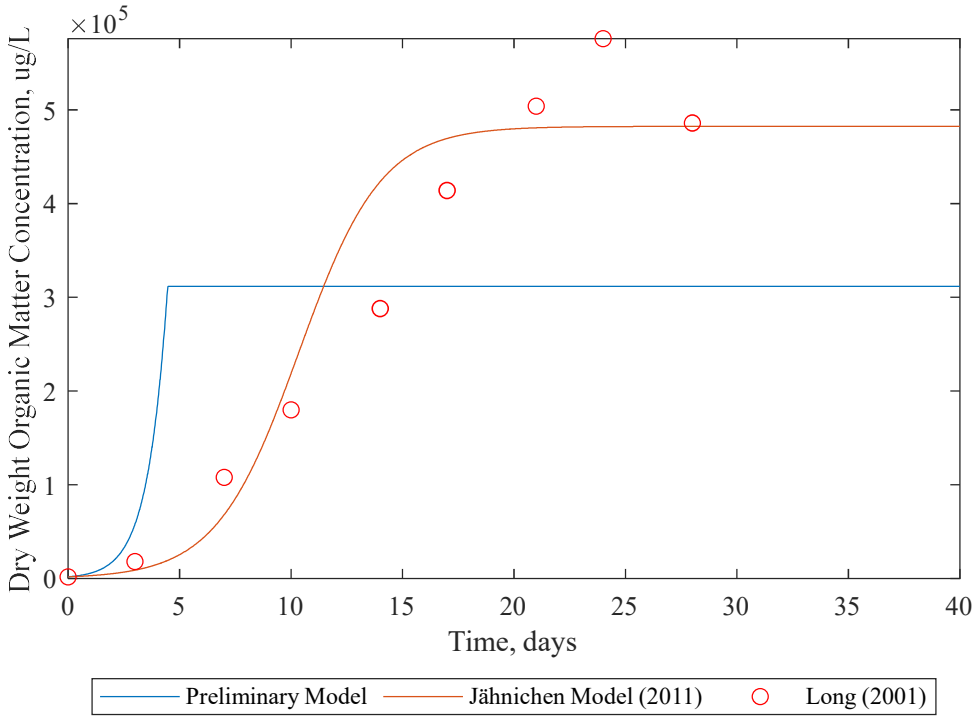

Figure 4-3 Comparison of microcystin producing cyanobacteria (Microcystis aeruginosa) concentration between preliminary model and Jähnichen et al. (2011) without light limitation and a_{Na}=0.002. Long (2001) values are estimated from figures. Mean error of -37092 µg L^{-1}.

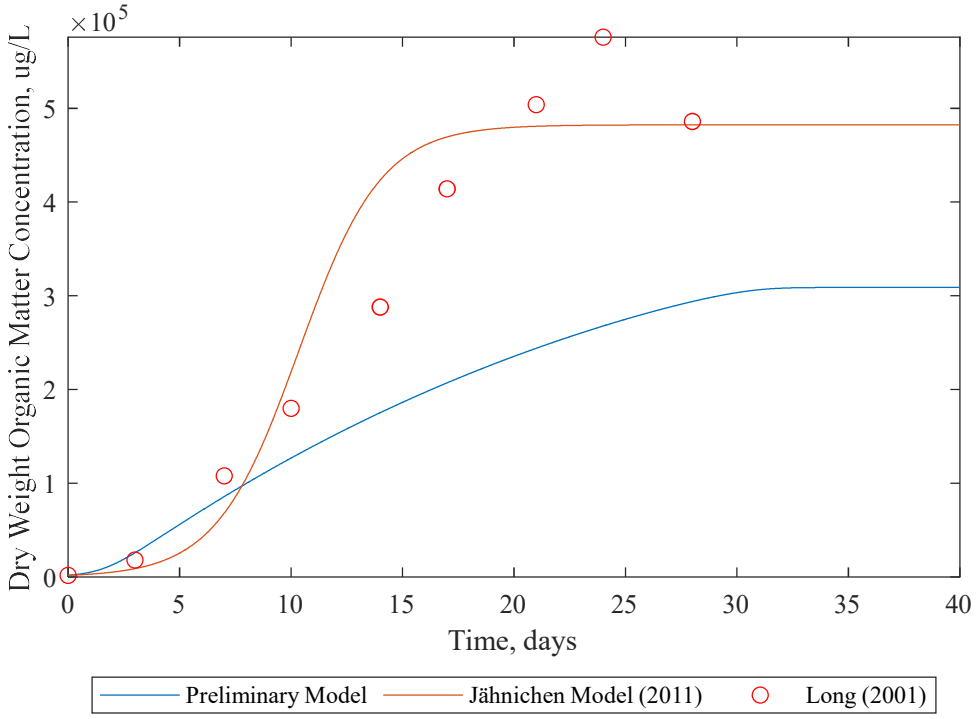

Figure 4-4 Comparison of microcystin producing cyanobacteria (Microcystis aeruginosa) concentration between preliminary model and Jähnichen et al. (2011) with light limitation, a_{Na}=0.002, and H=H_2=0.01. Long (2001) values are estimated from figures. Mean error of -12748 µg L^{-1}.

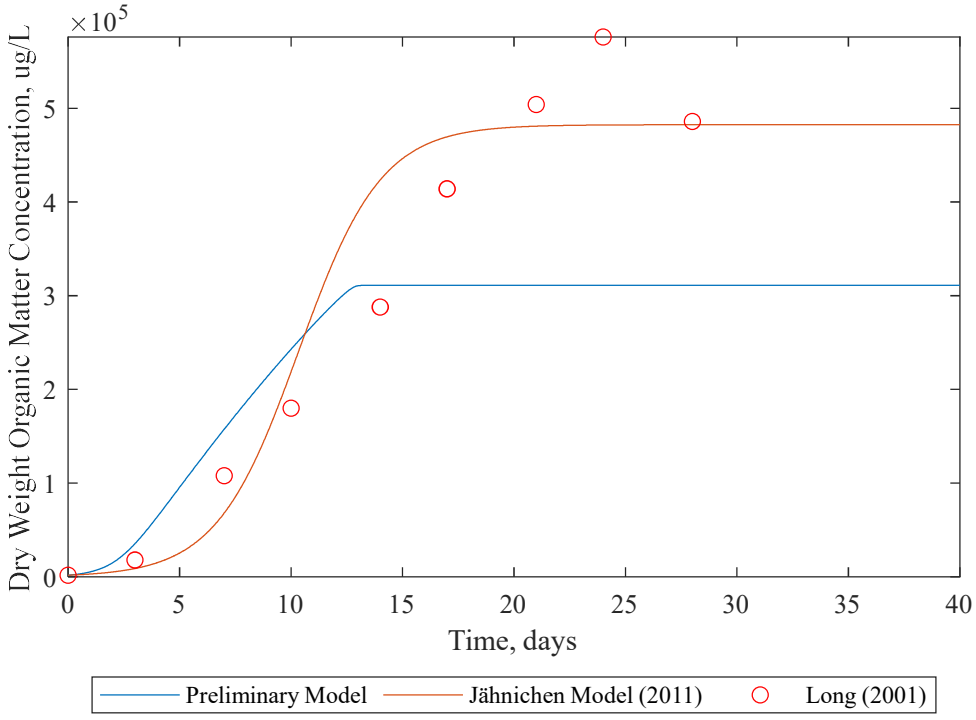

Figure 4-5 Comparison of microcystin producing cyanobacteria (Microcystis aeruginosa) concentration between preliminary model and Jähnichen et al. (2011) with light limitation, a_{Na}=0.002, and H=H_2=0.005. Long (2001) values are estimated from figures. Mean error of -64769 µg L^{-1}.

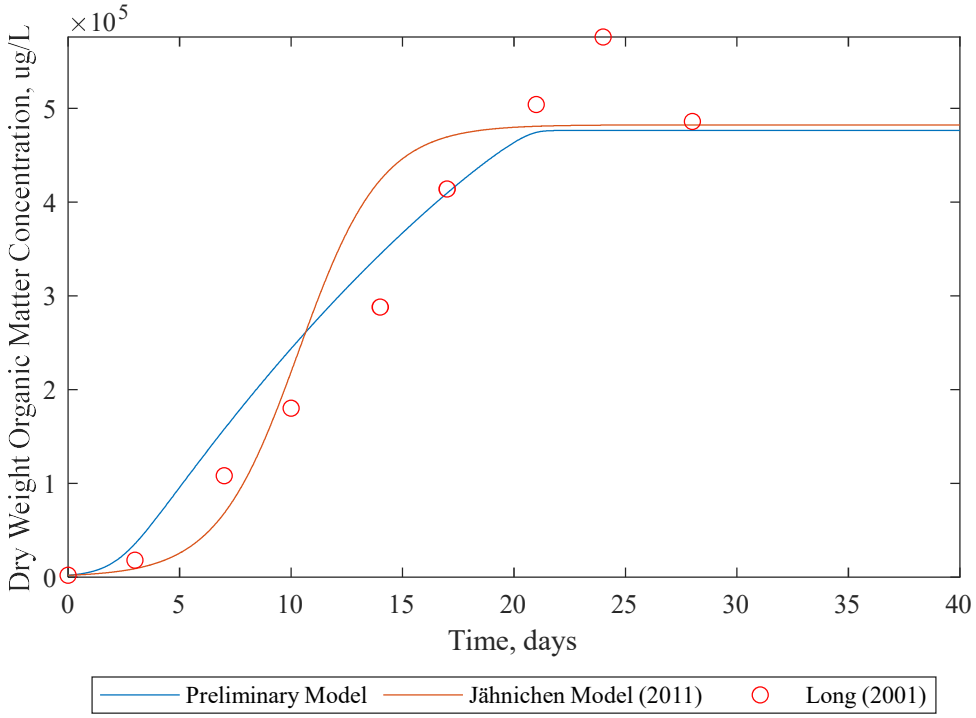

Figure 4-6 Comparison of microcystin producing cyanobacteria (Microcystis aeruginosa) concentration between preliminary model and Jähnichen et al. (2011) with light limitation, a_{Na}=0.0013, and H=H_2=0.005. Long (2001) values are estimated from figures. Mean error of 4863 µg L^{-1}.

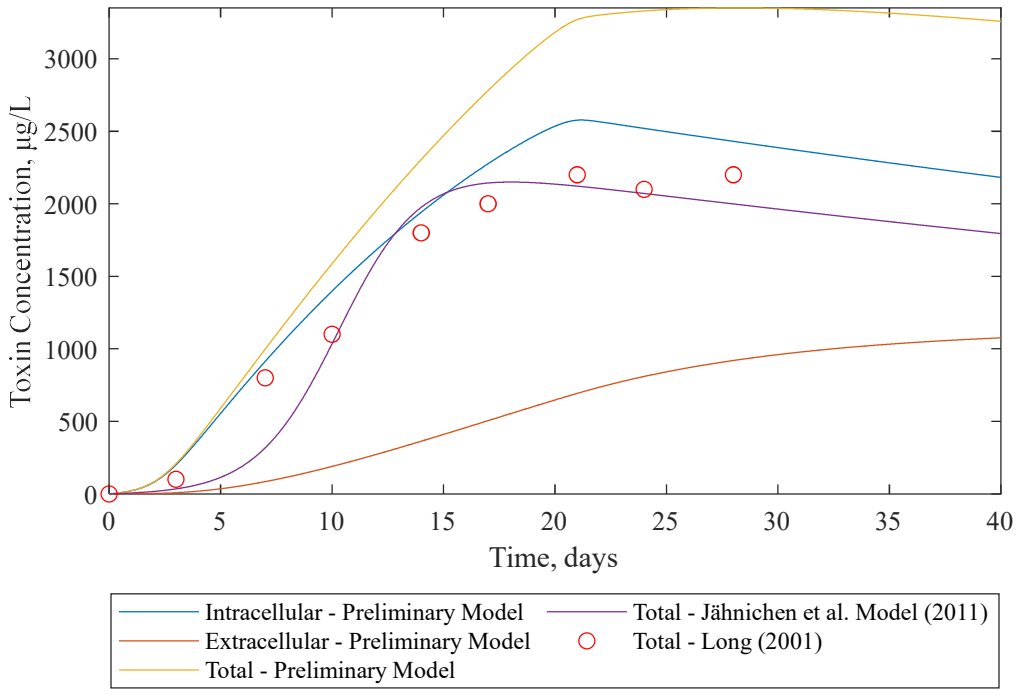

Figure 4-7 Comparison of microcystin concentration between preliminary model and Jähnichen et al. (2011) with light limitation, a_{Na}=0.0013, H=H_2=0.005, and β=0.006. Long (2001) values are estimated from figures. Mean error of 614 µg L^{-1}.

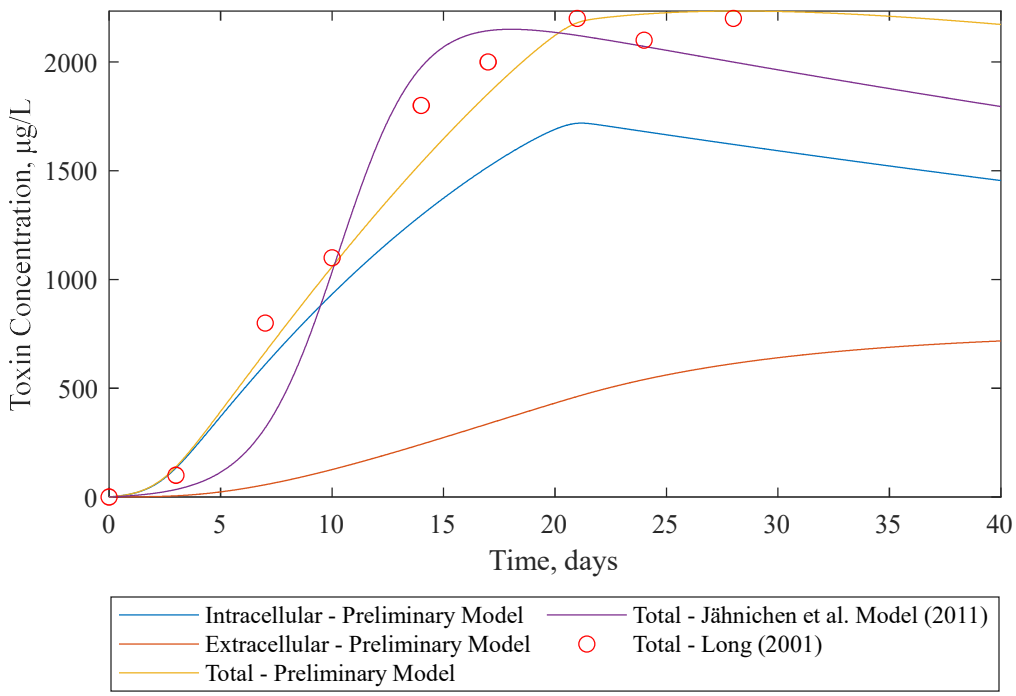

Figure 4-8 Comparison of microcystin concentration between preliminary model and Jähnichen et al. (2011) with light limitation, a_{Na}=0.0013, H=H_2=0.005, and β=0.004. Long (2001) values are estimated from figures. Mean error of -46 µg L^{-1}.

The preliminary model was able to achieve similar results to the model by Jähnichen *et al.* (2011), and the preliminary model was also able to closely match the experimental data. There were some slight variations in results between the two models and between the models and the experimental data. Assumptions were made regarding various parameters such as cell mass, nutrient concentrations, and nutrient constants that will affect the model results. The cyanobacteria concentration most closely matched the experimental data for the simulation with light limitation, a depth of 0.005 meters, and an a_{Na} value of 0.0013. This simulation had the smallest mean error of 4863 µg L^{-1}. The simulations with the smaller depth (0.005 meters as opposed to 0.01 meters) is most likely more representative of the experimental conditions as the cultures were grown in conical culture flasks where light was most likely able to penetrate the top and sides of

the culture reducing the impact of self-shading by the culture. The total toxin concentration most closely matched the experimental data for the simulation with a ratio of toxin to dry weight organic matter of 0.004 as opposed to 0.006. This simulation had a mean error of -46 μg L^{-1}. The simulations were able to capture the increase and then decline of total toxin overtime within a similar time period as the model by Jähnichen *et al.* (2011).

4.3 Comparison of Preliminary Model to Published Data: Cylindrospermopsin

Cylindrospermopsin concentration was modeled using the preliminary model and compared to results from Pierangelini *et al.* (2015) for a batch experiment of *Cylindrospermopsis raciborskii*. The values used for comparison are from the saturating light intensity experiment (labeled as 100 μmol photons m^{-2} s^{-1}). This experiment used Jaworski's medium which has both nitrogen and phosphorus, and the initial concentrations of each nutrient were estimated based on the medium composition as outlined by the Culture Collection of Autotrophic Organisms (Pierangelini *et al.*, 2015; CCALA, 2020). Both nutrients were included in the simulation so that the model could dynamically determine the limiting nutrient over time based on varying parameters since no information was provided on which nutrient was limiting. Table 4-2 shows the inputs that were used in the preliminary model to model cylindrospermopsin production and degradation.

Table 4-2 Input values used in preliminary model for cylindrospermopsin production and degradation.

Cylindrospermopsin			
Variable	**Abbreviation**	**Units**	**Value**
Initial cyanobacteria concentration, dry weight organic matter (OM)	a_0	mg m^{-3}	1200
Initial nutrient concentration (nitrogen)	N_0	mg m^{-3}	15400

Cylindrospermopsin			
Variable	**Abbreviation**	**Units**	**Value**
Initial nutrient concentration (phosphorus)	P_0	mg m^{-3}	6200
Initial intracellular toxin concentration	Cin_0	mg m^{-3}	0
Initial extracellular toxin concentration	Cex_0	mg m^{-3}	0
Ratio of nitrogen to dry weight organic matter (OM)	a_{Na}	mgNutrient $mgOM^{-1}$	0.05-0.075*
Nitrogen half-saturation constant	k_{sN}	mg m^{-3}	14
Ratio of phosphorus to dry weight organic matter (OM)	a_{Pa}	mgNutrient $mgOM^{-1}$	0.001-0.005*
Phosphorus half-saturation constant	k_{sP}	mg m^{-3}	3
Maximum growth rate at 20 °C	$k_{g,20}$	day^{-1}	0.34-0.90*
Temperature correction coefficient	θ	unitless	1.066
Temperature	T	°C	25
Light extinction due to factors other than phytoplankton	k'_e	m^{-1}	0
Bottom layer elevation	H_2	m	0.005
Top layer elevation	H_1	m	0
Layer depth	H	m	0.005
Optimal light level for growth	I_s	µmol photons m^{-2} s^{-1}	100
Maximum light level	I_{max}	µmol photons m^{-2} s^{-1}	100
Ratio of intracellular toxin to dry weight organic matter (OM)	β	mgToxin $mgOM^{-1}$	0.0007-0.001*
Rate of cell respiration	k_r	day^{-1}	0.02
Rate of cell excretion	k_e	day^{-1}	0.02
Rate of cell death	k_d	day^{-1}	0.01
Rate of intracellular toxin release from cell due to leakage	k_{leak}	day^{-1}	0
Rate of intracellular toxin decay inside the cell	k_{decay_intra}	day^{-1}	0.005
Rate of intracellular toxin release from cell due to active release	k_{active}	day^{-1}	0.01
Rate of extracellular toxin decay during the day	$k_{decay\_extra\_day}$	day^{-1}	0.03
Rate of extracellular toxin decay during the night	$k_{decay\_extra\_night}$	day^{-1}	0.012

*Range of values modeled

The initial cyanobacteria concentration (a_0) was obtained from the saturating light intensity experiment of Pierangelini *et al.* (2015) by converting cells per liter to dry weight organic matter using a value of 20E-12 g $cell^{-1}$ based on the values reported by

Long *et al* (2001) for *Microcystis aeruginosa* at similar growth rates to the one used in this model. The initial cell concentration was estimated from a figure in Pierangelini *et al.* (2015) to be 6E4 cells mL^{-1}. The initial nutrient concentrations were estimated to be 0.2 mM for phosphorus and 1.1 mM for nitrogen from the Jaworski's medium used in the experiment (Pierangelini *et al.*, 2015; CCALA, 2020). The initial nitrogen and phosphorus concentrations (N_0, P_0) were estimated from the molar concentrations. The initial intracellular and extracellular concentrations (Cin_0, Cex_0) were assumed to be zero. The limiting nutrient parameters (a_{Na}, k_{sN}, a_{Pa}, k_{sP}) were estimated from the CE-QUAL-W2 manual (Wells, 2020a). A minimum value of 0.05 and a maximum value of 0.075 for the ratio of nitrogen to dry weight organic matter (a_{Na}), and a minimum value of 0.001 and a maximum value of 0.005 for the ratio of phosphorus to dry weight organic matter (a_{Pa}) were chosen to compare the sensitivity of the model to these parameters and to identify the limiting nutrient.

A maximum growth rate at 20 degrees Celsius ($k_{g,20}$) was not provided for this species of cyanobacteria, so two growth rates were chosen to compare to the model results. One growth rate of 0.34 day^{-1} was back-calculated from the maximum growth of 0.47 day^{-1} observed at 25 degrees Celsius in Pierangelini *et al.* (2015). An additional growth rate of 0.9 day^{-1} was chosen since the maximum growth of 0.47 day^{-1} observed might not be the actual maximum growth possible at that temperature due to growth limitations of the experiment. The temperature of the model (T) was obtained from the experiments of Pierangelini *et al.* (2015). The temperature correction coefficient (θ) value was obtained from Chapra (2008). It was assumed that there was no light extinction due to factors other than the growth of the cyanobacteria ($k'_e = 0$). A culture

volume and flask size were not provided, but it was assumed a similar culture size to the experiments done by Long (2001) was used for the experiment of Pierangelini *et al.* The layer depth and bottom layer elevation (H, H_2) were assumed to be 0.005 meters. The optimal light level for growth (I_s) of *Cylindrospermopsis raciborskii* was estimated from experiments done previously by Pierangelini *et al.* (2014). The maximum light level was obtained from the experiments of Pierangelini *et al.* (2015), and light was applied to the cultures in a 12 hour/12 hour light-dark cycle. The model sensitivity to light limitation was also tested by setting the light attenuation factor to 1.0 (no light limitation) to compare to the results with light limitation.

The ratio of intracellular toxin to dry weight organic matter (β) was estimated from values provided by Preußel *et al.* (2006) and Cirés *et al.* (2011). A minimum value of 0.0007 and a maximum value of 0.001 for the ratio of toxin to dry weight organic matter were chosen to compare the sensitivity of the model to this parameter. The rates of cell respiration (k_r), cell excretion (k_e), and cell death (k_d) were assumed based on values provided in the CE-QUAL-W2 manual. The rate of cell death was assumed to be small since there would be no grazing losses. The rate of toxin leakage from cells (k_{leak}) was assumed to be zero but the rate of active release of toxins from cells (k_{active}) was provided a value based on the results of the study done by Preußel *et al.* (2014) that indicated cylindrospermopsin is actively released from cells. The rate of intracellular toxin decay inside the cell (k_{decay_intra}) was provided a small value based on the results of Jähnichen *et al.* (2011) for *Microcystis* species. The rate of extracellular toxin decay during the day ($k_{decay\_extra\_day}$) was estimated from the decay rate due to light observed by

León *et al.* (2019). The rate of extracellular decay during the night ($k_{decay\_extra\_night}$) was estimated from the decay rates observed by Chiswell *et al.* (1999).

4.3.1 Results

The results obtained from the preliminary model were compared to experimental data from Pierangelini *et al.* (2015) as estimated from figures. Figure 4-9 through Figure 4-13 show the change in concentration over time of cyanobacteria (in dry weight organic matter) for both the model and experimental data and the limiting nutrients as predicted by the preliminary model. The results are shown with and without light limitation, a_{Na} of 0.05 or 0.075, a_{Pa} of 0.001 or 0.005, and $k_{g,20}$ of 0.34 or 0.90 as indicated on each figure. The mean error between the preliminary model and the experimental data is shown on each figure.

Figure 4-14 and Figure 4-15 show the change in concentration over time of intracellular and extracellular toxin for the preliminary model and the experimental data from Pierangelini *et al.* (2015). The toxin results are shown with light limitation, a_{Pa} of 0.005, a_{Na} of 0.075, $k_{g,20}$ of 0.90, and with a ratio of toxin to dry weight organic matter of 0.0007 or 0.001 as indicated on each figure. The mean errors between the preliminary model intracellular and extracellular toxin concentrations and the experimental data are shown on each figure.

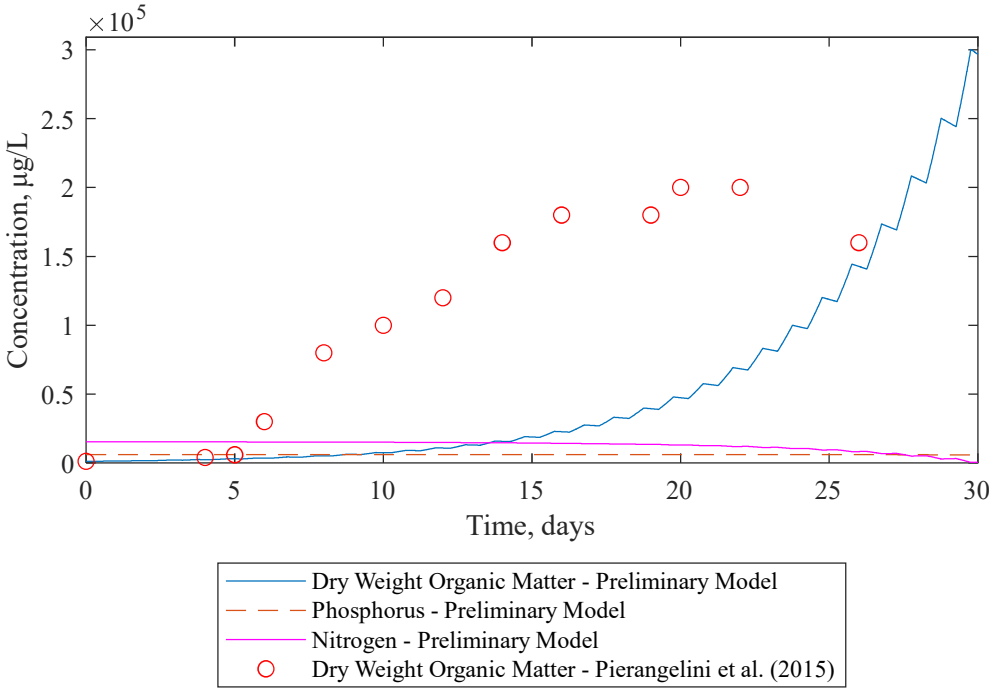

Figure 4-9 Comparison of cylindrospermopsin producing cyanobacteria (Cylindrospermopsis raciborskii) concentration between preliminary model and Pierangelini et al. (2015) without light limitation, a_{Na}=0.05, a_{Pa}=0.001, and $k_{g,20}$=0.34. Pierangelini et al. (2015) values are estimated from figures. Mean error of -80827 µg L^{-1}.

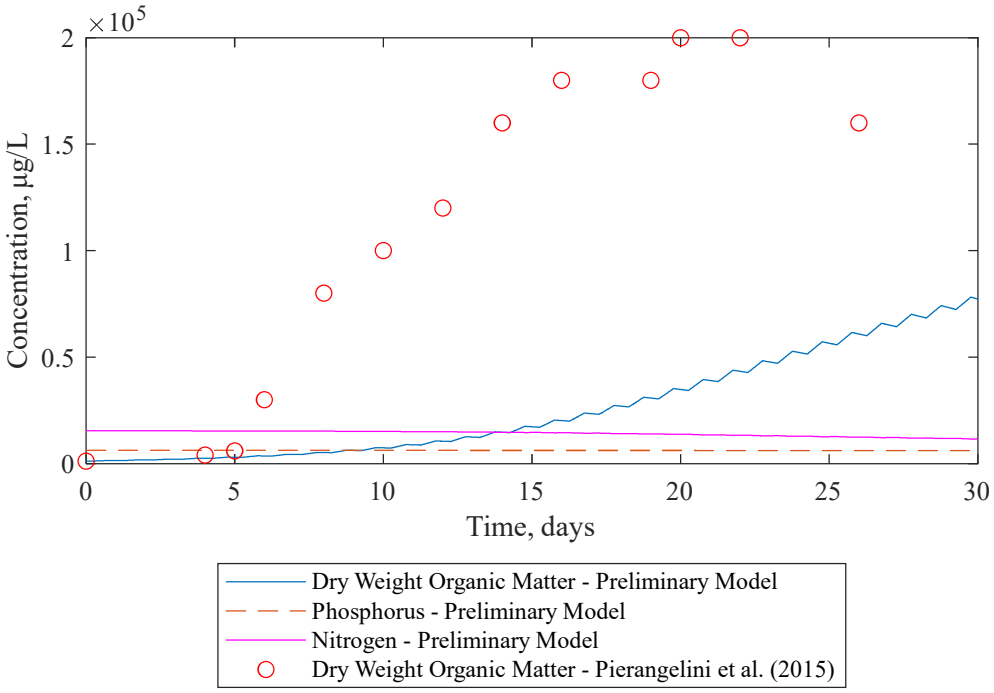

Figure 4-10 Comparison of cylindrospermopsin producing cyanobacteria (Cylindrospermopsis raciborskii) concentration between preliminary model and Pierangelini et al. (2015) with light limitation, a_{Na}=0.05, a_{Pa}=0.001, and $k_{g,20}$=0.34. Pierangelini et al. (2015) values are estimated from figures. Mean error of -91012 µg L^{-1}.

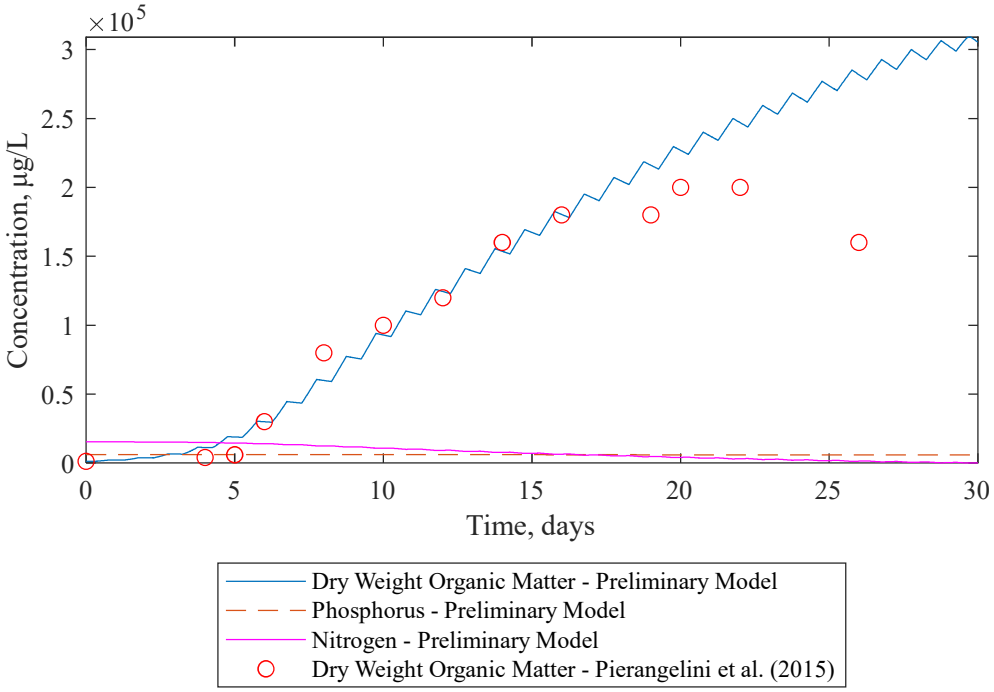

Figure 4-11 Comparison of cylindrospermopsin producing cyanobacteria (Cylindrospermopsis raciborskii) concentration between preliminary model and Pierangelini et al. (2015) with light limitation, a_{Na}=0.05, a_{Pa}=0.001, and $k_{g,20}$=0.90. Pierangelini et al. (2015) values are estimated from figures. Mean error of 17182 µg L^{-1}.

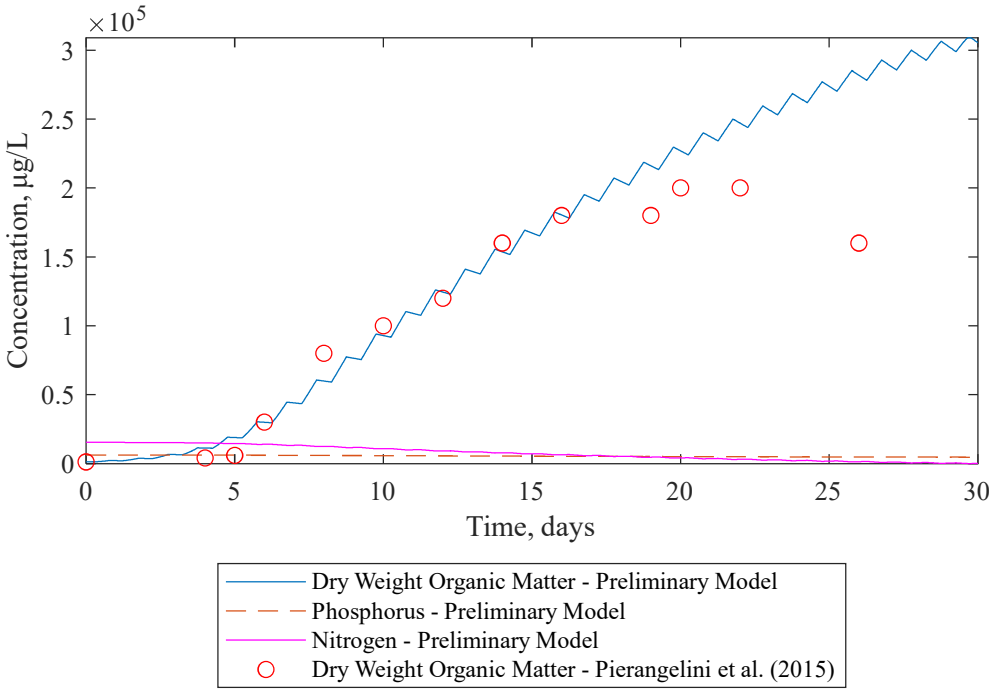

Figure 4-12 Comparison of cylindrospermopsin producing cyanobacteria (Cylindrospermopsis raciborskii) concentration between preliminary model and Pierangelini et al. (2015) with light limitation, a_{Na}=0.05, a_{Pa}=0.005, and $k_{g,20}$=0.90. Pierangelini et al. (2015) values are estimated from figures. Mean error of 17182 µg L^{-1}.

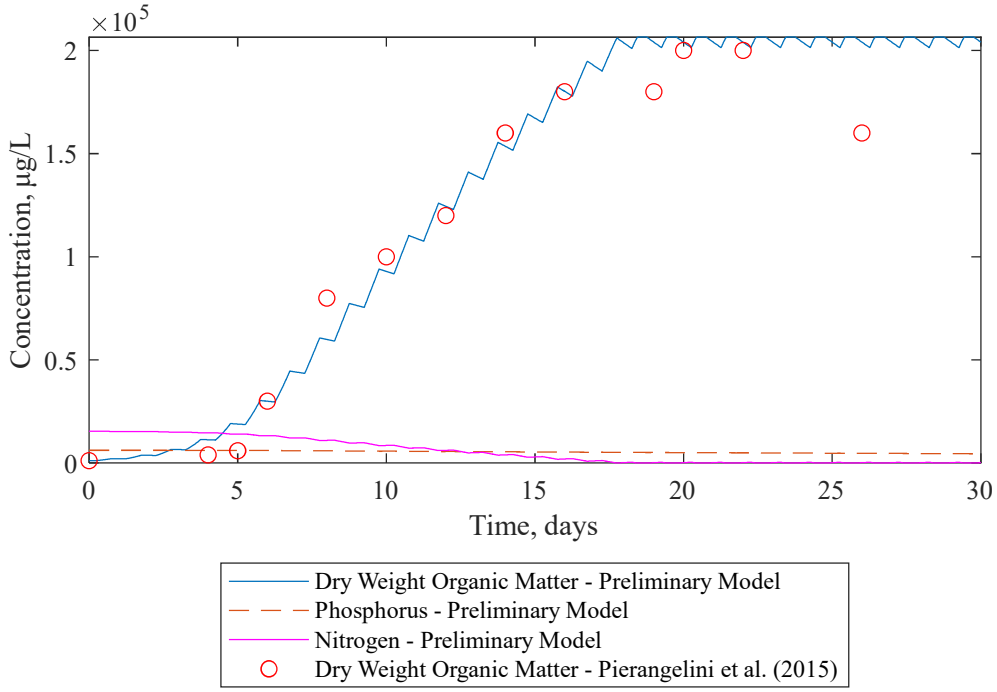

Figure 4-13 Comparison of cylindrospermopsin producing cyanobacteria (Cylindrospermopsis raciborskii) concentration between preliminary model and Pierangelini et al. (2015) with light limitation, a_{Na}=0.075, a_{Pa}=0.005, and $k_{g,20}$=0.90. Pierangelini et al. (2015) values are estimated from figures. Mean error of 5174 µg L^{-1}.

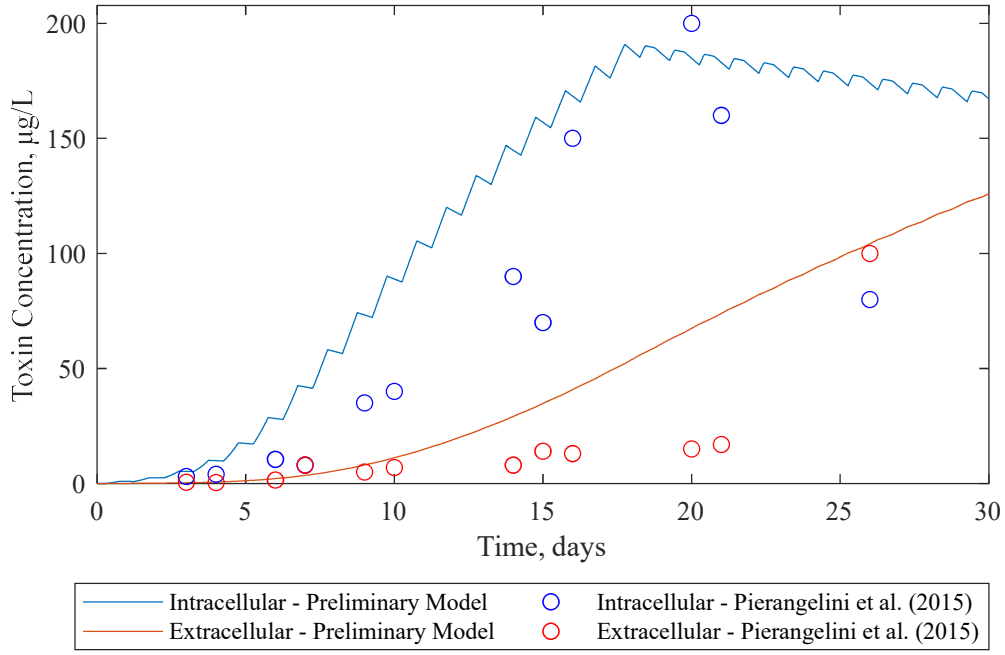

Figure 4-14 Comparison of cylindrospermopsin concentration between preliminary model and Pierangelini et al. (2015) with light limitation, a_{Na}=0.075, a_{Pa}=0.005, $k_{g,20}$=0.90, and β=0.001. Pierangelini et al. (2015) values are estimated from figures. Mean error of 34 µg L^{-1} for intracellular and 16 µg L^{-1} for extracellular.

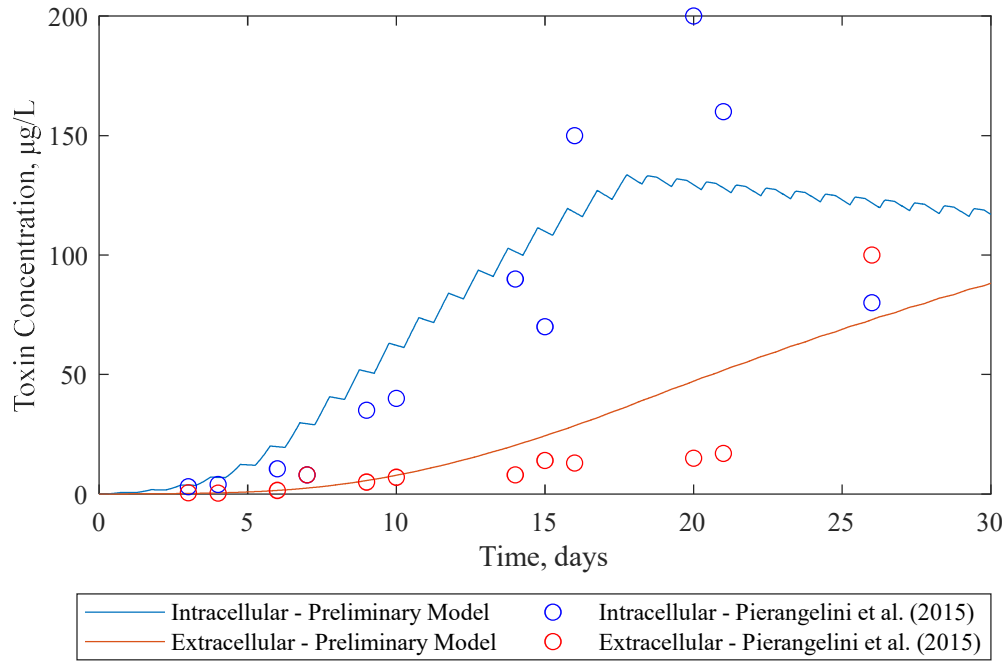

Figure 4-15 Comparison of cylindrospermopsin concentration between preliminary model and Pierangelini et al. (2015) with light limitation, a_{Na}=0.075, a_{Pa}=0.005, $k_{g,20}$=0.90, and β=0.0007. Pierangelini et al. (2015) values are estimated from figures. Mean error of 2.6 µg L^{-1} for intracellular and 6.2 µg L^{-1} for extracellular.

The preliminary model was able to closely match the experimental data. There were slight variations between the model and the experimental data. The initial concentration of cyanobacteria used in the preliminary model and the experimental values of cyanobacteria concentration were converted to mass concentrations from cellular concentrations by using an estimated value of cell mass for a different cyanobacteria species than the one in the experiment. This may have added some error to the model. The initial nutrient concentration used in the model was estimated based on one example of the medium, but this may not be the actual composition of the medium used which could contribute to some of the variation as well. The assumed depth could also be a source of error in the model. However, all concentrations were within the same

order of magnitude for all the simulations. The variations in nutrient parameters tested showed that nitrogen was the limiting nutrient in the selected simulations.

The cyanobacteria concentration most closely matched the experimental data for the simulation with light limitation, a_{Na}=0.075, a_{Pa}=0.005, and $k_{g,20}$=0.90. This simulation had the smallest mean error of 5174 μg L^{-1}. A maximum growth rate at 20 Celsius of 0.90 day^{-1} more closely matched the experimental data than the observed maximum growth rate of 0.47 day^{-1} at 25 degrees Celsius. It may be that the observed growth rate of 0.47 day^{-1} was the average growth over both the light and dark conditions. Since there is no growth in the absence of light, a maximum growth of approximately 1.0 day^{-1} would be observed only during the day if 0.47 day^{-1} is the average over the entire period. The toxin concentrations most closely matched the experimental data for the simulation with the ratio of toxin to dry weight equal to 0.0007. This simulation had a mean error of 2.6 μg L^{-1} for the intracellular toxin and 6.2 μg L^{-1} for the extracellular toxin. Both the model and the experimental data showed a peak intracellular toxin concentration after which the intracellular concentration decreased over time. The model and the data also both showed a continuous increase in extracellular toxin concentration over time for the time period simulated.

Chapter 5: Integration into CE-QUAL-W2

5.1 Overview

CE-QUAL-W2 is a two-dimensional (longitudinal and vertical), laterally averaged, hydrodynamic and water quality model. The model uses meteorological, bathymetry, flow, temperature, and water quality input data to model state variables (such as temperature, nutrients, and algae) at longitudinal segments and vertical layers in the waterbody. The model is divided into longitudinal segments that typically range between 100-1000 meters and vertical layer depths typically range between 0.5 and 2 meters. The model uses input parameters (kinetic rates and coefficients) that are adjusted using the model control file.

The intracellular and extracellular toxin equations presented previously have been modified to account for variability in cyanobacteria species within a model algal group since typically only one group is chosen to model all the cyanobacteria present. The concentration of cyanobacteria (a) has been multiplied by a fraction (*CTP*) of how much of that concentration is predicted to produce a specific toxin. For example, if half of the cyanobacteria concentration in a reservoir consists of predicted microcystin producers then *CTP_MC* would be set to 0.5. The *CTP* value is also used to determine whether an algal group is a toxin producer. If an algal group is not a toxin producer, then all the *CTP* values will be set to zero. For a given algal group, the total of all *CTP* values can be greater than one since some algal species may produce more than one toxin. It is up to the user to determine what species are most often present in the waterbody and which toxins each species is likely to produce. In addition, the toxin equations have been simplified for initial testing of the equations in CE-QUAL-W2 and the algal kinetic rates

have been adjusted to match the symbology used in the CE-QUAL-W2 user manual as follows:

$$C_{intra} = \sum_{i=1}^{n\ algal\ groups} (CTP) * \Phi_a * \beta \qquad \textbf{(5-1)}$$

$$\frac{dC_{extra}}{dt} = K_{am} * \Phi_a * \beta * (CTP) + k_{release} * C_{intra} - k_{decay} * C_{extra} \qquad \textbf{(5-2)}$$

The intracellular toxin is calculated based only on the concentration of algae present in a model cell and the fraction of algae producing that toxin. The intracellular concentration is summed for all the algal groups that produce that toxin. There are no decay or other rates associated with the intracellular toxin concentration for the initial integration and testing of the model in the CE-QUAL-W2 code. The extracellular rate equation is only a function of the death rate of algae, the release rate of intracellular toxin and the extracellular decay. Only one value is allowed for the release rate and decay rate for each toxin being modeled.

The simplified intracellular and extracellular toxin mass balances were incorporated into the CE-QUAL-W2 model and corresponding updates were made to the control file to adjust toxin parameters. Table 5-1 shows new categories that were added to the control file for toxin production, where the yellow cells indicate locations where inputs are adjusted.

Table 5-1 Cyanotoxin Control File Updates.

Cyanotoxins Control File	ON/ OFF	DEBUG
TOXINCONTROL: ATOX (turn ON/OFF all algae toxins), ATOX_DEBUG (turn on debugging output)		
MICROCYSTIN	ALG1	ALG2
CTP_MC, fraction of algae concentration producing MC		
CTB_MC, ratio of intracellular toxin to dry weight biomass (mg-toxin mg-DW^{-1})		
CTR_MC, release rate day^{-1}		
CTD_MC, extracellular decay day^{-1}		
CYLINDROSPERMOPSIN	ALG1	ALG2
CTP_CYN, fraction of algae concentration producing CYN		
CTB_CYN, ratio of intracellular toxin to dry weight biomass (mg-toxin mg-DW^{-1})		
CTR_CYN, release rate day^{-1}		
CTD_CYN, extracellular decay day^{-1}		
ANATOXIN-A	ALG1	ALG2
CTP_ATX, fraction of algae concentration producing ATX		
CTB_ATX, ratio of intracellular toxin to dry weight biomass (mg-toxin mg-DW^{-1})		
CTR_ATX, release rate day^{-1}		
CTD_ATX, extracellular decay day^{-1}		
SAXITOXIN	ALG1	ALG2
CTP_STX, fraction of algae concentration producing STX		
CTB_STX, ratio of intracellular toxin to dry weight biomass (mg-toxin mg-DW^{-1})		
CTR_STX, release rate day^{-1}		
CTD_STX, extracellular decay day^{-1}		

Each of the four toxins (microcystin, cylindrospermopsin, anatoxin-a, and saxitoxin) have been added as state variables to the CE-QUAL-W2 code with the option to turn any of them “on” or “off” depending on the cyanobacteria species that grow in the waterbody of interest. The control file updates include a separate section for each of the four toxins for the user to select rates and ratios that best represent production and decay of that toxin. Table 5-2 lists suggested ranges of values to use for each parameter based on literature values and model tests.

Table 5-2 Model parameter ranges to use in CE-QUAL-W2 toxin models.

Parameter	MC	CYN	ATX-A	STX
CTP, fraction of algae concentration producing toxin	Waterbody dependent, determined by species present			
CTB, ratio of intracellular toxin to dry weight biomass (mg-toxin mg-DW^{-1})	0.0005-0.024	0.0005-0.007	0.001-0.01	0.001-0.004
CTR, release rate day^{-1}	Approx. equal to 0-1 times excretion rate	Approx. equal to 1-2 times excretion rate	Approx. equal to 0-1 times excretion rate	Approx. equal to 0-1 times excretion rate
CTD, extracellular decay day^{-1}	0.05-0.2	0.01-0.06	0.05-0.2	0.01-0.07

DW, dry weight

5.2 Comparison of CE-QUAL-W2 Code Updates to Experimental Data

The simplified equations that were incorporated into CE-QUAL-W2 (Equations (5-1) and (5-2)) were tested on the same laboratory data as described in Chapter 4 to verify functionality of the simplified models. The same model parameters for cyanobacteria growth and initial conditions that were used to produce Figure 4-8 and Figure 4-15 were used for the microcystin and cylindrospermopsin model tests, respectively. The values of the model parameters in Equations (5-1) and (5-2) that were used in the tests are summarized in Table 5-3.

Table 5-3 Model parameters used for testing simplified CE-QUAL-W2 toxin equations on experimental data.

Parameter	MC	CYN
CTP, fraction of algae concentration producing toxin	1.0	1.0
CTB, ratio of intracellular toxin to dry weight biomass (mg-toxin mg-DW^{-1})	0.004	0.0007
CTR, release rate day^{-1}	0.03	0.03
CTD, extracellular decay day^{-1}	0.1	0.03

DW, dry weight

The microcystin release rate of 0.03 day^{-1} was chosen to match the excretion rate that was used in the original model test. The cylindrospermopsin release rate of 0.03 day^{-1} was chosen to equal the sum of the excretion rate and active release rate that were used in the original model test. Figure 5-1 and Figure 5-2 show the results from the updated

CE-QUAL-W2 model equations as compared to field data from the laboratory experiments.

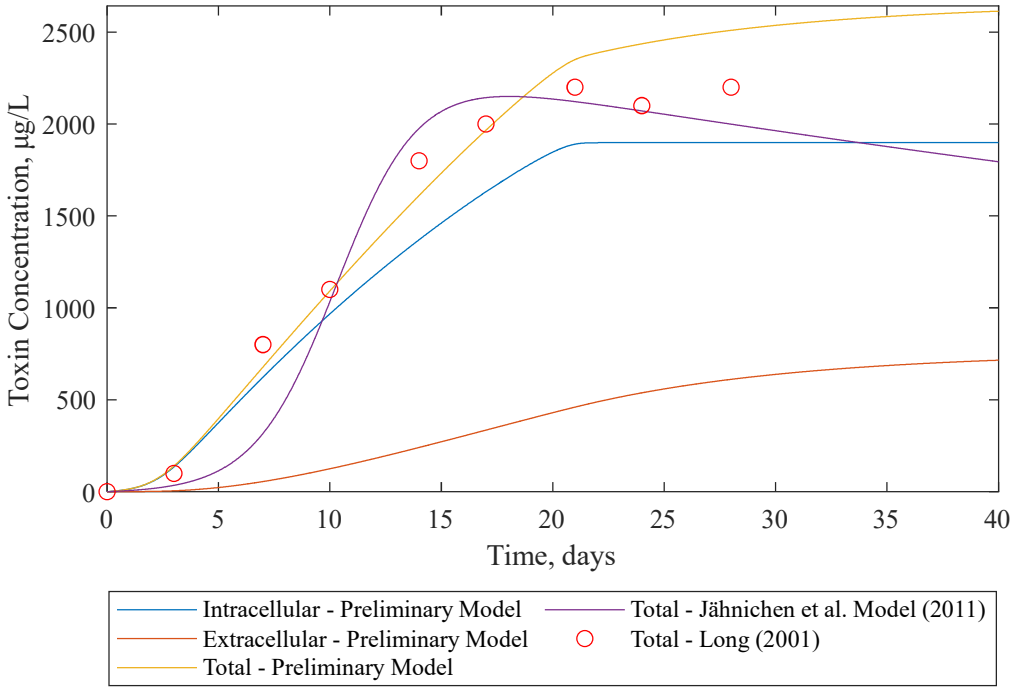

Figure 5-1 Comparison of microcystin concentration between CE-QUAL-W2 model equations and Jähnichen et al. (2011). Long (2001) values are estimated from figures. Mean error of 54 µg L^{-1} between total toxin concentrations of the preliminary model and experimental data from Long (2001).

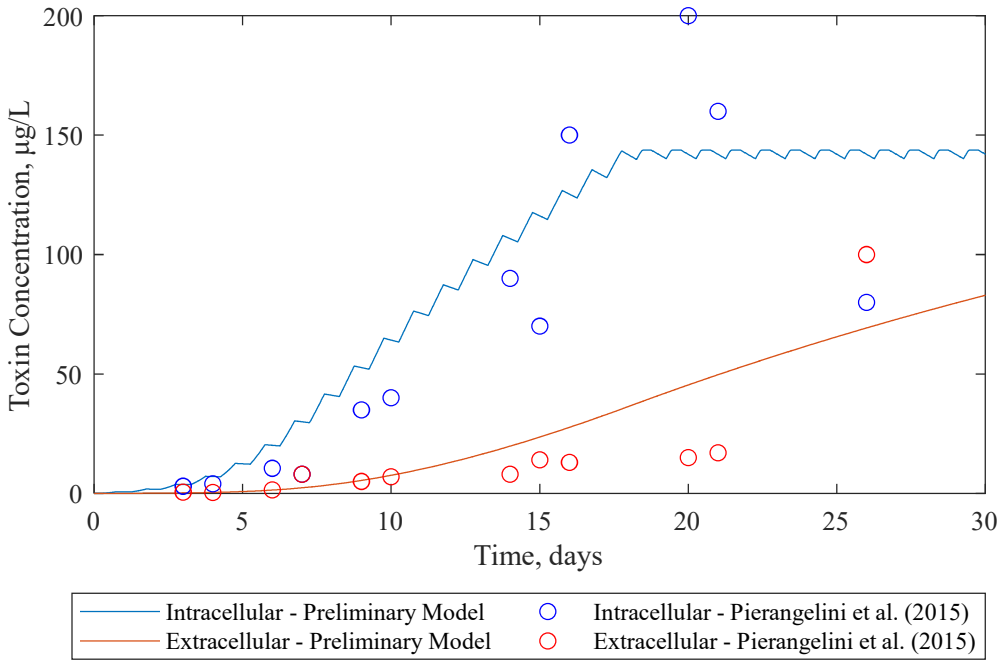

Figure 5-2 Comparison of cylindrospermopsin concentration between CE-QUAL-W2 model equations and Pierangelini et al. (2015). Pierangelini et al. (2015) values are estimated from figures. Mean error of 8.4 µg L^{-1} for intracellular and 5.3 µg L^{-1} for extracellular.

The simplified equations incorporated into CE-QUAL-W2 were able to produce similar results as the original toxin models and were able to predict similar toxin concentrations as the laboratory data.

5.3 CE-QUAL-W2 Code Updates

The preliminary models and control file updates described previously were incorporated into the CE-QUAL-W2 code. The code updates include two loops, one each for the intracellular toxins and extracellular toxins. Each loop calculates the concentration of each toxin that is a function of the algal kinetics (growth, excretion, respiration, and mortality) as well as any release or decay of the toxin. The loop goes through each algal group that is producing toxins and then sums the concentrations together from each algal group for a specific toxin. The total intracellular or extracellular concentration will be the sum of the toxin produced by all the algal groups. In practice,

there will likely only be one algal group producing toxins in a CE-QUAL-W2 model, but this code update allows for multiple algal groups to produce toxins. The preliminary models included the option to have a night decay rate and a day decay rate for the extracellular toxin, but for initial testing of the model in CE-QUAL-W2, only one value for extracellular decay was included for simplicity. Refer to Appendix A: CE-QUAL-W2 Code Updates for a detailed description of the updates that were added to the fortran90 code of the CE-QUAL-W2 W2 Modules subroutine and Water Quality subroutine. New code additions from this study are highlighted.

Chapter 6: Testing of CE-QUAL-W2

The cyanotoxin model was tested on Henry Hagg Lake using measured toxin data in the lake for 2019 to compare to the model results.

6.1 Henry Hagg Lake Model 2020 Update

Henry Hagg Lake is located on Scoggins Creek, Oregon (approximately 25 miles to the west of Portland, Oregon) and impounded by Scoggins Dam. The lake was built as part of the United States Bureau of Reclamation Tualatin Project in 1978 (USBR, 2021). The lake is used for irrigation, recreation, flood control, and water supply to the Tualatin River. A model for Henry Hagg Lake had been previously developed in CE-QUAL-W2 that simulated water quality parameters from January 1, 2013 (Julian day 1) through December 2015 with temperature simulation through the end of 2019. This model was updated through the end of 2020 (Julian Day 2922) with all water quality and temperature parameters. The following input files were updated to include data through 2020: meteorological, flow, temperature, and concentration. Figure 6-1 shows an aerial map of Henry Hagg Lake. Figure 6-2 and Figure 6-3 show the model grid and tributaries of the lake that had previously been developed for the original model.

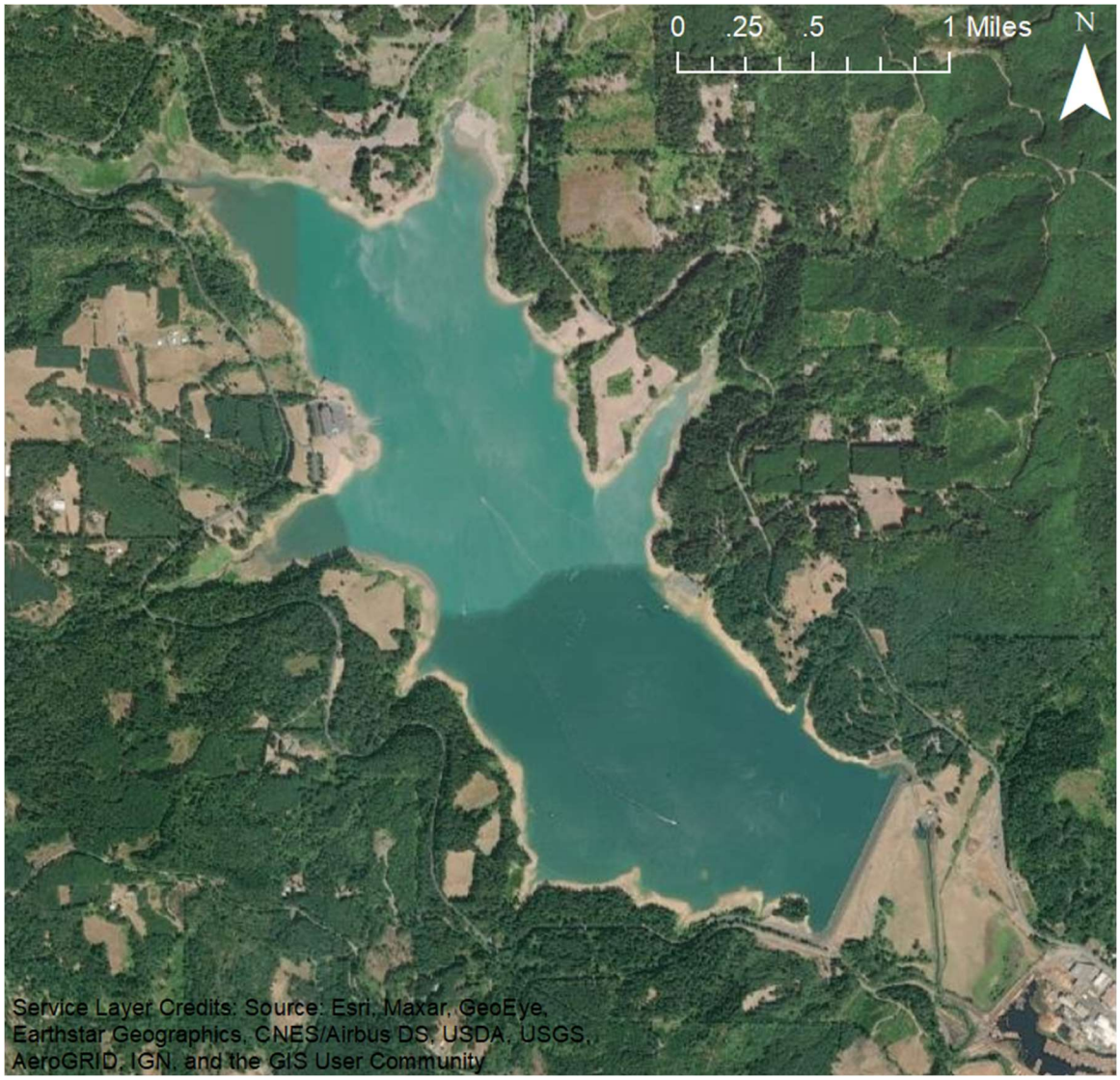

Figure 6-1 Aerial view of Henry Hagg Lake.

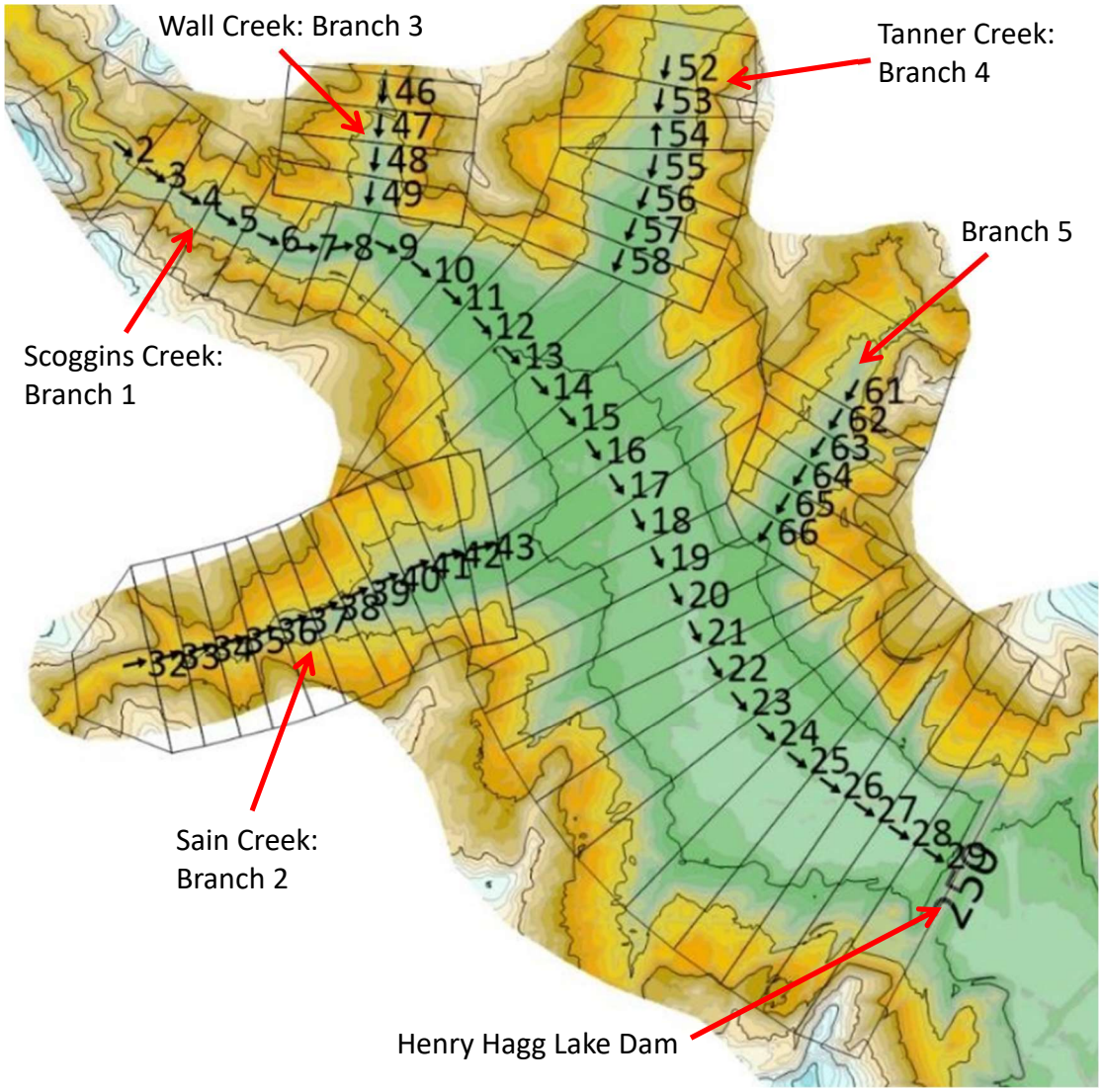

Figure 6-2 Model grid and tributaries of Henry Hagg Lake, reproduced after Wells and Berger (2019).

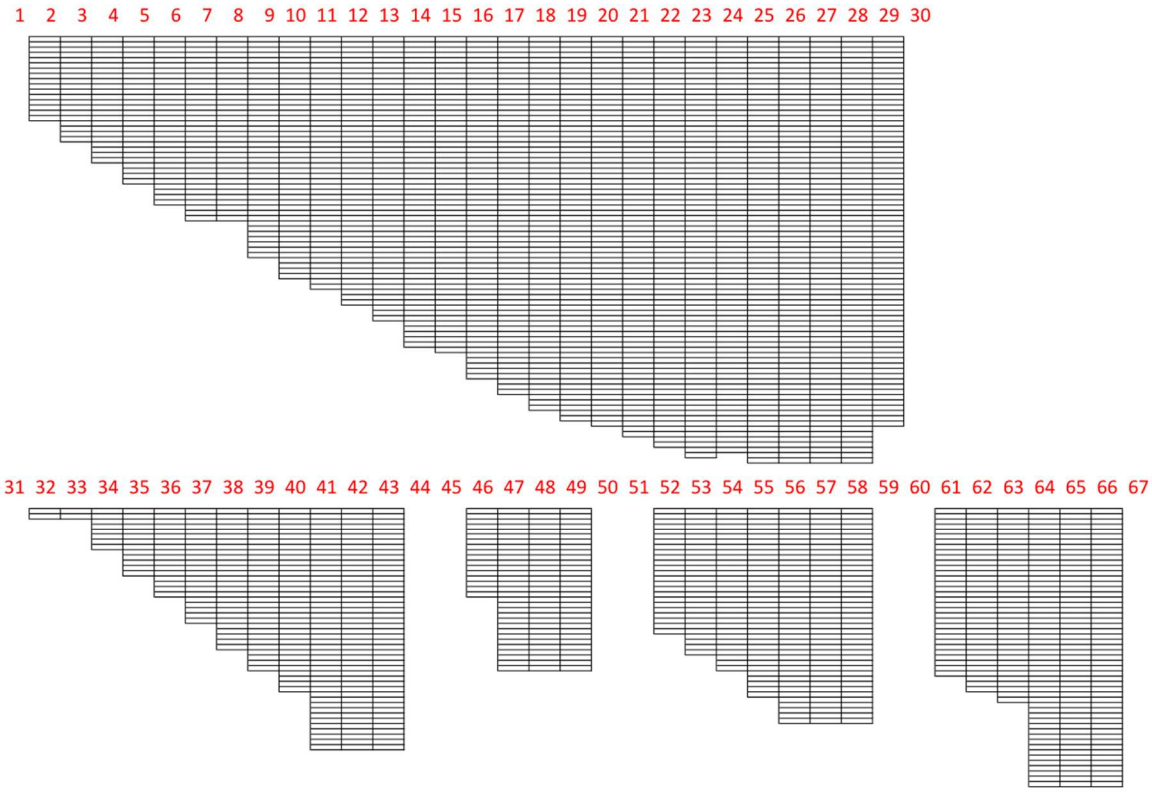

Figure 6-3 Profile schematic of Henry Hagg Lake model segments (horizontal) and vertical layers. Each layer is 0.61 m (2 ft) deep and segment lengths vary between 150-200 m long.

6.1.1 Meteorological Inputs

Meteorological inputs consist of air temperature, dew point temperature, wind velocity, wind direction, cloud coverage, and solar radiation. The United States Bureau of Reclamation Hydromet station SCOO (Scoggins Creek below Henry Hagg Lake) was used to acquire instantaneous air temperature, the Reclamation Hydromet station SCO (Scoggins Dam and Henry Hagg Lake) was used to acquire wind speed and wind direction, and the Reclamation Agrimet station FOGO (Forest Grove) was used to acquire dew point and solar radiation data. Cloud cover inputs were calculated using measured and theoretical solar radiation. Theoretical clear sky solar radiation was calculated based on latitude and longitude using code from CE-QUAL-W2 (Wells, 2020b). Cloud cover was then calculated using Equation **(**6-1**)**:

$$\phi_{s\_data} = \phi_{s\_clearsky}(1 - 0.65C^2) \quad \textbf{(6-1)}$$

where ϕ_{s_data} is the measured short wave solar radiation, $\phi_{s\_clearsky}$ is the theoretical clear sky short wave solar radiation, and C is the fraction of cloud cover between 0 and 1 (Wunderlich, 1972; Wells, 2020a). During the water quality calibration process, it was discovered that the minimum wind velocity values should be increased to better match the field data. The updated model through 2020 used a minimum wind velocity of 0.5 m s^{-1} as a wind velocity of zero is very uncommon and likely the result of equipment sensitivity. Time series graphs of the six meteorological inputs are shown in Figure 6-4.

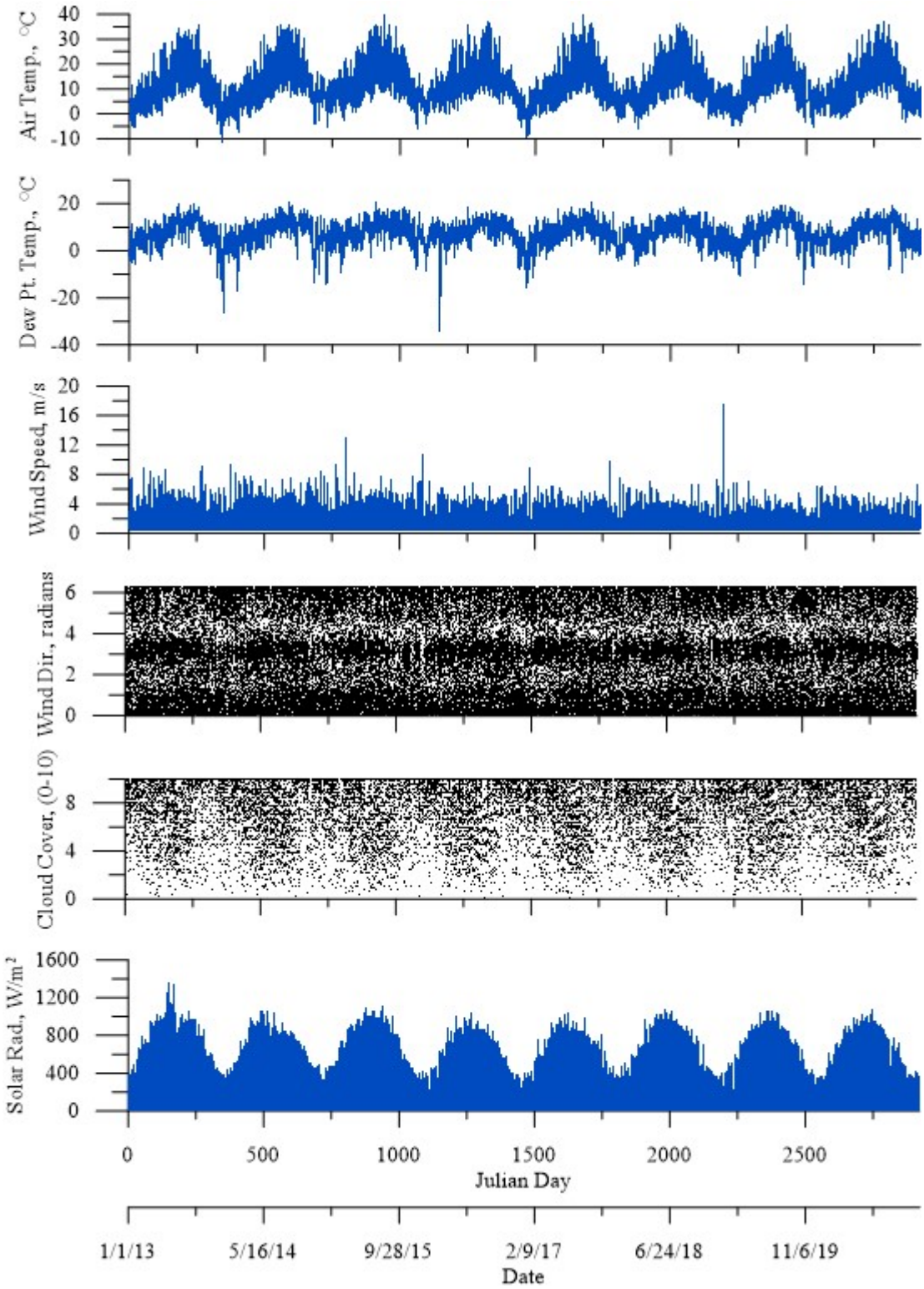

Figure 6-4 Time series graphs of meteorological inputs: air temperature, dew point temperature, wind velocity, wind direction, cloud coverage, and solar radiation.

6.1.2 Flow Inputs

There are five tributaries that enter Henry Hagg Lake as shown in Figure 6-2, but only three of these tributaries have recorded flow measurements: Scoggins Creek (Branch 1), Sain Creek (Branch 2), and Tanner Creek (Branch 4). Flows for Branch 3 and Branch 5 were set to zero since no field data was available and these appear to be minor tributaries. There is also a distributed tributary applied to Branch 1 to account for any sources and sinks of flow not accounted for in the model with the other branches. The water balance tool provided with the CE-QUAL-W2 model was used to compare the measured water level with the simulated water level to calculate the required distributed tributary flow to balance the measured inflows and outflows from the lake.

Water level data was obtained from the Reclamation Hydromet station SCO station. Outflow values were obtained from the Reclamation Hydromet station SCOO. The model simulates release from the dam using a gate with a 350 cubic feet per second limit. Any flow above this limit is sent to the spillway. Flow data for Scoggins Creek was obtained from Reclamation Hydromet station SCLO (Scoggins Creek above Henry Hagg Lake). Flow data for Sain Creek was obtained from the Oregon Water Resource Department (OWRD) station 14202920 (Sain Creek near Gaston). Flow data for Tanner Creek was obtained from the Tualatin Valley Irrigation District (TVID) manual recordings with available data through 2019 and a regression with Sain Creek was used to estimate 2020 flow values. A time series graph of the tributary branch inflows is shown in Figure 6-5. A time series graph of the distributed tributary inflows and dam outflows is shown in Figure 6-6.

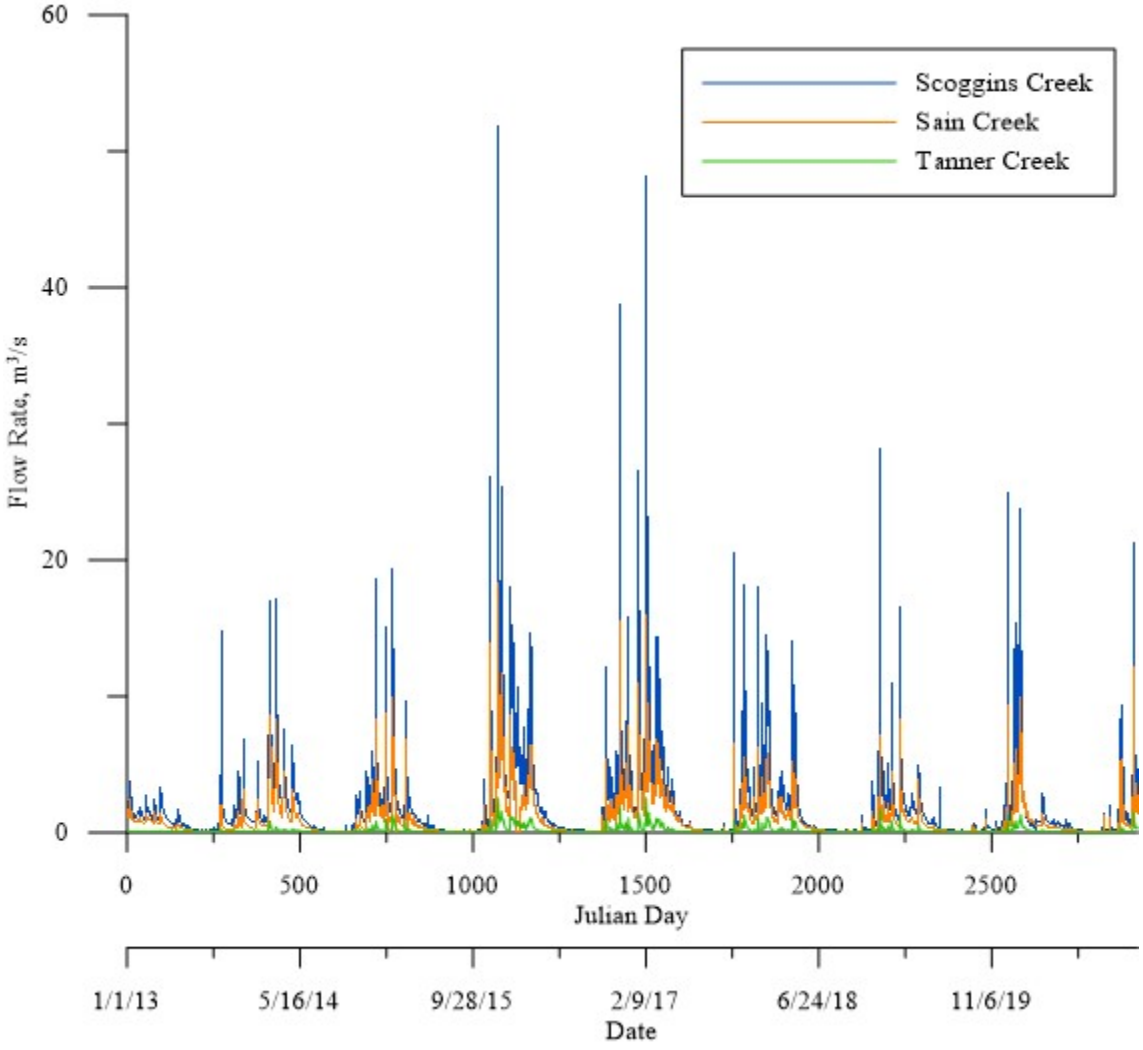

Figure 6-5 Time series graph of tributary inflows.

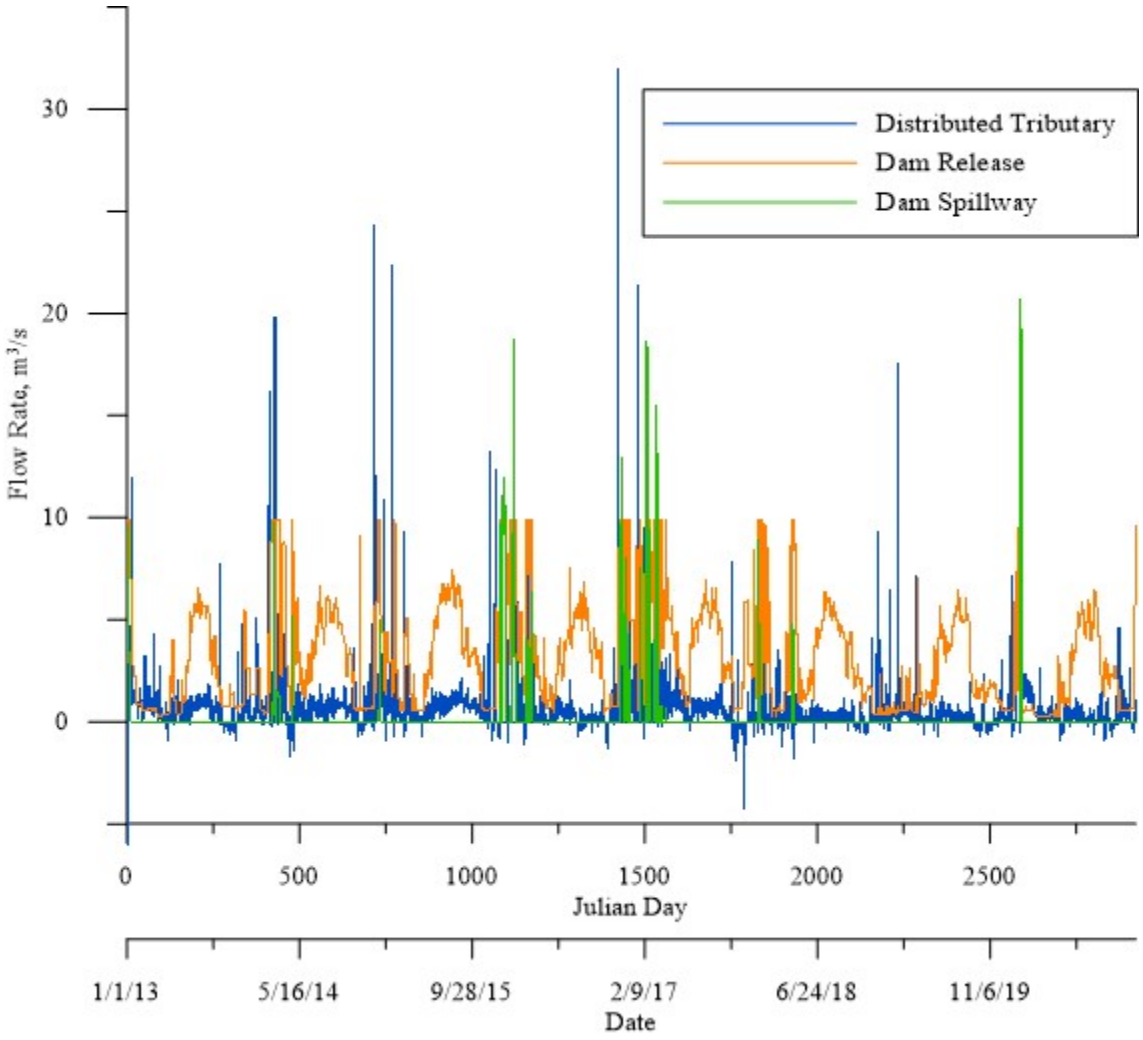

Figure 6-6 Time series graph of distributed tributary inflow and dam outflows.

6.1.3 Temperature Inputs

Water temperature input values were obtained from the Reclamation Hydromet station SCLO which is located immediately upstream of the lake. These temperature values were originally applied to all the branches and the distributed tributary, but during calibration it was discovered that the modeled temperature was too cold. The temperature of Branch 1 was kept the same, but an additional 0.5 degrees Celsius was added to the other two branches and the distributed tributary during the months of December, January, and February for the entire model simulation period to better match

the field data. Figure 6-7 shows a time series graph of the temperature inputs for Branch 1.

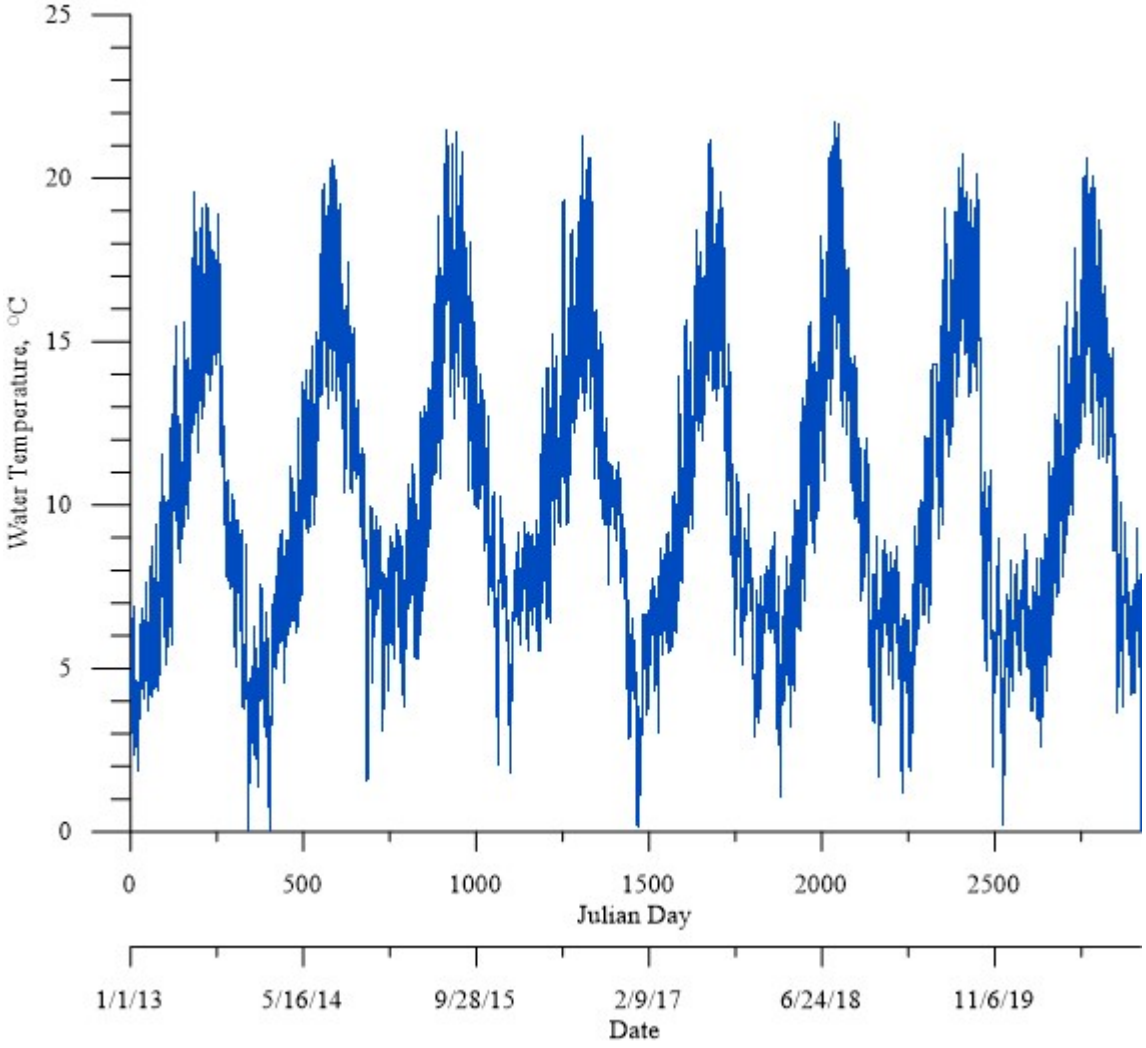

Figure 6-7 Time series graph of temperature inputs measured at Reclamation Hydromet station SCLO.

6.1.4 Concentration Inputs

Concentration inputs were obtained from the City of Hillsboro and the Joint Water Commission (JWC) for Scoggins Creek, Sain Creek, and Tanner Creek. The distributed tributary input concentrations were estimated as equal to Scoggins Creek (Branch 1) concentrations. Table 6-1 shows the parameters used in calculating input

concentrations with the corresponding dates of field data available. Data collection began in October 2014 at Henry Hagg Lake. Since the model simulation begins in January 2013, average values of concentration inputs were used prior to the start of data collection. Field data was measured approximately once per month, but since the model uses continuous inflow data, values from missing dates were calculated by interpolating between field measurements. The average values of dissolved organic carbon and total suspended solids were used after their last dates of measurement since no values after August 2017 were measured for these two parameters. The last value of measurement for all other constituents were kept constant till the end of the model simulation.

Table 6-1 Concentration parameters used for input files.

Parameter	Dates of Measurements
Algae Biomass	10/15/14-10/19/20
Alkalinity	10/15/14-12/09/20
Ammonia-N	11/06/14-10/19/20
Chlorophyll	10/15/14-12/09/20
Conductivity	10/15/14-12/09/20
Dissolved Organic Carbon (DOC)	10/15/14-08/09/17
Dissolved Oxygen (DO)	10/15/14-12/09/20
E. Coli	10/15/14-10/19/20
Nitrate-N/Nitrite-N	10/15/14-10/19/20
Ortho-Phosphate	10/15/14-10/19/20
pH	10/15/14-12/09/20
Temperature	10/15/14-12/09/20
Total Kjeldahl Nitrogen (TKN)	12/17/14-10/19/20
Total Organic Carbon (TOC)	10/15/14-10/19/20
Total Phosphorus (TP)	12/17/14-10/19/20
Total Suspended Solids (TSS)	10/15/14-08/09/17

The following equations show the calculations in developing the constituent inputs using field data and assumptions (Wells and Berger, 2019; Wells, 2020a). These equations were reproduced from those used to develop the concentration input files for

the original model simulation period. Equation (6-2) shows the calculation of total organic matter:

$$\Phi_{TOM} = \frac{\Phi_{TOC}}{orgc} - \Phi_{algae} \quad \textbf{(6-2)}$$

where Φ_{TOM} is total organic matter, Φ_{TOC} is total organic carbon (from data), $orgc$ is the stoichiometric equivalent between organic matter and carbon set equal to 0.45, and Φ_{algae} is the total algae concentration. Equation (6-3) shows the calculation of dissolved organic matter:

$$\Phi_{DOM} = \frac{\Phi_{DOC}}{orgc} \quad \textbf{(6-3)}$$

where Φ_{DOM} is dissolved organic matter and Φ_{DOC} is dissolved organic carbon (from data). There was no DOC data recorded for Tanner Creek so the ratio of Scoggins Creek average DOC to average TOC was used to convert Tanner Creek TOC to DOC. Equation (6-4) shows the calculation of particulate organic matter:

$$\Phi_{POM} = \Phi_{TOM} - \Phi_{DOM} \quad \textbf{(6-4)}$$

where Φ_{POM} is particulate organic matter. Dissolved and particulate organic matter are each made up of labile (fast decaying) and refractory (slow decaying) portions. It was assumed that 10 percent of both the particulate and dissolved organic matter was labile and that 90 percent was refractory. Equations **(**6-5**)** through **(**6-8**)** show the calculations of labile and refractory organic matter:

$$\Phi_{LDOM} = 10\% * \Phi_{DOM} \quad \textbf{(6-5)}$$

$$\Phi_{RDOM} = 90\% * \Phi_{DOM} \quad \textbf{(6-6)}$$

$$\Phi_{LPOM} = 10\% * \Phi_{POM} \quad \textbf{(6-7)}$$

$$\Phi_{RPOM} = 90\% * \Phi_{POM} \quad \textbf{(6-8)}$$

where Φ_{LDOM} is labile dissolved organic matter, Φ_{RDOM} is refractory dissolved organic matter, Φ_{LPOM} is labile particulate organic matter, and Φ_{RPOM} is refractory particulate organic matter. Equation **(**6-9**)** shows the calculation of inorganic suspended solids:

$$\Phi_{ISS} = \Phi_{TSS} - \Phi_{POM} - \Phi_{algae} \quad \textbf{(6-9)}$$

where Φ_{ISS} is inorganic suspended solids and Φ_{TSS} is the total suspended solids concentration (from data).

The calculation of algae concentrations was updated for the inflow files. The original calibration of the model calculated algae group 1 concentrations as $chl\ a\left(\frac{\mu g}{L}\right) * 0.1\left(\frac{mg\ algae}{\mu g\ chl\ a}\right)$, and calculated algae group 2 and algae group 3 concentrations as a constant 0.001 mg L^{-1}. The calculations of algae group 2 and algae group 3 concentrations were updated to mimic the algae group 1 calculation but using $0.05\left(\frac{mg\ algae}{\mu g\ chl\ a}\right)$ for algae group 2 and $0.03\left(\frac{mg\ algae}{\mu g\ chl\ a}\right)$ for algae group 3. These are approximate values of the biomass to chlorophyll a ratio for green algae (estimated with group 2) and cyanobacteria (estimated with group 3) as shown in Equations **(**6-10**)** through **(**6-12**)**:

$$\Phi_{algae1} = \Phi_{chla} * achla1 \quad \textbf{(6-10)}$$

$$\Phi_{algae2} = \Phi_{chla} * achla2 \quad \textbf{(6-11)}$$

$$\Phi_{algae3} = \Phi_{chla} * achla3 \quad \textbf{(6-12)}$$

where Φ_{algae} is the concentration of algae in each group, Φ_{chla} is chlorophyll a (from data), and $achla$ is the ratio of algae biomass to chlorophyll a for each algae group (0.1, 0.05, or 0.03 as described previously). Zooplankton was not measured, but the

zooplankton input concentration was set to a constant 0.001 mg L^{-1}. This is a relatively small value but was used to "seed" the reservoir. If the input concentration was set to zero, then no zooplankton would grow.

The total amount of phosphorus in organic matter was calculated using Equation (6-13):

$$\Phi_{OM-P} = \Phi_{TP} - \Phi_{PO4-P} - \sum(\Phi_{algae} * algp) \quad \textbf{(6-13)}$$

where Φ_{OM-P} is the total amount of phosphorus in organic matter, Φ_{TP} is the total phosphorus (from data), Φ_{PO4-P} is ortho-phosphorus (from data), and $algp$ is the stoichiometric equivalent between algae and phosphorus set equal to 0.015. The phosphorus from algae is the sum of phosphorus in all algal groups. The fractions of labile dissolved organic matter – phosphorus (Φ_{LDOM-P}), refractory dissolved organic matter – phosphorus (Φ_{RDO}), labile particulate organic matter – phosphorus (Φ_{LPOM-P}), and refractory particulate organic matter – phosphorus (Φ_{RPOM-P}) were estimated as follows:

$$\Phi_{LDOM-P} = \frac{\Phi_{OM-P} * \Phi_{LDOM}}{\Phi_{TOM}} \quad \textbf{(6-14)}$$

$$\Phi_{RDOM-P} = \frac{\Phi_{OM-P} * \Phi_{RDOM}}{\Phi_{TOM}} \quad \textbf{(6-15)}$$

$$\Phi_{LPOM-P} = \frac{\Phi_{OM-P} * \Phi_{LPOM}}{\Phi_{TOM}} \quad \textbf{(6-16)}$$

$$\Phi_{RPOM-P} = \frac{\Phi_{OM-P} * \Phi_{RPOM}}{\Phi_{TOM}} \quad \textbf{(6-17)}$$

The total amount of nitrogen in organic matter was calculated using Equation (6-18):

$$\Phi_{OM-N} = \Phi_{TKN} - \Phi_{NH3-N} - \sum(\Phi_{algae} * algn) \quad \textbf{(6-18)}$$

where Φ_{OM-N} is the total amount of nitrogen in organic matter, Φ_{TKN} is total Kjeldahl nitrogen (from data), Φ_{NH3-N} is ammonia nitrogen (from data), and $algn$ is the stoichiometric equivalent between algae and nitrogen set equal to 0.08. The nitrogen from algae is the sum of nitrogen in all algal groups. The fractions of labile dissolved organic matter – nitrogen (Φ_{LDOM-N}), refractory dissolved organic matter – nitrogen (Φ_{RDOM-}), labile particulate organic matter – nitrogen (Φ_{LPOM-N}), and refractory particulate organic matter – nitrogen (Φ_{RPOM-N}) were estimated as follows in the original model simulation:

$$\Phi_{LDOM-N} = \frac{\Phi_{OM-N} * \Phi_{LDOM}}{\Phi_{TOM}} \quad \textbf{(6-19)}$$

$$\Phi_{RDOM-N} = \frac{\Phi_{OM-N} * \Phi_{RDOM}}{\Phi_{TOM}} \quad \textbf{(6-20)}$$

$$\Phi_{LPOM-N} = \frac{\Phi_{OM-N} * \Phi_{LPOM}}{\Phi_{TOM}} \quad \textbf{(6-21)}$$

$$\Phi_{RPOM-N} = \frac{\Phi_{OM-N} * \Phi_{RPOM}}{\Phi_{TOM}} \quad \textbf{(6-22)}$$

During the water quality calibration process, it was discovered that switching the Φ_{RDOM-N} and Φ_{RPOM-N} values better matched the field data. The updated model through 2020 used the following equations to calculate these two values, where the fractions of refractory particulate and dissolved organic matter were switched:

$$\Phi_{RDOM-N} = \frac{\Phi_{OM-N} * \Phi_{RPOM}}{\Phi_{TOM}} \quad \textbf{(6-23)}$$

$$\Phi_{RPOM-N} = \frac{\Phi_{OM-N} * \Phi_{RDOM}}{\Phi_{TOM}} \quad \textbf{(6-24)}$$

The total inorganic carbon concentration was estimated using the subroutine PH_CO2 located within the CE-QUAL-W2 source code which calculates total inorganic carbon as a function of pH, alkalinity, and temperature where alkalinity values are from field data. The subroutine is based on the equilibrium reaction between carbonate and bicarbonate. Figure 6-8 through Figure 6-12 show the concentration inputs used in the Henry Hagg Lake model. TDS, chloride, and sulfate concentrations were based on average concentrations measured in the Upper Tualatin River at Cherry Grove.

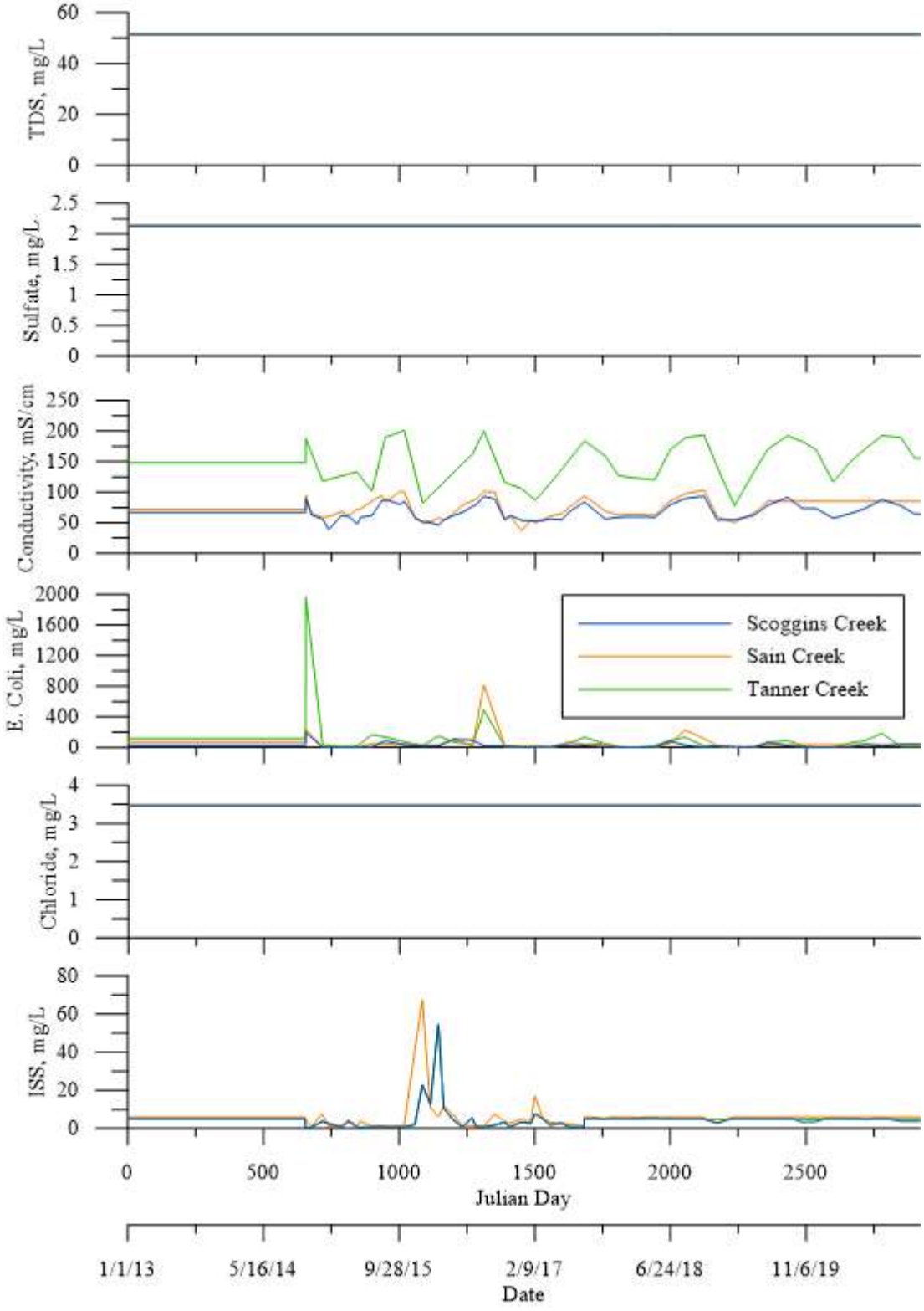

Figure 6-8 Time series graphs of concentration inputs for total dissolved solids, sulfate, conductivity, E. coli, chloride, and inorganic suspended solids.

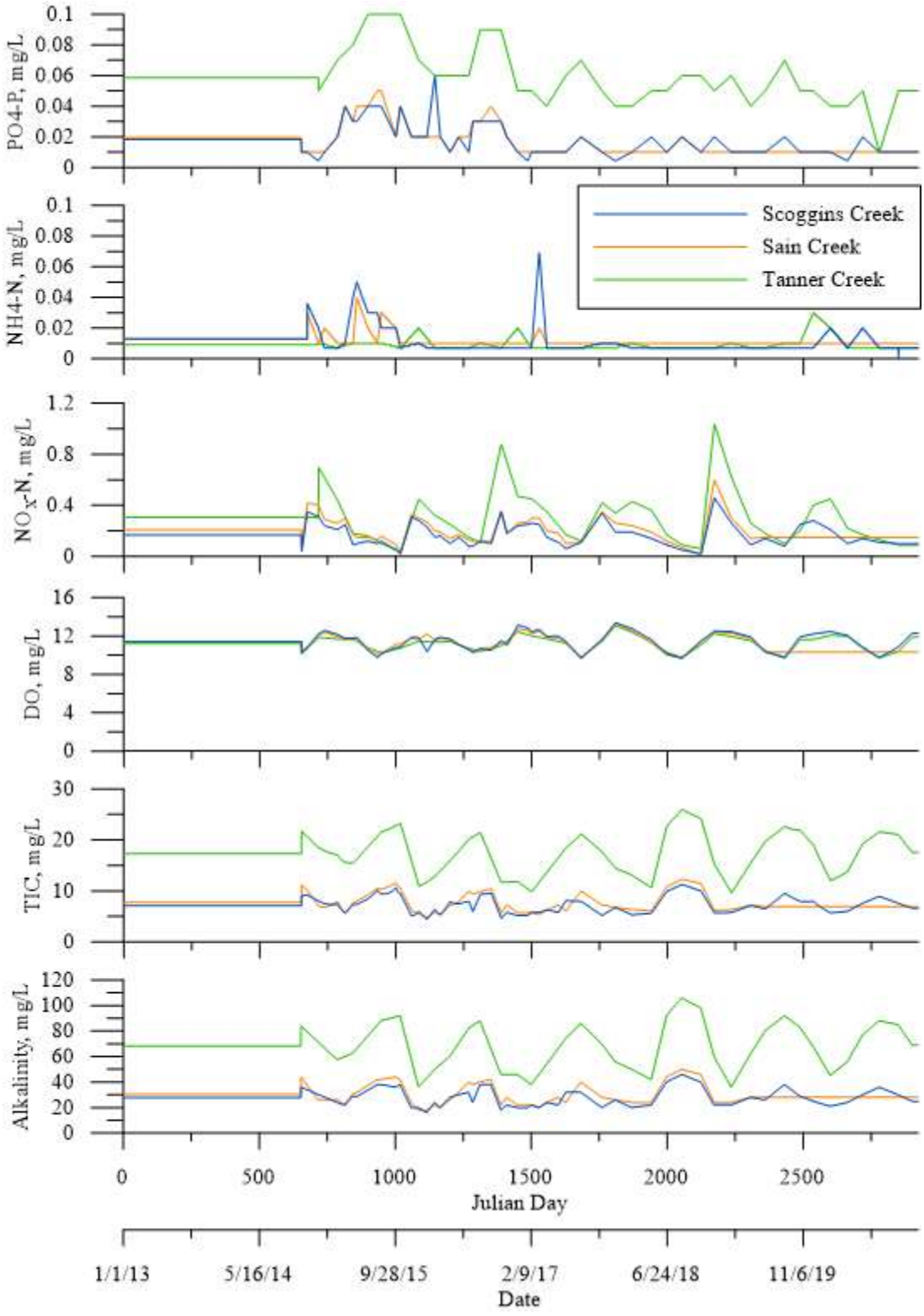

Figure 6-9 Time series graphs of concentration inputs for dissolved ortho-phosphate, ammonia, nitrate+nitrite, dissolved oxygen, total inorganic carbon, and alkalinity.

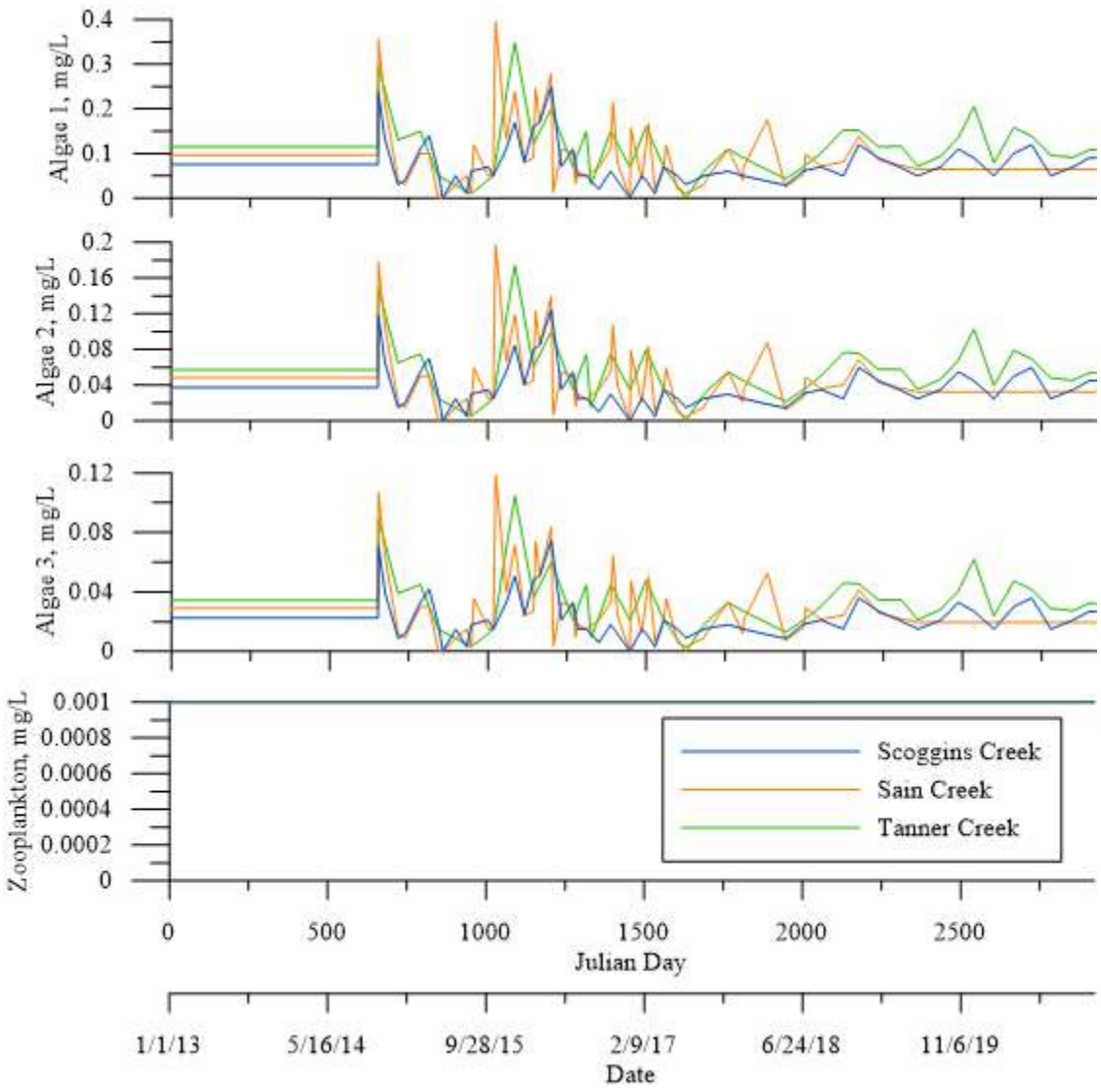

Figure 6-10 Time series graphs of concentration inputs for algae group 1, algae group 2, algae group 3, and zooplankton.

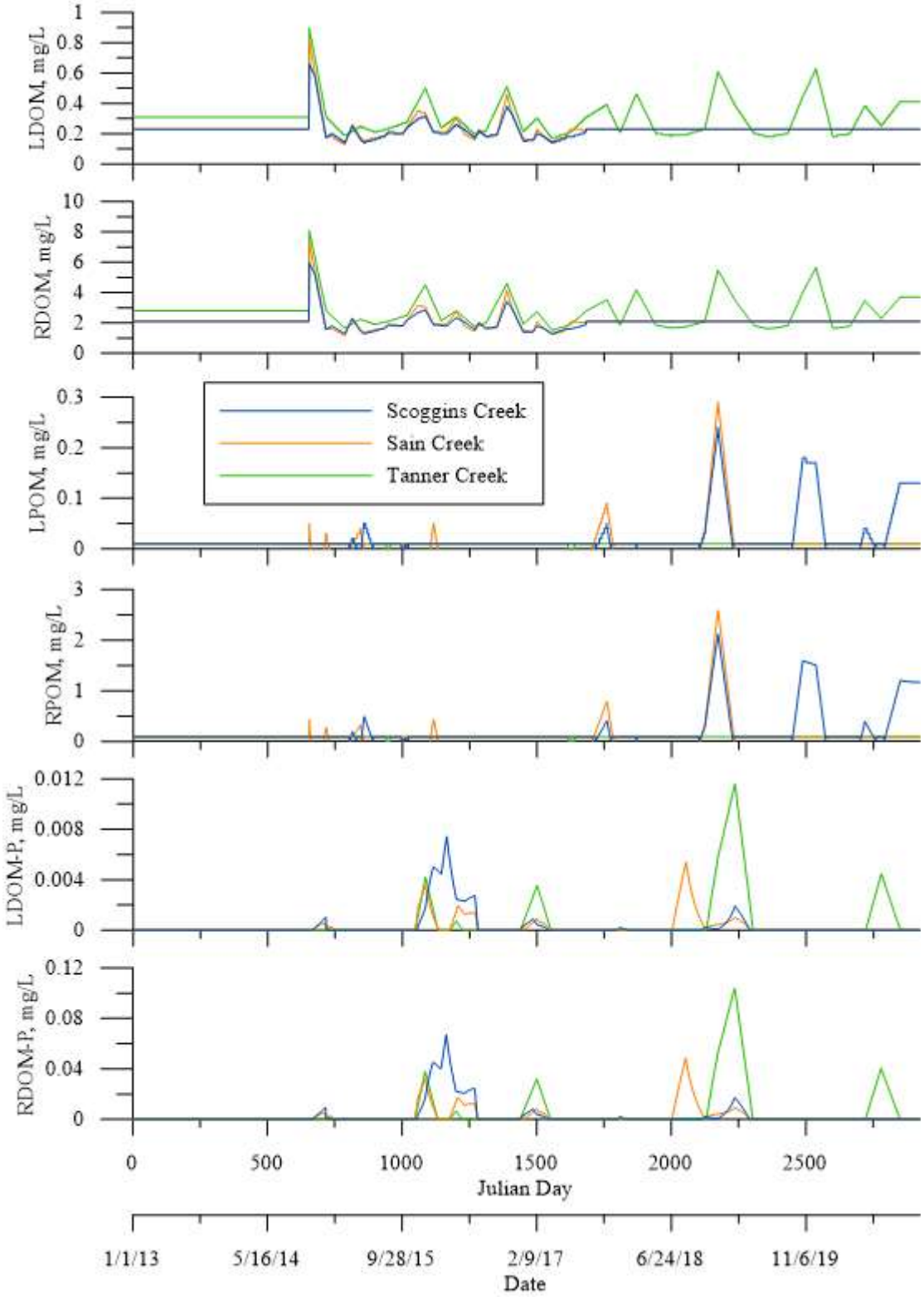

Figure 6-11 Time series graphs of concentration inputs for LDOM, RDOM, LPOM, RPOM, LDOM-P, and RDOM-P.

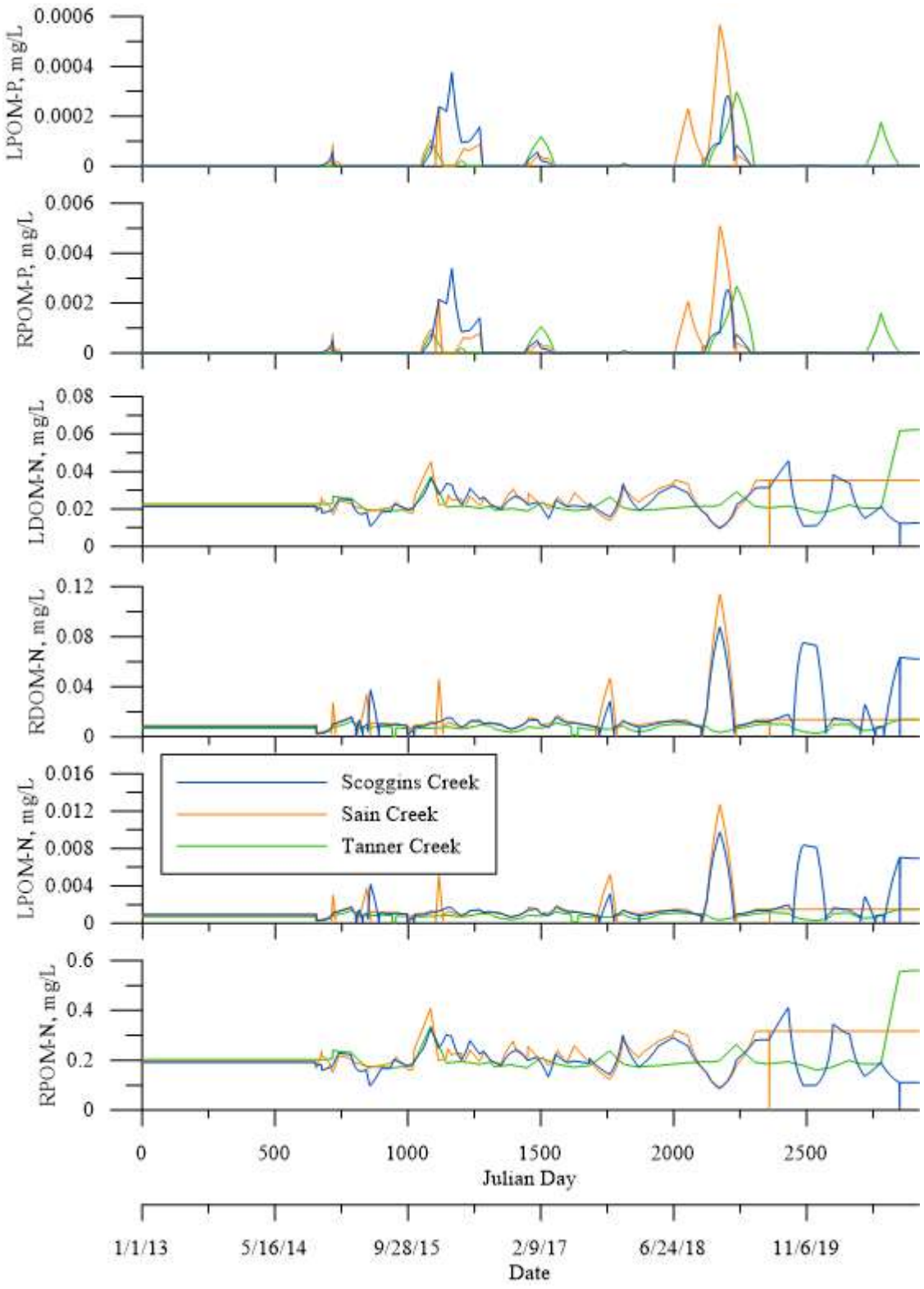

Figure 6-12 Time series graphs of concentration inputs for LPOM-P, RPOM-P, LDOM-N, RDOM-N, LPOM-N, and RPOM-N.

6.2 Henry Hagg Lake Water Quality Calibration

As previously mentioned, a model for Henry Hagg Lake had been developed in CE-QUAL-W2 for January 1, 2013 through December 31, 2015, but further refinement of the model for water quality, including data collected through 2020, was performed prior to adding cyanotoxins to the model for Henry Hagg Lake. Water quality was calibrated by comparing Henry Hagg Lake depth profiles and dam outflow values between the model results and collected field data for the following water quality parameters: algae, temperature, dissolved oxygen, pH, chlorophyll a, and nutrients. To refine these parameters, model updates were made to algal groups, light extinction, sediment, nutrients, and boundary conditions. Field measurements for the dam outflow were obtained from the United States Geological Survey (USGS) gage 14202980 (Scoggins Creek below Henry Hagg Lake), and measurements for depth profiles within the lake were obtained from the City of Hillsboro and the Joint Water Commission (JWC).

Calibration statistics of mean error, absolute mean error, and root mean square error were calculated for each comparison of the model predictions to field measurements. The equation used for the mean error is shown in Equation **(**6-25**)**

$$Mean\ Error\ (ME) = \frac{\sum_1^n (model - data)}{n} \qquad \textbf{(6-25)}$$

where *n* is the number of observations, *model* is the model predicted state variable, and *data* is the field data variable. The mean absolute error between model and field data is shown in Equation **(**6-26**)**

$$Absolute\ Mean\ Error\ (AME) = \frac{\sum_1^n abs(model - data)}{n} \quad \textbf{(6-26)}$$

The root mean square error between the model and field data is shown in Equation (6-27)

$$Root\ Mean\ Square\ Error\ (RMSE) = \sqrt{\frac{\sum_1^n (model - data)^2}{n}} \quad \textbf{(6-27)}$$

The mean error represents model bias where a positive value indicates the model is overpredicting a specific parameter and a negative value indicates the model is underpredicting this parameter. The absolute mean error is used as an overall representation of how closely the model predictions match the field data. The smaller the absolute mean error, the closer the model matches field data. The root mean square error will add more weight to larger errors than smaller errors and will indicate if there is a wide range of error sizes.

6.2.1 Algae

Algae was calibrated by comparing chlorophyll a depth profiles just before the dam at Henry Hagg Lake between the model results and collected field data as well as comparing the percent biovolume of the three groups between the model and field data.

6.2.1.1 Algal Groupings

Algae and cyanobacteria can be modeled as a single assemblage or as multiple groups in CE-QUAL-W2. While there is no limit to how many groups can be used, it is often preferred to use as few groups as possible to model the algal dynamics. Since each algal group contains 28 variables, and the presence of each algal group affects the other groups, it can become difficult to calibrate the model if using more than a few groups. In

addition, a simpler model that can accurately predict the dynamics and water quality is preferred over a more complex model.

Eight algal groups have been recorded in Henry Hagg Lake over the past six years: cyanobacteria, chrysophytes, cryptophytes, diatoms, dinoflagellates, euglenoids, greens, and unidentified flagellates. Three algal groups were simulated in the Henry Hagg Lake model to represent the eight algal groups identified at the Lake. Group 1 represented diatoms, group 2 represented chrysophytes, cryptophytes, dinoflagellates, euglenoids, greens, and unidentified flagellates, and group 3 represented cyanobacteria. The model groups were chosen based on how much of each species was present at different temperatures and the seasonal variation of species throughout the past few years. Figure 6-13 shows the percent of measured biovolume at various temperatures for each algal group in Henry Hagg Lake from October 2014 through December 2018 and Figure 6-14 shows the seasonal variation of each algal group from October 2014 through December 2020. While diatoms and cryptophytes tend to be present at colder temperatures, cryptophytes often increased in prevalence during the times that diatoms decreased in prevalence, therefore cryptophytes were placed in group 2. Cyanobacteria were placed in a group of their own in order to apply cyanotoxin dynamics to this group separately.

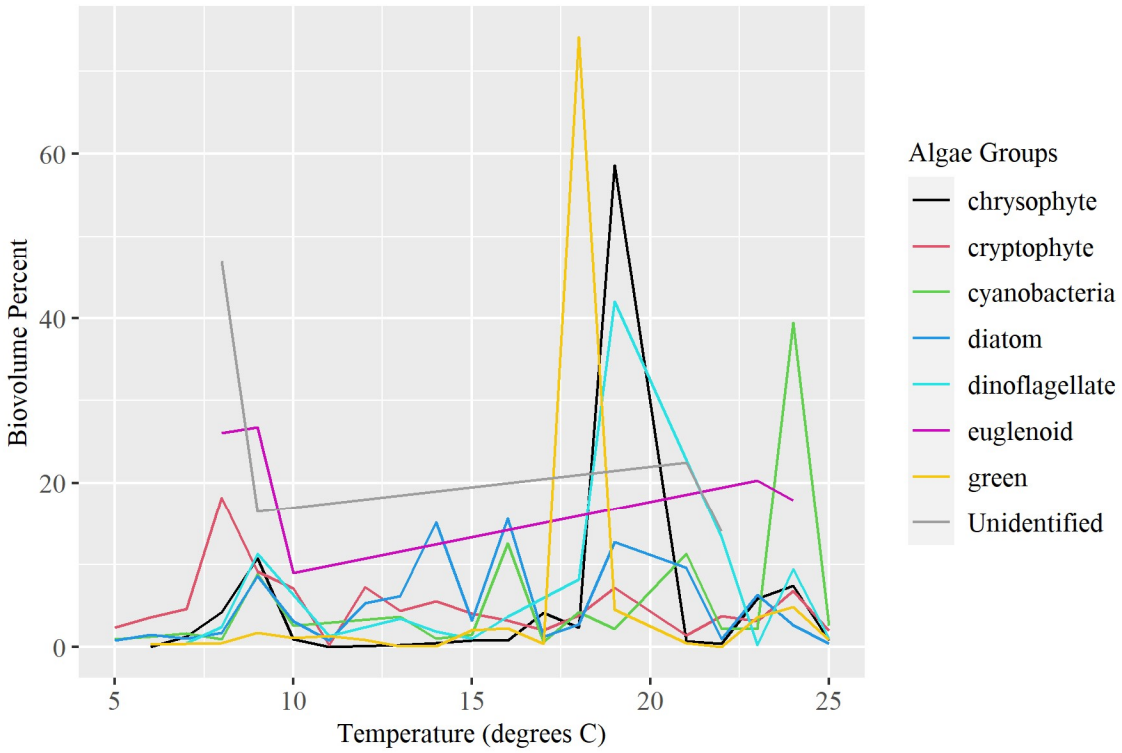

Figure 6-13 Percent of measured biovolume at various temperatures for each algal group in Henry Hagg Lake using field data from 2014-2018.

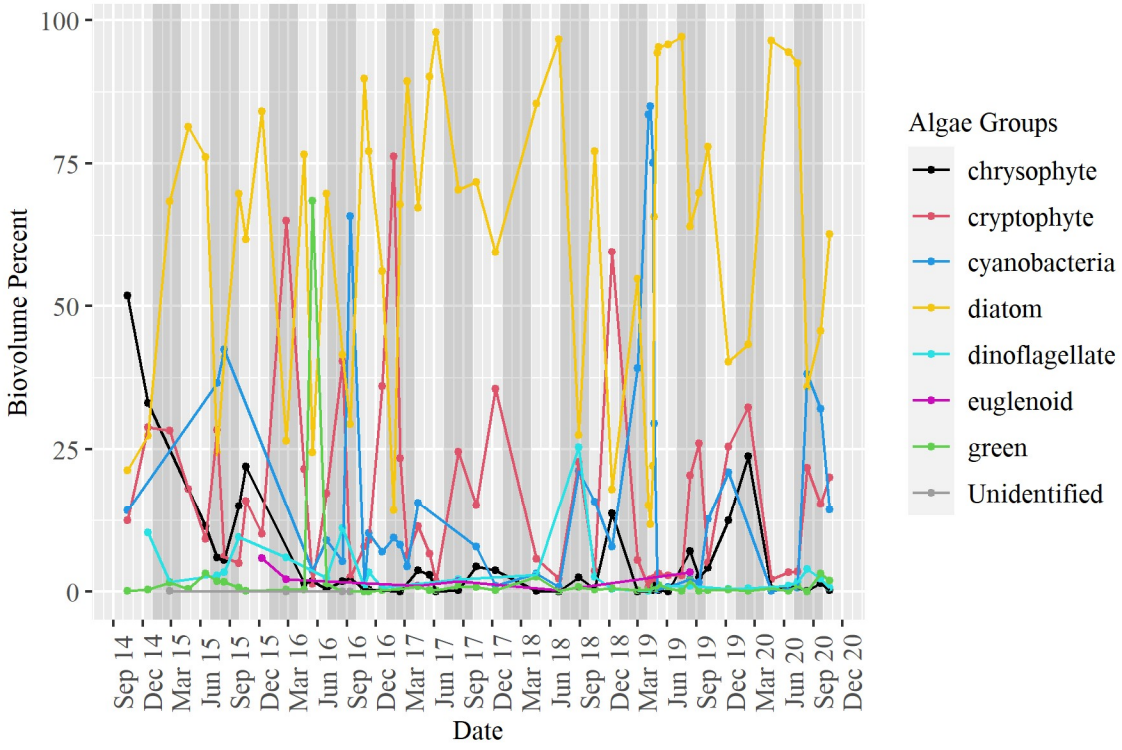

Figure 6-14 Seasonal variation of each algal group in Henry Hagg Lake using field data from 2014-2020.

Data collected in 2019 showed a spike of cyanobacteria in February through April at colder lake temperatures. This skewed the biovolume to colder temperatures which is not representative of the typical temperature range of cyanobacteria and so 2019 data was not used in determining the algal groups. Figure 6-15 shows the percent of measured biovolume at various temperatures in Henry Hagg Lake using the 2019 data.

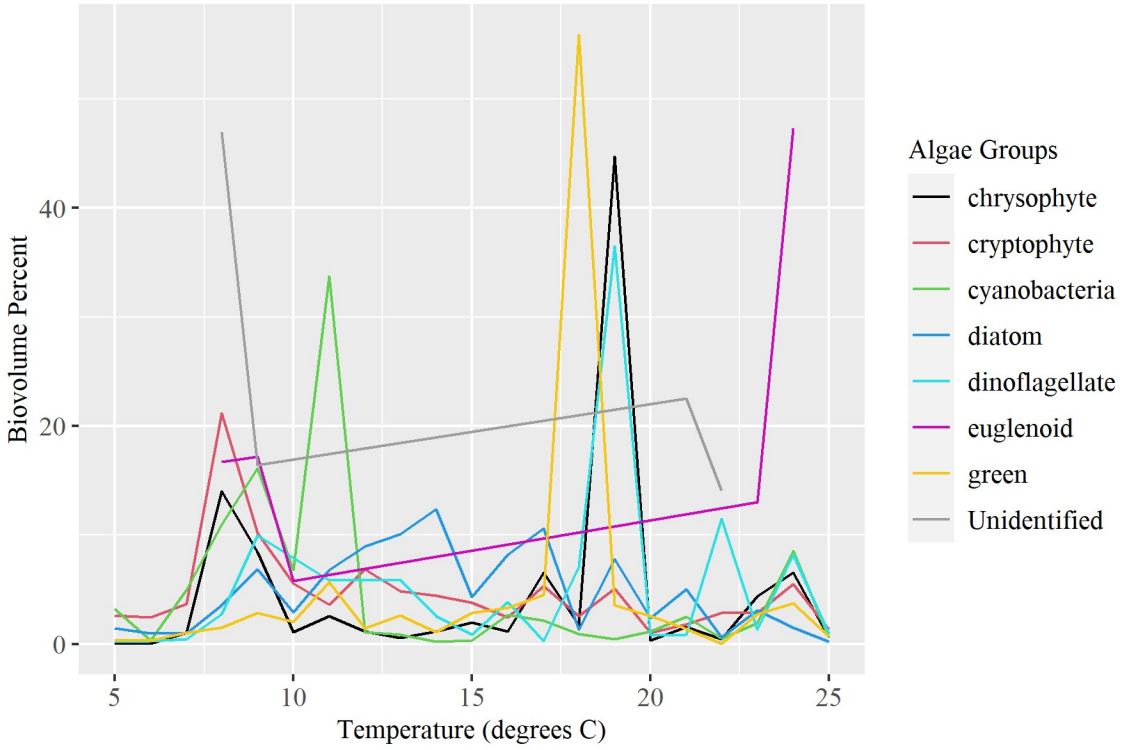

Figure 6-15 Percent of measured biovolume at various temperatures for each algal group in Henry Hagg Lake using field data from 2014-2020.

Figure 6-16 shows a comparison of the percent biomass of each algal group between the model results and field measurements for each season. The percent biomass for an algal group was calculated as the sum of the group's biomass at all depths for a particular season divided by the sum of all algal biomass at all depths for that season. Equation (6-28) shows an example calculation for the percent biomass for group 1 in the summer:

$$Percent\ biomass\ Group\ 1, summer$$

$$= \frac{\Sigma Group\ 1\ biomass\ at\ all\ depths\ in\ all\ summer\ months}{\Sigma Total\ biomass\ at\ all\ depths\ in\ all\ summer\ months} * 100\% \quad \textbf{(6-28)}$$

where the same calculation would be applied to each group during each season. Winter was defined as January 1 – March 31, spring was defined as April 1 – June 30, summer was defined as July 1 – September 30, and fall was defined as October 1 – December 31.

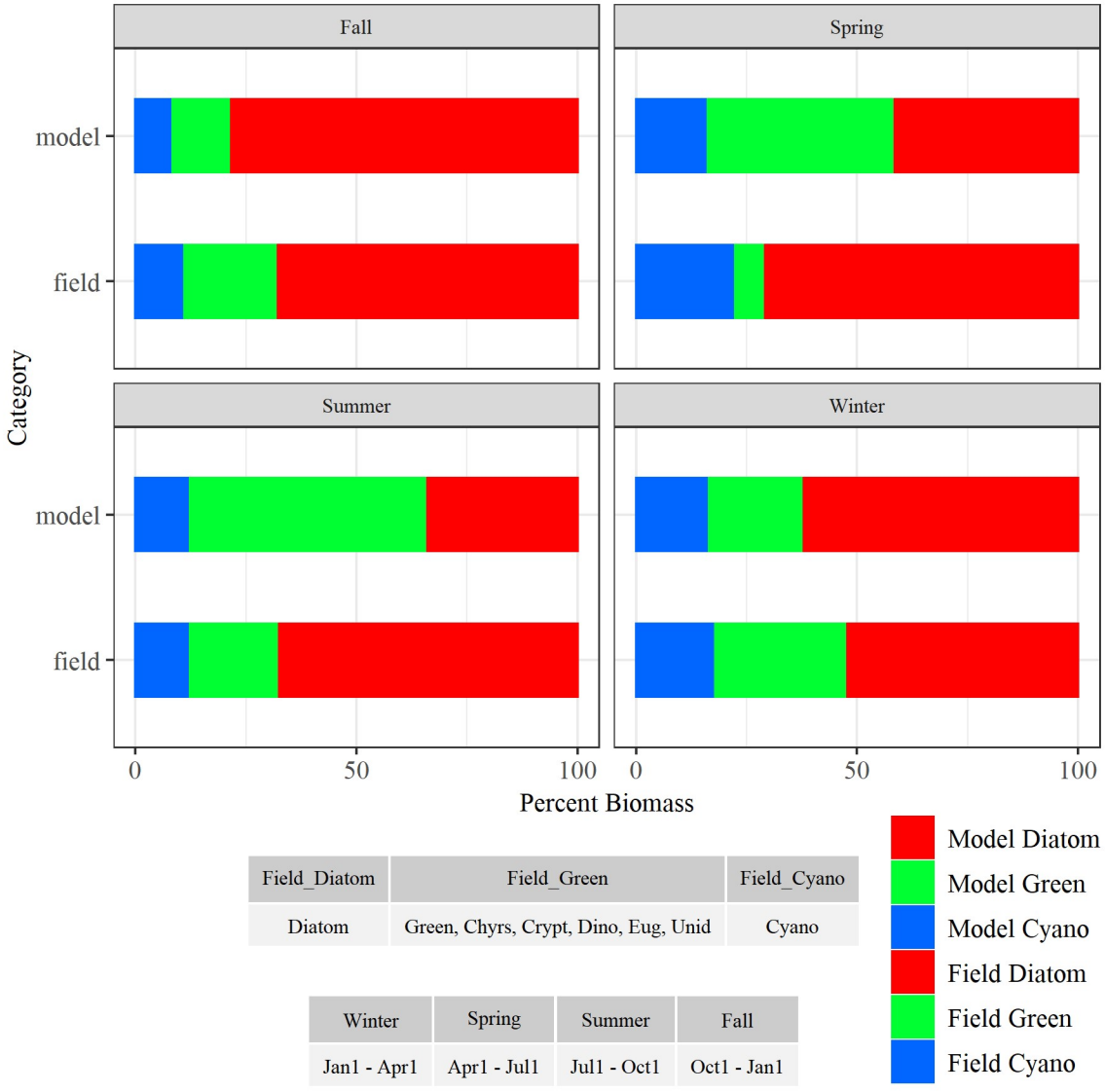

Field_Diatom	Field_Green	Field_Cyano
Diatom	Green, Chyrs, Crypt, Dino, Eug, Unid	Cyano

Winter	Spring	Summer	Fall
Jan1 - Apr1	Apr1 - Jul1	Jul1 - Oct1	Oct1 - Jan1

Figure 6-16 Average percent biomass comparison for each algal group in Henry Hagg Lake.

6.2.1.2 Algal Rates and Coefficients

Of the updates made to the algal rates and coefficients, the algal light saturation intensity (ASAT) and algal settling rate (AS) had some of the most pronounced effects on the relative abundance of each species. ASAT values were decreased for all species to get more photoinhibition at the surface and encourage growth at slightly lower depths to better match the field data. The AS values were also decreased for all groups to allow for more competition between the three algal groups so that one species did not dominate. Other updates to nutrient rates and coefficients were made to improve model results. Table 6-2 shows the rates and coefficients that were updated in the model to better match the field measurements for the water quality parameters.

Table 6-2 Model updates to algal rates and coefficients.

Parameter	Parameter Name	Previous Value	Updated Value
AG (ALG1, 2, 3)	Max algal growth rate, d^{-1}	2.3, 2.1, 2.1	3, 2.5, 2.5
AS (ALG1, 2, 3)	Algal settling rate, m d^{-1}	0.5, 0.5, 0.5	0.1, 0.1, 0.0
AHSP (ALG1, 2, 3)	Algal half-saturation for Phosphorus limited growth, g m^{-3}	0.003, 0.003, 0.003	0.001, 0.005, 0.005
AHSN (ALG1, 2, 3)	Algal half-saturation for Nitrogen limited growth, g m^{-3}	0.014, 0.014, 0.014	0.01, 0.014, 0.001
ASAT (ALG1, 2, 3)	Light saturation intensity at max photosynthetic rate, W m^{-2}	70, 70, 70	50, 70, 70
AT1 (ALG1, 2, 3)	Lower temp. for algal growth, ^oC	4, 4, 4	4, 10, 10
AT2 (ALG1, 2, 3)	Lower temp. for max algal growth, ^oC	12, 20, 15	10, 20, 25
AT3 (ALG1, 2, 3)	Upper temp. for max algal growth, ^oC	19, 23.5, 21	20, 25, 30
AT4 (ALG1, 2, 3)	Upper temp. for algal growth, ^oC	40, 40, 40	25, 30, 40
AK1 (ALG1, 2, 3)	Fraction of algal growth rate at AT1	0.3, 0.07, 0.07	0.2, 0.1, 0.1
ALGP (ALG1, 2, 3)	Stoichiometric equivalence between algal biomass and phosphorus, fraction	0.015, 0.015, 0.015	0.003, 0.03, 0.019
ALGSI (ALG1, 2, 3)	Stoichiometric equivalence between algal biomass and silica, fraction	0, 0, 0	0.18, 0.18, 0.18
ACHLA (ALG1, 2, 3)	Ratio between algal biomass and chl a, mg-algae µg-$chla^{-1}$	0.1, 0.01, 0.01	0.1, 0.05, 0.03
O2AG (ALG1, 2, 3)	Oxygen stoichiometry for algal primary production, mg-O_2 mg-algae OM^{-1}	1.4, 1.4, 1.4	1.8, 1.8, 1.8

chl a, chlorophyll a; OM, organic matter
(Bowie *et al.*, 1985; Wells, 2020a)

6.2.2 Light Extinction

The previous version of the model used a separate file to read in extinction coefficients over time. This was turned off in the updated model in order to have the model dynamically predict light extinction coefficients and allow for more flexibility when extending the model simulation period. Dynamic light predictions also make the model more predictive when simulating management scenarios since the modeled organic matter, algae, and inorganic suspended solids will affect light extinction. Switching the model to dynamically predict light extinction instead of reading in an external file required some of the other light extinction parameters to be updated to better match the field measurements. The baseline extinction coefficient (EXH2O) and algal light extinction coefficient (EXA) were both increased in the updated model while the extinction coefficient due to inorganic suspended solids (EXSS) and the extinction coefficient due to organic matter (EXOM) were both decreased to obtain better model statistics. Table 6-3 shows the extinction coefficients that were updated in the model. Figure 6-17 shows the comparison of the light extinction coefficient over time between the external file and the dynamic time-series model output.

Table 6-3 Model updates to light extinction coefficients.

Parameter	Parameter Name	Previous Value	Updated Value
EXH2O	Baseline extinction coefficient, m^{-1}	0.25	0.45
EXSS	Extinction due to ISS, m^{-1} $(g\ m^{-3})^{-1}$	0.3	0.1
EXOM	Extinction due to OM, m^{-1} $(g\ m^{-3})^{-1}$	0.3	0.1
EXC	Read extinction coefficients	ON	OFF
EXA (all algal groups)	Algal light extinction, m^{-1} $(g\ m^{-3})^{-1}$	0.3	0.6

ISS, inorganic suspended solids; OM, organic matter
(Wells, 2020a)

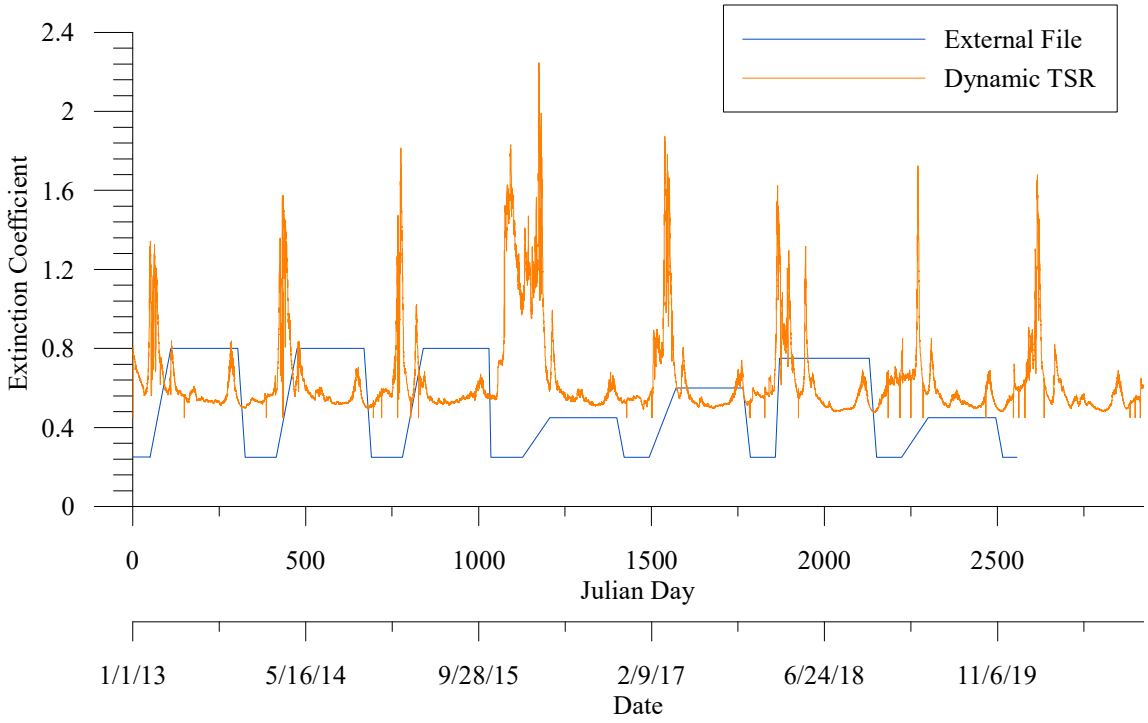

Figure 6-17 Comparison of dynamic and external file extinction coefficients.

6.2.3 Sediment

Two sediment parameters were updated to the model. The first order sediment decay rate was increased from 0.01 to 0.14. This was done to allow for more decay in the bottom of the lake which would subsequently decrease the DO at the bottom to better match the field data. The zero-order sediment oxygen demand was increased from 1.1 to 1.3 for the model segments near the dam to also decrease the DO at the bottom of the lake. Table 6-4 summarizes the sediment rates that were updated in the model.

Table 6-4 Model updates to sediment rates.

Parameter	Parameter Name	Previous Value	Updated Value
SEDK	First order sediment decay rate, d^{-1}	0.01	0.14
SOD (segments 20-30)	Zero-order sediment oxygen demand, g m^{-2} d^{-1}	1.1	1.3

(Wells, 2020a)

6.2.4 Nutrients

The model typically overpredicted nutrients such as ammonia and nitrate. In order to decrease the model predictions of these nutrients, the ammonium decay rate was increased to promote more decay and the lower temperatures for decay of ammonia and nitrate were reduced to increase the range of temperatures at which decay would occur. Other updates to nutrient rates and coefficients were made to improve model results. Table 6-5 summarizes the nutrient rates and coefficients that were updated in the model.

Table 6-5 Model updates to nutrient rates and coefficients.

Parameter	Parameter Name	Previous Value	Updated Value
PO4R	Sediment release rate of phosphorus, fraction of SOD	0	0.001
NH4R	Sediment release rate of Ammonium, fraction of SOD	0	0.001
NH4DK	Ammonium decay rate, d^{-1}	0.2	0.3
NH4T2	Lower temp. for max ammonia decay, ^oC	30	20
O2NH4	Oxygen stoichiometry for nitrification, $mg\text{-}O_2$ $mg\text{-}Nitrogen^{-1}$	4.33	4.57
NO3T2	Lower temp. for max nitrate decay, ^oC	30	25

SOD, sediment oxygen demand
(Wells, 2020a)

6.2.5 Boundary Conditions

Six boundary conditions were updated in the model. As mentioned previously, the calculations for algae group 2 and group 3 concentrations were updated in all input files from the original model calculations to better match nutrient concentrations in the lake. Also, the fraction of refractory dissolved organic matter – nitrogen (RDOMN) and the fraction of refractory particulate organic matter – nitrogen (RPOMN) were switched in all input files from the original model calculations to better match nutrient concentrations in the lake. As was mentioned previously, the water temperature inputs for Branch 1 were obtained from the station immediately upstream of the lake. The same

temperatures were applied to the other two branches and the distributed tributary with an additional 0.5 degrees Celsius added to the months of December, January, and February to increase the modeled temperature to better match the field data. The wind sheltering coefficient was updated from a variable value between 1.8-2.2 to a constant value of 2.0. This was done to allow for more flexibility when extending the model simulation period. As a result of making the wind sheltering coefficient a constant value, the minimum wind velocities in the meteorological input file were increased from 0 to 0.5 m s^{-1} so that the water quality parameter would better match the field data. As was mentioned previously, a wind velocity of zero is very uncommon, and likely the result of equipment sensitivity. Due to potential sediment build up in the bottom of the lake near the outflow, the bottom layer below which selective gate withdrawal will not occur was updated to layer 73 from layer 75. Table 6-6 summarizes the boundary condition values that were updated in the model.

Table 6-6 Model updates to boundary condition values.

Parameter	Parameter Name	Previous Value	Updated Value
Algae2, Algae3 (branch inflow files + distributed tributary file)	Algae inflow concentrations	Updated calculations	
RDOMN & RPOMN (branch inflow files + distributed tributary file)	Refractory dissolved organic matter - Nitrogen, Refractory particulate organic matter - Nitrogen	Switched values in these two columns	
Water temperature for Branch 2, Branch 4, and distributed tributary	Water temperature input	Added 0.5 degree Celsius to measured values in December, January, and February	
Met file wind velocity	Meteorological input file Minimum wind velocity	0	0.5
WSC	Wind sheltering coefficient	1.8-2.2	2.0
KBUGT	Bottom layer below which selective gate withdrawal will not occur	75	73

(Wells, 2020a)

6.2.6 Results

Depth profiles were created for the location of the lake just before the dam to compare model predictions to measured field data. Model segment 29 is the last segment of Henry Hagg Lake before the dam (Figure 6-2). Model results at this segment were compared with field data obtained at the sampling location titled "V – Hagg Lake".

Calibration statistics of mean error, absolute mean error, and root mean square error were calculated for each comparison of the model predictions to field measurements. Values that were recorded as "no detect" were input into the profiles and statistical calculations as one half of the minimum value recorded over the entire period of data collection. Comparisons of model predictions to field data for the dam outflow were also created along with associated statistics. Refer to Appendix B: Henry Hagg Lake Profile Plots and Appendix C: Henry Hagg Lake Outflow Plots for the results. The statistics for the profiles are summarized in Table 6-7 and the statistics for the dam outflow are summarized in Table 6-8.

Table 6-7 Error statistics for vertical profile water quality data at segment 29.

Parameter	No. of Data	Mean Error	Absolute Mean Error	Root Mean Square Error
Temperature (°C)	1168	-0.25	0.747	0.975
Dissolved Oxygen (mg L^{-1})	1136	-0.281	0.738	1.118
pH	1152	0.081	0.28	0.404
Chlorophyll a (µg L^{-1})	1222	-0.766	1.344	1.962
Ammonia (mg L^{-1})	149	0.007	0.013	0.018
Nitrate-Nitrite (mg L^{-1})	148	0.043	0.073	0.093
Total Kjeldahl Nitrogen (mg L^{-1})	134	-0.048	0.089	0.161
Phosphate (mg L^{-1})	149	0.004	0.01	0.012
Total Phosphorus (mg L^{-1})	135	0.015	0.019	0.023
Dissolved Organic Carbon (mg L^{-1})	34	-0.282	0.312	0.375
Total Organic Carbon (mg L^{-1})	161	-0.06	0.25	0.332
Alkalinity (mg L^{-1})	150	0.842	2.286	3.261
Total Suspended Solids (mg L^{-1})	33	-1.176	2.1	4.185

Table 6-8 Error statistics for Henry Hagg Lake dam outflows compared with continuous water quality data.

Parameter	No. of Data	Mean Error	Absolute Mean Error	Root Mean Square Error
Temperature (°C)	139739	-0.226	0.806	1.032
Dissolved Oxygen (mg L^{-1})	139709	0.132	0.372	0.499
pH	139644	-0.033	0.171	0.325
Conductivity (µS cm^{-1})	135337	4.622	4.673	5.863

The model predictions closely matched the field data for most of the water quality parameters. The temperature errors were all within one degree Celsius, and the predicted profiles matched the data for every day sampled. The negative mean error is due to the model underpredicting temperatures, especially in the hypolimnion. Further increasing the tributary inflow temperatures or adjusting the extinction coefficients could help improve the statistics, but overall, the model is able to successfully predict the lake temperatures throughout the simulation period. The profile statistics were the largest for alkalinity and total suspended solids. There was limited data available for total suspended solids which makes it difficult to accurately compare the model to the field data. The alkalinity values are very high (between 20-40 mg L^{-1}) so the error statistics of 2-4 mg L^{-1} are more reasonable than for a parameter with lower average values.

The dissolved oxygen and pH profiles closely matched the field data for most of the days sampled, and the model predictions generally followed the trend of higher values of dissolved oxygen and pH near the surface and lower values at deeper locations. The model was not able to capture the peak of dissolved oxygen and pH that occurred on some days below the surface at a depth of approximately ten meters. The lack of dissolved oxygen and pH could be related to algae photosynthesis and algae stoichiometry. While the model was able to successfully predict chlorophyll a peaks

below the surface, the model predictions were generally lower than the field data. Further refinement of the algae groups and algae coefficients to improve the chlorophyll a predictions in the model might also improve the pH and dissolved oxygen statistics since the stoichiometry and growth of algae can greatly affect these two parameters. As shown in Figure 6-16 (percent biomass comparison for each algal group), the modeled algal groups closely matched the relative biomass percentages of the field data for the fall and winter seasons, but the diatom and green groups in the spring and summer seasons did not match as closely. However, the model cyanobacteria group closely matched the field data in all seasons. Increasing diatom growth in the spring and summer months might improve the chlorophyll a statistics since April through July are typically the months that the model is not able to capture the chlorophyll a peak below the surface. One source of error in the algal groupings is that the field data was sampled approximately once per month which limits the available data to compare with the model predictions. Changes in relative abundance of each algal species between sampling periods will not be captured in the field data used for comparison and will affect the results.

The model predictions for nutrients generally matched the field data. The concentrations for the nitrogen species, phosphate, and total phosphorus were all very low, but the model predictions were very close to the field data. The model predictions for nitrate-nitrite generally matched the field data trend of lower concentrations near the surface and higher concentrations lower in the lake. The field data showed very little variation throughout the water column for phosphate and total phosphorus, but the model predicted slightly higher concentrations near the bottom. The model predictions for

dissolved organic carbon and total organic carbon were also close to the field data values, although there was not very much data available for dissolved organic carbon.

The model predictions of the dam outflow for temperature, dissolved oxygen, and pH all matched the general trends of the field data. Similar to the profiles for temperature, the model predicted slightly colder temperatures on average as indicated by the negative mean error. The model successfully predicted the yearly fluctuations in dissolved oxygen and pH. The sharp decreases and increases in dissolved oxygen shown in the field data are likely the result of equipment error, but overall, the model closely matched the field data. The model was not able to match the conductivity in the outflow as closely as the other three parameters, but the model was able to capture the general trend of the conductivity fluctuations.

6.3 Testing of CE-QUAL-W2 Toxin Model on Henry Hagg Lake

The code updates to the water quality subroutine were compiled with the entire CE-QUAL-W2 code and modeled using Henry Hagg Lake. Toxin data was available at Henry Hagg Lake between April 3, 2019 to May 6, 2019 for microcystin and cylindrospermopsin. All the recorded values for cylindrospermopsin were classified as non-detects, and all but four measurements for microcystin were recorded as non-detects. Values of 0.15 and 0.43 ng mL^{-1} were recorded on April 3, 2019 and values of 0.15 and 0.2 ng mL^{-1} were recorded on April 22, 2019 at the surface of the water. The toxin results from the Henry Hagg Lake model were compared to these four values as an estimated range of toxins at the lake. Figure 6-18 shows the relative abundance of the different cyanobacteria species in Henry Hagg Lake over the entire period of data collection (2014 – 2020).

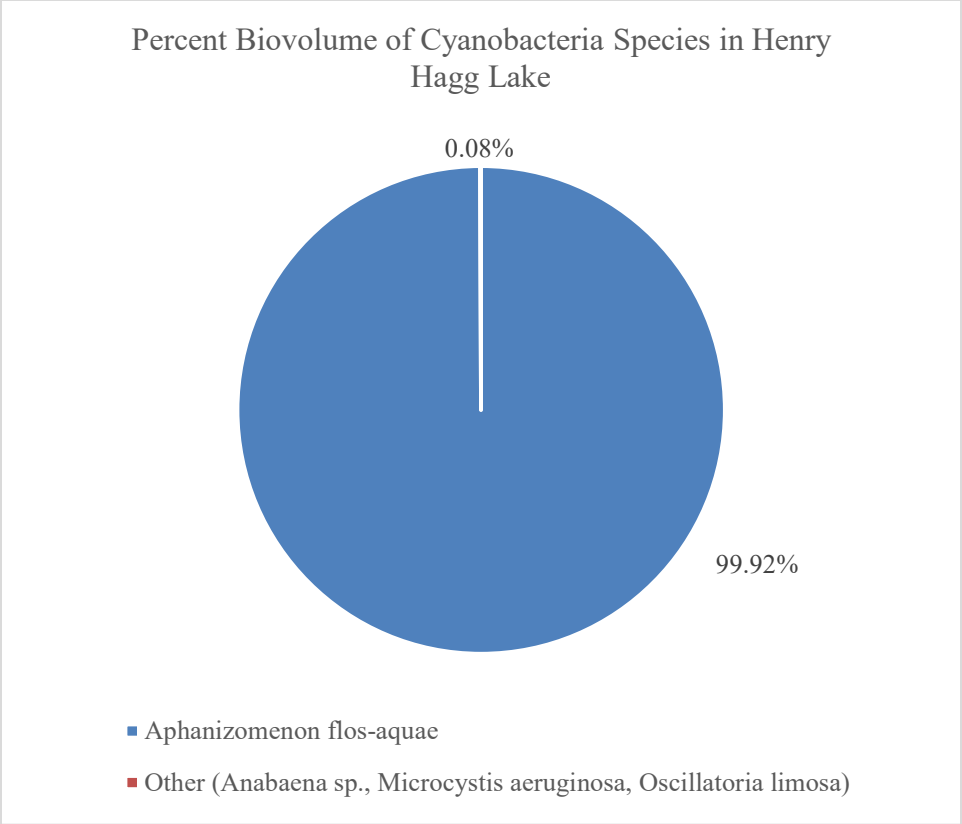

Figure 6-18 Relative abundance of cyanobacteria species in Henry Hagg Lake from 2014 through 2020.

Strains from the *Aphanizomenon flos-aquae* species are known to produce cylindrospermopsin which contribute to more than 99 percent of the total biomass in the lake. The other species, *Anabaena sp., Microcystis aeruginosa,* and *Oscillatoria limosa*, account for less than one percent of the total biomass in the lake. Strains from *Microcystis aeruginosa* and *Anabaena sp.* are known to produce microcystin.

Four model scenarios were conducted to test the functionality of the code updates. The first model scenario tested the toxin decay in the reservoir without any toxin production by the algal groups within the lake. This was achieved by adding an initial toxin to the lake and setting all the *CTP* (fraction of algal group producing a toxin) values to zero for all the algal groups. The second model scenario tested toxin decay and

production by cyanobacteria death only and for only one algal group (algal group 3). The third scenario tested toxin decay and production by cyanobacteria death and release for only algal group 3. The fourth scenario tested toxin decay and production with all three algal groups set as toxin producers to test the ability of the model to add together intracellular toxins for multiple groups. Model results from the third scenario were compared to field data of toxin concentrations in Henry Hagg Lake. This scenario was chosen because it modeled all four of the toxin parameters for the two toxins of concern at the lake and from only the cyanobacteria group. Table 6-9 summarizes the control file parameters chosen for each scenario based on Equations (5-1) and (5-2).

Table 6-9 Summary of toxin model test scenarios for Henry Hagg Lake.

Parameter	Scenario 1		Scenario 2		Scenario 3		Scenario 4	
	MC	**CYN**	**MC**	**CYN**	**MC**	**CYN**	**MC**	**CYN**
CTP, fraction	0	0	0.1	0.3	0.1	0.3	0.1	0.3
CTB, fraction	0	0	0.02	0.005	0.02	0.005	0.02	0.005
CTR, day^{-1}	0	0	0	0	0.01	0.03	0.01	0.03
CTD, day^{-1}	0.1	0.05	0.1	0.05	0.1	0.05	0.1	0.05
Initial concentration	10 ng/mL		0 ng/mL		0 ng/mL		0 ng/mL	

6.3.1 Results

Extracellular toxin concentrations as predicted by CE-QUAL-W2 at the surface of the lake in segment 29 for each of the four scenarios are shown in Figure 6-19, Figure 6-20, Figure 6-21, and Figure 6-22.

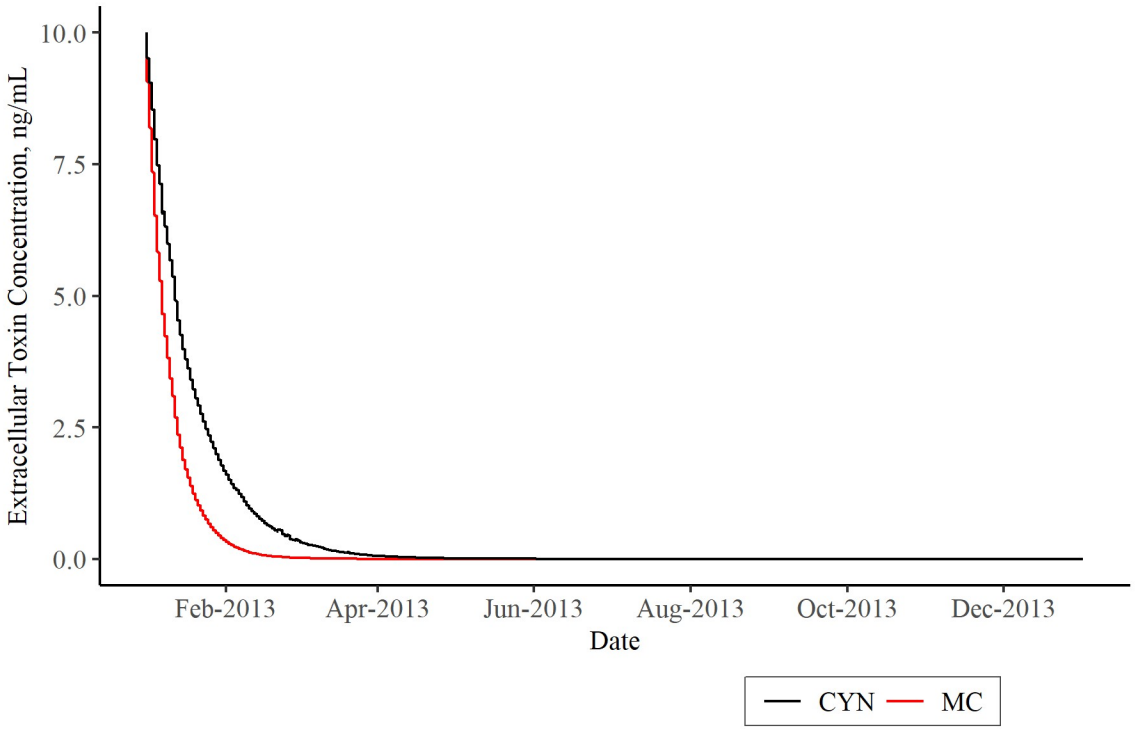

Figure 6-19 CE-QUAL-W2 toxin results for scenario 1 at the surface of segment 29.

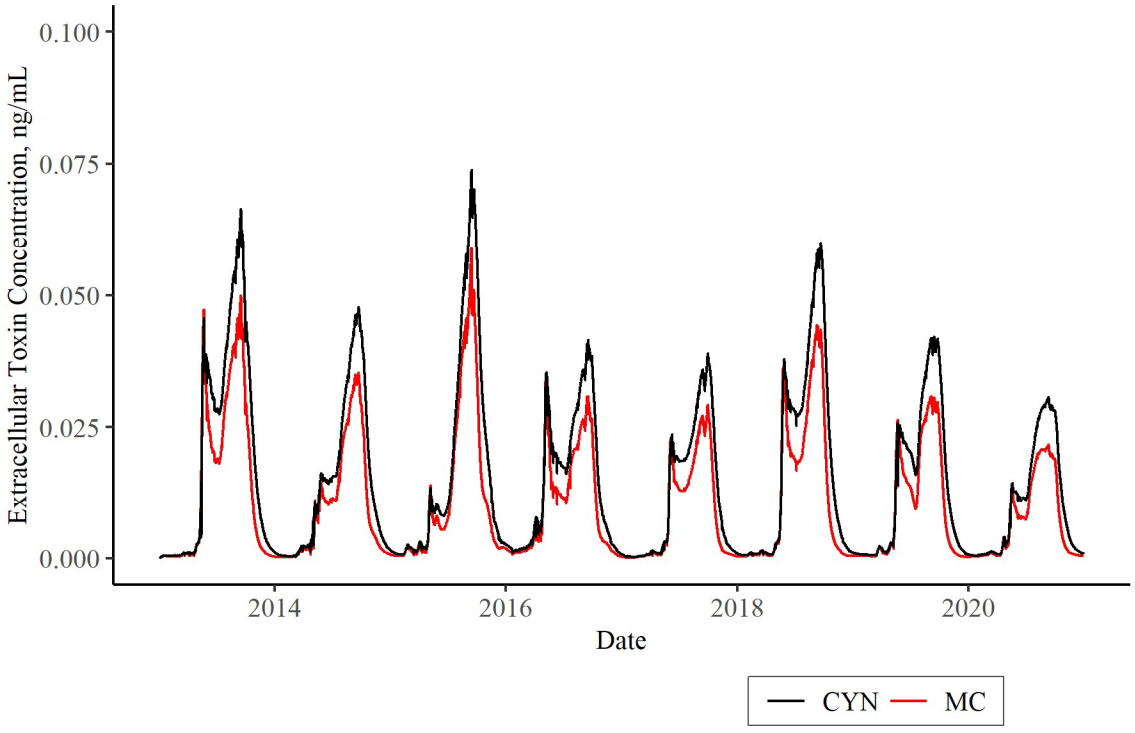

Figure 6-20 CE-QUAL-W2 toxin results for scenario 2 at the surface of segment 29.

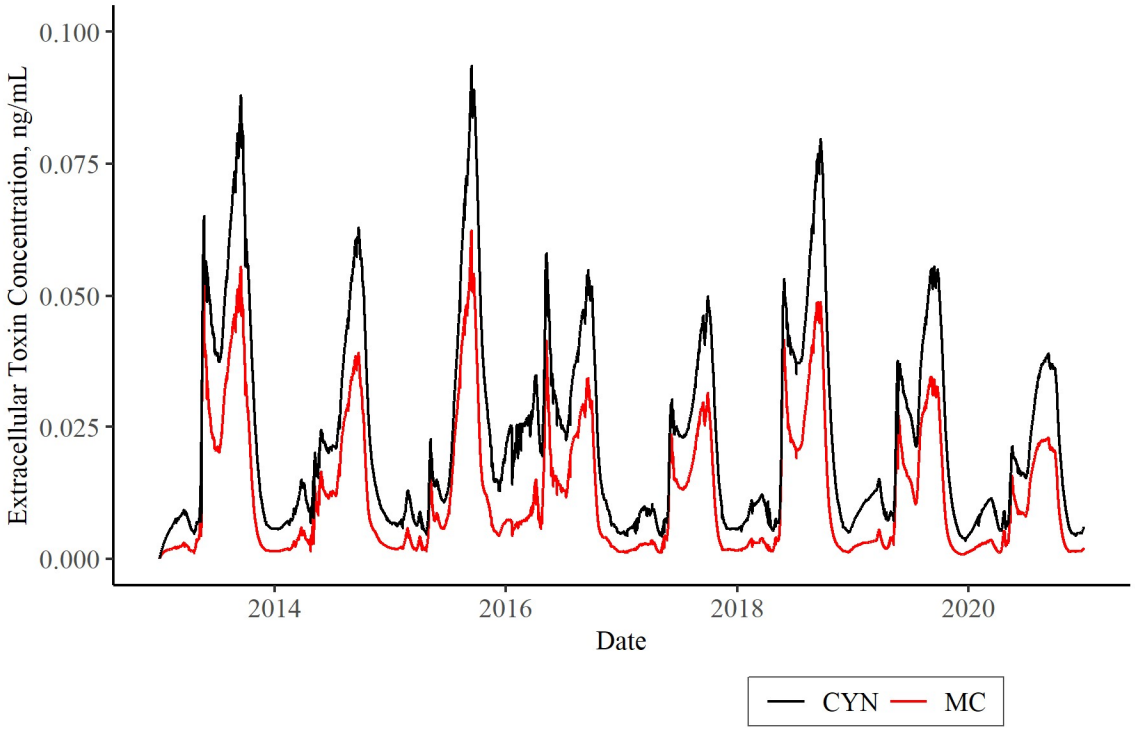

Figure 6-21 CE-QUAL-W2 toxin results for scenario 3 at the surface of segment 29.

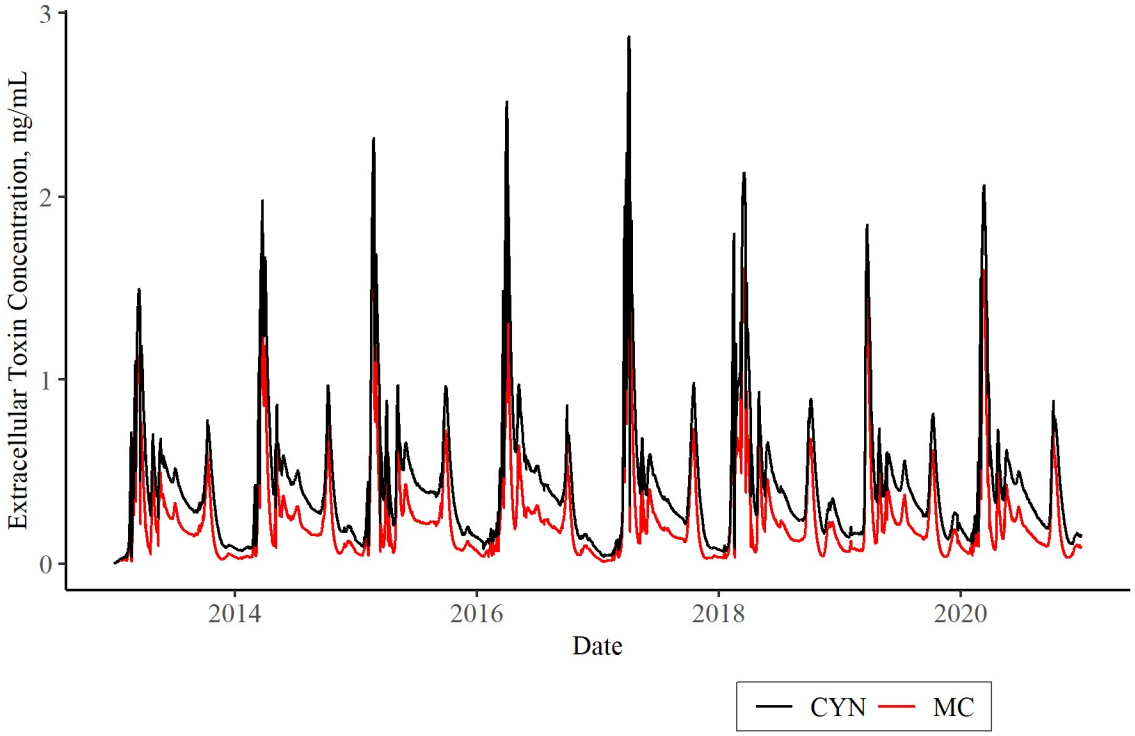

Figure 6-22 CE-QUAL-W2 toxin results for scenario 4 at the surface of segment 29.

The results from each scenario matched the predicted outcomes as based on the toxin parameters chosen for each scenario. The results for the first scenario showed a faster decay for microcystin than cylindrospermopsin which agrees with the higher decay rate for microcystin chosen than cylindrospermopsin. The results for the second scenario showed peaks of extracellular concentrations in the summer with concentrations close to zero in the winter months. Cylindrospermopsin was given a larger *CTP* value and a slower decay rate which result in the higher cylindrospermopsin concentrations than microcystin. The results for the third scenario showed peaks at similar time periods to the second scenario but the overall concentrations were higher. Since both toxins were provided release rates for this third scenario it matches the expected outcome that the concentrations would be higher than the second scenario. The fourth scenario showed an even greater increase in concentrations for both toxins which is what was expected to occur since all three algal groups were turned on as toxin producers.

Conservation of the toxin mass was assessed using the snapshot output file generated by the model. The model is conserving mass for each constituent if the spatially integrated mass (change in mass for each branch) is equal to the temporally integrated mass (difference in the sum of all incoming mass and sum of all outgoing mass). If the two values are equal to each other then mass is not being created or destroyed. Percent errors between the two values should be on the order of 10^{-6} to 10^{-13} which means the model is conserving mass to machine accuracy (Wells, 2020a). Percent errors are on the order of 10^{-8} at the beginning of the model run (12 hours of simulation) for microcystin and cylindrospermopsin in branch 1. All other constituents have the same order of magnitude of error. Percent errors are on the order of 10^{0} and 10^{-1} at the

end of the model run (2919 days and 12 hours of simulation) for microcystin and cylindrospermopsin, respectively. The percent error for the other constituents are on the order of 10^{-2} to 10^{1}. The error at the end of the model simulation is greater than the desired error which means that some mass is being created or destroyed for the two toxins. However, since all the other constituents have similar percent errors, it does not appear that the toxin masses are being conserved differently. There may be a small bug in the code or stability issue in the model that caused these discrepancies in the mass balances of the constituents.

Model results from the third scenario were compared to the measured toxin values for microcystin (0.15 to 0.43 ng mL^{-1}) and cylindrospermopsin (no toxin detected). Even though no cylindrospermopsin was detected in the lake, the toxin was still included in the model simulations to test the model's ability to predict multiple toxin concentrations and to test how the dynamics vary between microcystin and cylindrospermopsin. Figure 6-23 shows the concentration and percent for intracellular and extracellular microcystin and Figure 6-24 shows the concentration and percent for intracellular and extracellular cylindrospermopsin for the third scenario.

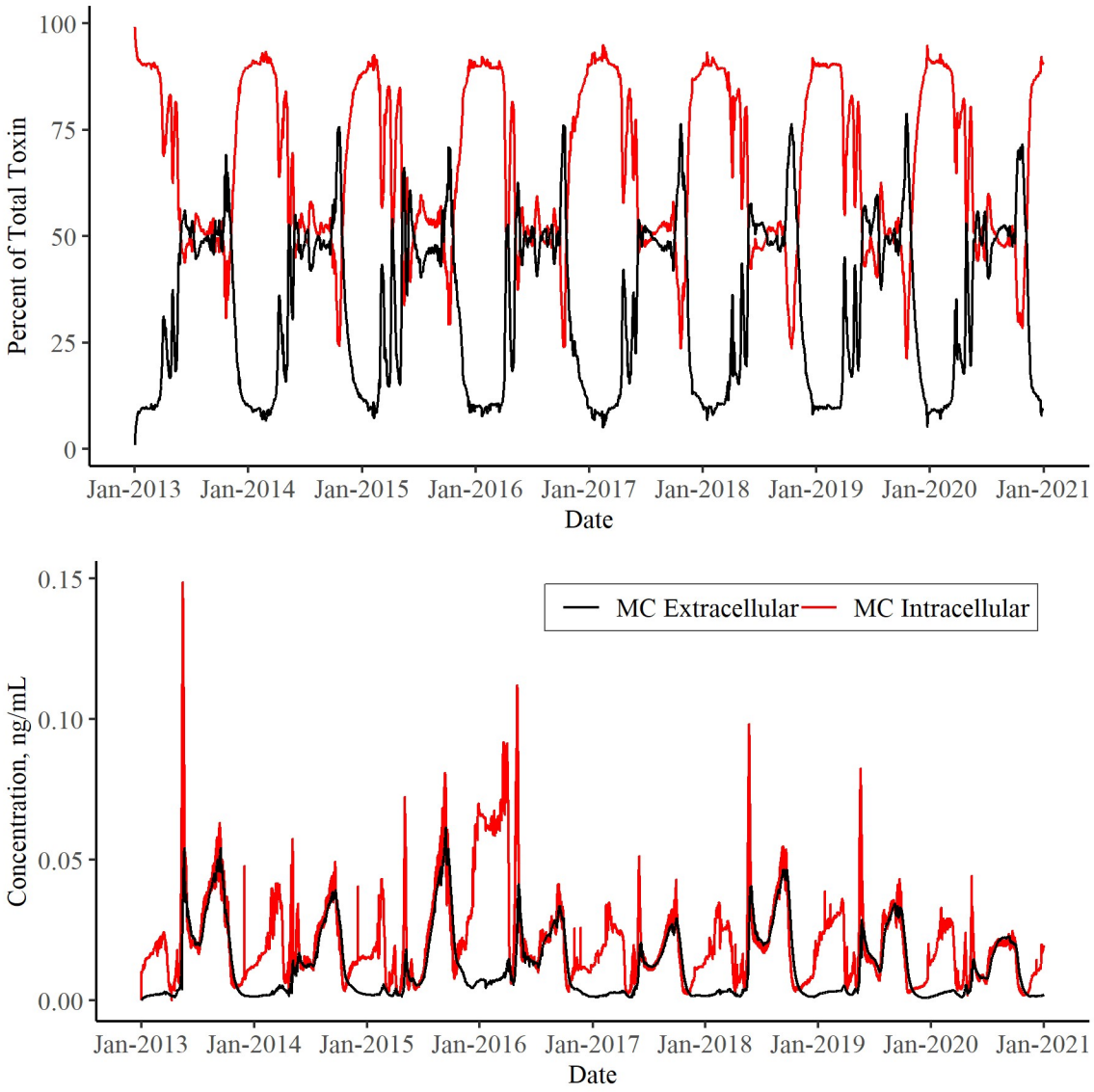

Figure 6-23 Scenario 3 toxin results for microcystin: (top) intracellular and extracellular percent of the total toxin concentration, (bottom) intracellular and extracellular toxin concentrations.

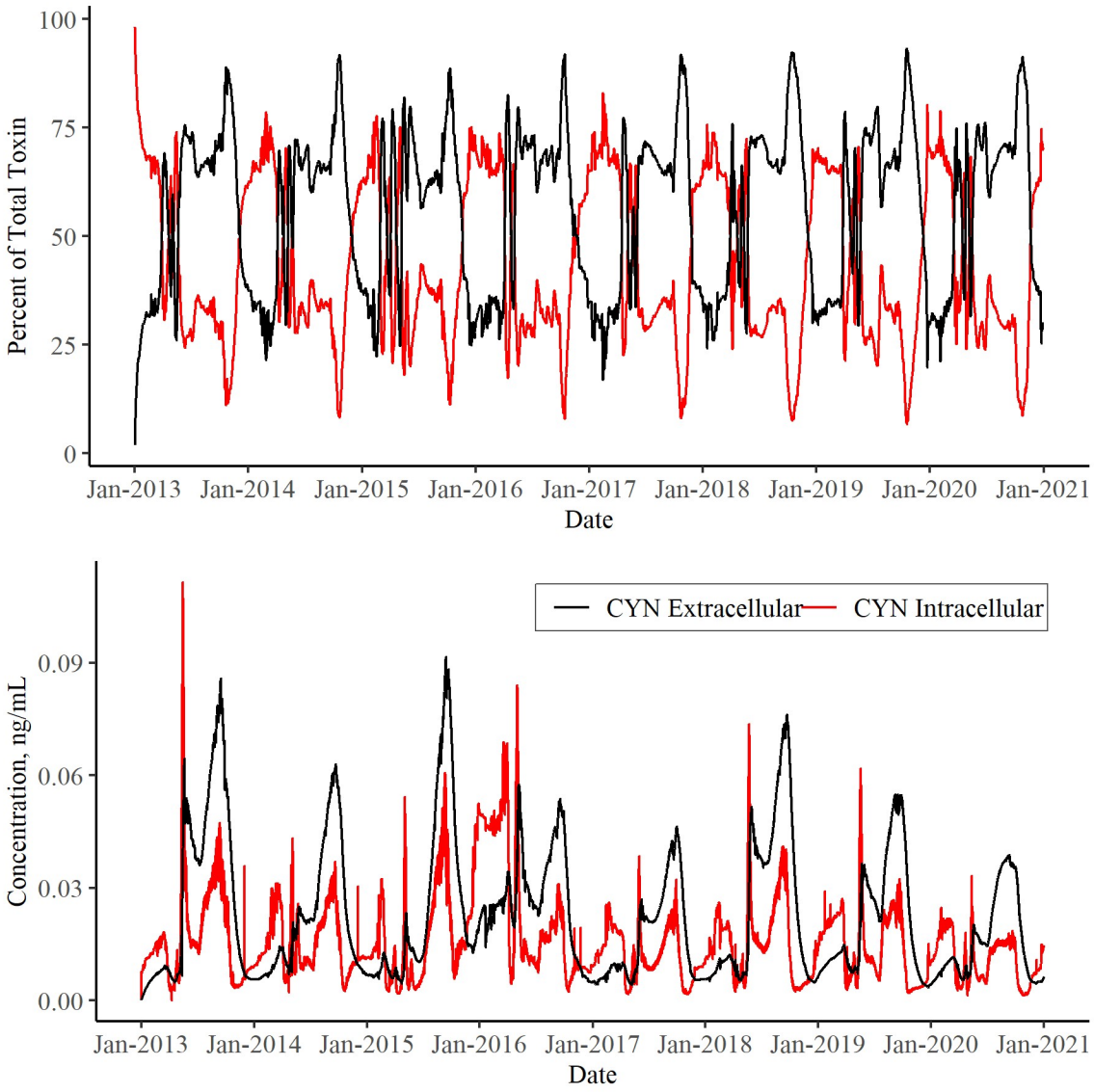

Figure 6-24 Scenario 3 toxin results for cylindrospermopsin: (top) intracellular and extracellular percent of the total toxin concentration, (bottom) intracellular and extracellular toxin concentrations.

The model results show peak microcystin concentrations that ranged from about 0.05 to 0.17 ng mL^{-1} in the summer months and peak cylindrospermopsin concentrations that ranged from about 0.05 to 0.15 ng mL^{-1} in the summer months. The lab method for measuring microcystin was ELISA (enzyme-linked immunosorbent assay) with a detection limit of 0.15 ng mL^{-1}, and the lab method for measuring cylindrospermopsin was LC-MS (liquid chromatography, mass spectrometry) with a detection limit of 0.05 ng

mL^{-1}. Both methods provide an analysis of total toxin concentrations (sum of intracellular and extracellular) since a triple freeze and thaw process is used to lyse intact cells prior to analysis (Wendelken, 2015; Zaffiro, Rosenblum and Wendelken, 2016). The lowest microcystin values recorded were 0.15 ng mL^{-1} which is the lowest that MC can be detected. It is likely that there was microcystin present at concentrations below 0.15 ng mL^{-1} in the lake but was not able to be detected. The peak microcystin concentrations as predicted by the model are in the approximate range of those measured in the field, but since there is minimal field data it is difficult to adequately compare these values. No cylindrospermopsin was recorded in the lake during the time of measurements even though the majority of the species present have cylindrospermopsin producing strains. This is an indicator that the strains present of *Aphanizomenon flos-aquae* do not produce toxins or produce toxins at low levels not able to be detected in the field measurements.

The relative fractions of the intracellular and extracellular components of each toxin are similar to literature values reported for microcystin and cylindrospermopsin. The intracellular fraction of microcystin is often found at a higher percent than the extracellular fraction. Figure 6-23 shows that the model predicted approximately equal fractions of intracellular and extracellular microcystin during the summer months and predicted the intracellular toxin to be about 90 percent of the total toxin concentration during winter months. Intracellular microcystin is usually found at about 70 percent of the total toxin concentration, so the model results in the summer are about 20 percent lower than what would be expected. Increasing the decay rate or decreasing the release rate would provide for a lower extracellular concentration. Cylindrospermopsin is more

often found at higher extracellular concentrations. Figure 6-24 shows that the model predicted extracellular CYN to be about 75 percent of the total toxin concentration which is in agreement with CYN being found at higher extracellular concentrations. The model predicted that most of the toxin would be present as intracellular toxin in the winter for both cylindrospermopsin and microcystin. This is likely due to increased flows and more mixing in the winter that lead to dilution and removal of the extracellular toxin that exceed the amount of toxin being produced during those months.

Chapter 7: Conclusions and Continuing Research

The goals of this research were to develop models for the transport and fate of cyanotoxins in surface waterbodies and to incorporate the models into the two-dimensional (longitudinal and vertical) hydrodynamic and water quality model CE-QUAL-W2. Additional goals of this research were to update and improve the water quality predictions of the existing CE-QUAL-W2 Henry Hagg Lake model. Preliminary models for the transport and fate of intracellular and extracellular cyanotoxins were developed and tested using published laboratory data. The preliminary models were able to successfully achieve similar results to published data from laboratory experiments for both microcystin and cylindrospermopsin. The models contain various parameters that can be adjusted depending on the type of toxin being produced or the species producing the toxin such as the leakage and loss rates, decay rates, and ratio of intracellular toxin to dry weight organic matter (β). These parameters allow for flexibility in applying the model to different cyanobacteria species and different toxins. While the model allows for flexibility in choosing values for each parameter, the preliminary model is limited in its ability to dynamically predict toxin concentrations based on varying environmental conditions. The overall quantity of intracellular toxin is dependent on the growth and loss kinetics of cyanobacteria mass which are functions of light, temperature, and nutrients, but the ratio of intracellular toxin to dry weight organic matter is a constant value. Some cyanobacteria species may only produce toxins under certain conditions, and the quantity of toxin can vary depending on the environmental conditions. Using a constant value for the ratio of toxin to biomass will not capture these dynamics. The decay rates have also been shown to vary depending on environmental parameters.

Future work is needed to develop each of the model parameters as functions of changing environmental conditions such as light, temperature, and pH.

A model for Henry Hagg Lake had been previously developed in CE-QUAL-W2 for the simulation period of January 2013 through December 2015. Part of this research was to increase the simulation period of the model through the end of 2020. This was done by updating all the input files (meteorological, flow, temperature, and concentration) through 2020 and then calibrating the model using data observed in the lake. Data used for the meteorological, flow, and temperature input files were available on a near continuous basis, but the concentration data used for the input files was only measured approximately once per month. Concentration values were interpolated between field measurements to use in the model. The methodology used to develop the concentration inputs using the measured field data was reproduced from those used to develop the data for the original Henry Hagg Lake model.

The model was calibrated to field data measured through the end of 2020 by updating values in the model for algal groups, light extinction, sediment, nutrients, and boundary conditions. The model predictions were compared to field data measured in the lake just before the dam and at the dam outflow. The model was able to match the general trend of the field data for most of the water quality parameters tested. Temperature, dissolved oxygen, pH, and chlorophyll a had the most data measurements for comparison at the location before the dam. Temperature error statistics were within 1.0 degree Celsius, dissolved oxygen errors were within 1.2 mg L^{-1}, pH errors were within 0.5 pH units, and chlorophyll a errors were within 2 μg L^{-1}. The model was not able to capture the peak concentrations below the surface for pH and dissolved oxygen.

The model was able to capture some peaks of chlorophyll a below the surface, but the model predictions were generally lower than the field data. Further refinement of chlorophyll a will likely improve the statistics for pH and dissolved oxygen as well.

The algal groups were also refined in the model to better match relative biomass percentages of the algae measured at the lake. Three algal groups were simulated in the model to represent the eight algal groups identified at Henry Hagg Lake. Group 1 was compared to diatoms, group 2 was compared to the sum of chrysophytes, cryptophytes, dinoflagellates, euglenoids, greens, and unidentified flagellates, and group 3 was compared to cyanobacteria. The modeled algal groups most closely matched the relative biomass percentages of the field data in fall and winter. Group 1 and group 2 did not match the field data as closely in the spring or summer, but group 3 (cyanobacteria) was able to closely match the field data for cyanobacteria in these seasons. Additional work is required to better match the biomass percentages for the spring and summer seasons. One possible option is to create a second diatom group that grows faster at warmer temperatures. This may allow for separation of algal dynamics between the two diatom groups to better match the field data. However, since the field data is only collected once per month, variations in algal growth between sampling events will not be captured and lead to limitations in the comparisons between the model results and field data. In addition, algae growth can be patchy across a waterbody so that the concentration measured at one location might be very different than the concentration at another location also impacting the overall comparisons. Overall, the model was able to provide water quality predictions that closely matched the field data for many of the parameters tested.

The preliminary toxin models were simplified and then incorporated into the CE-QUAL-W2 code and tested on the Henry Hagg Lake model. Four scenarios were used to test the functionality of the toxin models in CE-QUAL-W2. The model results from each scenario matched the predicted outcomes based on the toxin parameters chosen for each scenario. There was limited field data available for the toxins which made it difficult to adequately compare the model results to the measured values. Overall, the model predicted microcystin concentrations close to those that were measured in the field. No cylindrospermopsin was detected in the field so no comparisons can be made between the model results of cylindrospermopsin and the field data. However, the model results of the relative fractions of cylindrospermopsin concentrations matched what would be expected based on literature data if cylindrospermopsin was produced in the lake. The model results showed that intracellular concentrations of both toxins were higher than the extracellular concentrations in the winter months. This is likely due to higher flows and more mixing in the winter leading to dilution of the extracellular concentration.

As mentioned previously, the model parameters are currently input as constant values and are therefore limited in their ability to predict toxin concentrations under changing environmental conditions that may affect the quantity of toxin produced and the rate at which the toxins decay. Additional work is needed to model the parameters as functions of environmental parameters. The toxin data available in Henry Hagg Lake was limited so it was difficult to compare the model results to the field data. Additional work is required to fully test the toxin model in CE-QUAL-W2. Further applications of the model to waterbodies with more consistent toxin data will help verify the accuracy of the CE-QUAL-W2 model at predicting toxin concentrations. Currently only four toxins

are included in the model, but additional toxins could be incorporated through more research into their production and decay rates. The toxin model developed as part of this project is a first step in modeling toxin fate and transport in surface waterbodies using CE-QUAL-W2.

References

Almuhtaram, H. *et al.* (2018) 'Cyanotoxins and Cyanobacteria Cell Accumulations in Drinking Water Treatment Plants with a Low Risk of Bloom Formation at the Source', *Toxins*, 10(11), p. 430. doi: 10.3390/toxins10110430.

Antoniou, M. G., de la Cruz, A. A. and Dionysiou, D. D. (2005) 'Cyanotoxins: New Generation of Water Contaminants', *Journal of Environmental Engineering*, 131(9), pp. 1239–1243. doi: 10.1061/(ASCE)0733-9372(2005)131:9(1239).

Ballot, A. *et al.* (2010) 'First report of anatoxin-a-producing cyanobacterium Aphanizomenon issatschenkoi in northeastern Germany', *Toxicon*, 56(6), pp. 964–971.

Banker, R. *et al.* (2000) '7-Epicylindrospermopsin, a Toxic Minor Metabolite of the Cyanobacterium *Aphanizomenon o valisporum* from Lake Kinneret, Israel', *Journal of Natural Products*, 63(3), pp. 387–389. doi: 10.1021/np990498m.

Bouma-Gregson, K., Power, M. E. and Bormans, M. (2017) 'Rise and fall of toxic benthic freshwater cyanobacteria (Anabaena spp.) in the Eel river: Buoyancy and dispersal', *Harmful Algae*, 66, pp. 79–87. doi: 10.1016/j.hal.2017.05.007.

Bowie, G. L. *et al.* (1985) 'Rates, constants, and kinetics formulations in surface water quality modeling', *EPA*, 600, pp. 3–85.

Buratti, F. M. *et al.* (2017) 'Cyanotoxins: producing organisms, occurrence, toxicity, mechanism of action and human health toxicological risk evaluation', *Archives of Toxicology*, 91(3), pp. 1049–1130. doi: 10.1007/s00204-016-1913-6.

Carmichael, W. (1992) 'Cyanobacteria secondary metabolites—the cyanotoxins', *Journal of applied bacteriology*, 72(6), pp. 445–459.

Carneiro, R. L. *et al.* (2013) 'Use of the cell quota and chlorophyll content for normalization of cylindropermopsin produced by two Cylindrospermopsis raciborskii strains grown under different light intensities', *Ecotoxicology and Environmental Contamination*, 8(1), pp. 93–100.

Carneiro, R. L., Pacheco, A. B. F. and De Oliveira e Azevedo, S. M. F. (2013) 'Growth and Saxitoxin Production by Cylindrospermopsis raciborskii (Cyanobacteria) Correlate with Water Hardness', *Marine Drugs*, 11(8), pp. 2949–2963. doi: 10.3390/md11082949.

Castro, D. *et al.* (2004) 'The effect of temperature on growth and production of paralytic shellfish poisoning toxins by the cyanobacterium Cylindrospermopsis raciborskii C10', *Toxicon*, 44(5), pp. 483–489. doi: 10.1016/j.toxicon.2004.06.005.

CCALA (2020) *Jaworski's Medium*, *Culture Collection of Autotrophic Organisms*. Available at: https://ccala.butbn.cas.cz/en/jaworskis-medium (Accessed: 26 February 2021).

Chapra, S. C. (2008) *Surface Water-Quality Modeling*. Waveland Press.

Chiswell, R. K. *et al.* (1999) 'Stability of cylindrospermopsin, the toxin from the cyanobacterium, Cylindrospermopsis raciborskii: Effect of pH, temperature, and sunlight on decomposition', *Environmental Toxicology*, 14(1), pp. 155–161. doi: 10.1002/(SICI)1522-7278(199902)14:1<155::AID-TOX20>3.0.CO;2-Z.

Chorus, I. and Welker, M. (2021) *Toxic cyanobacteria in water: a guide to their public health consequences, monitoring and management*. CRC Press.

Christensen, V. G. and Khan, E. (2020) 'Freshwater neurotoxins and concerns for human, animal, and ecosystem health: A review of anatoxin-a and saxitoxin', *Science of The Total Environment*, 736, p. 139515. doi: 10.1016/j.scitotenv.2020.139515.

Christiansen, G. *et al.* (2003) 'Microcystin Biosynthesis in Planktothrix: Genes, Evolution, and Manipulation', *Journal of Bacteriology*, 185(2), pp. 564–572. doi: 10.1128/JB.185.2.564-572.2003.

Cirés, S. *et al.* (2011) 'Cylindrospermopsin production and release by the potentially invasive cyanobacterium Aphanizomenon ovalisporum under temperature and light gradients', *Harmful Algae*, 10(6), pp. 668–675. doi: 10.1016/j.hal.2011.05.002.

Cires, S. and Ballot, A. (2016) 'A review of the phylogeny, ecology and toxin production of bloom-forming Aphanizomenon spp. and related species within the Nostocales (cyanobacteria)', *Harmful Algae*, 54, pp. 21–43.

Corbel, S., Mougin, C. and Bouaïcha, N. (2014) 'Cyanobacterial toxins: Modes of actions, fate in aquatic and soil ecosystems, phytotoxicity and bioaccumulation in agricultural crops', *Chemosphere*, 96, pp. 1–15. doi: 10.1016/j.chemosphere.2013.07.056.

Cruz, A. A. de la *et al.* (2013) 'A review on cylindrospermopsin: the global occurrence, detection, toxicity and degradation of a potent cyanotoxin', *Environmental Science: Processes & Impacts*, 15(11), pp. 1979–2003. doi: 10.1039/C3EM00353A.

Davis, T. W. *et al.* (2014) 'Investigating the production and release of cylindrospermopsin and deoxy-cylindrospermopsin by Cylindrospermopsis raciborskii over a natural growth cycle', *Harmful Algae*, 31, pp. 18–25. doi: 10.1016/j.hal.2013.09.007.

Facey, J. A., Apte, S. C. and Mitrovic, S. M. (2019) 'A Review of the Effect of Trace Metals on Freshwater Cyanobacterial Growth and Toxin Production', *Toxins*, 11(11). doi: 10.3390/toxins11110643.

Falconer, I. R. (2005) *Cyanobacterial toxins of drinking water supplies: cylindrospermopsins and microcystins*. Boca Raton, FL: CRC Press.

Fristachi, A. *et al.* (2008) 'Occurrence of cyanobacterial harmful algal blooms workgroup report', in *Cyanobacterial harmful algal blooms: state of the science and research needs*. Springer, pp. 45–103.

Gagnon, A. and Pick, F. R. (2012) 'Effect of Nitrogen on Cellular Production and Release of the Neurotoxin Anatoxin-A in a Nitrogen-Fixing Cyanobacterium', *Frontiers in Microbiology*, 3. doi: 10.3389/fmicb.2012.00211.

Glibert, P. M. (2020) 'Harmful algae at the complex nexus of eutrophication and climate change', *Harmful Algae*, 91, p. 101583. doi: 10.1016/j.hal.2019.03.001.

Gouvêa, S. P., Boyer, G. L. and Twiss, M. R. (2008) 'Influence of ultraviolet radiation, copper, and zinc on microcystin content in Microcystis aeruginosa (Cyanobacteria)', *Harmful Algae*, 7(2), pp. 194–205. doi: 10.1016/j.hal.2007.07.003.

Graham, J. L. *et al.* (2018) *Water-quality conditions with an emphasis on cyanobacteria and associated toxins and taste-and-odor compounds in the Kansas River, Kansas, July 2012 through September 2016*. 2328–0328. US Geological Survey.

Heath, M. W. *et al.* (2014) 'Effects of nitrogen and phosphorus on anatoxin-a, homoanatoxin-a, dihydroanatoxin-a and dihydrohomoanatoxin-a production by Phormidium autumnale', *Toxicon*, 92, pp. 179–185. doi: 10.1016/j.toxicon.2014.10.014.

Heisler, J. *et al.* (2008) 'Eutrophication and harmful algal blooms: A scientific consensus', *Harmful Algae*, 8(1), pp. 3–13. doi: 10.1016/j.hal.2008.08.006.

Hesse, K., Kohl, J. and Chorus, I. (2001) *Effects of light and nutrient supply on growth and microcystin concentration of different strains of Microcystis aeruginosa*, *Cyanotoxins: Occurrence, Effects, Controlling Factors*. Springer: Heidelberg/Berlin, Germany.

Huang, I.-S. and Zimba, P. V. (2019) 'Cyanobacterial bioactive metabolites—A review of their chemistry and biology', *Harmful Algae*, 86, pp. 139–209. doi: 10.1016/j.hal.2019.05.001.

Indrasena, W. M. and Gill, T. A. (2000) 'Storage stability of paralytic shellfish poisoning toxins', *Food Chemistry*, 71(1), pp. 71–77. doi: 10.1016/S0308-8146(00)00143-6.

Jähnichen, S. *et al.* (2007) 'Impact of Inorganic Carbon Availability on Microcystin Production by Microcystis aeruginosa PCC 7806', *Applied and Environmental Microbiology*, 73(21), pp. 6994–7002. doi: 10.1128/AEM.01253-07.

Jähnichen, S., Long, B. M. and Petzoldt, T. (2011) 'Microcystin production by Microcystis aeruginosa: Direct regulation by multiple environmental factors', *Harmful Algae*, 12, pp. 95–104. doi: 10.1016/j.hal.2011.09.002.

Jiang, Y. *et al.* (2015) 'Identification of genes for anatoxin-a biosynthesis in Cuspidothrix issatschenkoi', *Harmful Algae*, 46, pp. 43–48. doi: 10.1016/j.hal.2015.05.005.

Jones, G. J. and Negri, A. P. (1997) 'Persistence and degradation of cyanobacterial paralytic shellfish poisons (PSPs) in freshwaters', *Water Research*, 31(3), pp. 525–533.

Kayal, N., Newcombe, G. and Ho, L. (2008) 'Investigating the fate of saxitoxins in biologically active water treatment plant filters', *Environmental Toxicology*, 23(6), pp. 751–755. doi: 10.1002/tox.20384.

Kellmann, R. *et al.* (2008) 'Biosynthetic Intermediate Analysis and Functional Homology Reveal a Saxitoxin Gene Cluster in Cyanobacteria', *Applied and Environmental Microbiology*, 74(13), pp. 4044–4053. doi: 10.1128/AEM.00353-08.

León, C. *et al.* (2019) 'Study of cyanotoxin degradation and evaluation of their transformation products in surface waters by LC-QTOF MS', *Chemosphere*, 229, pp. 538–548.

Long, B. (2001) *The influence of growth conditions on the intracellular microcystin quota of Microcystis aeruginosa*. doi: 10.13140/RG.2.1.3420.7605.

Long, B. M., Jones, G. J. and Orr, P. T. (2001) 'Cellular microcystin content in N-limited Microcystis aeruginosa can be predicted from growth rate', *Appl. Environ. Microbiol.*, 67(1), pp. 278–283.

Lopez, C. B. *et al.* (2008) *Scientific assessment of freshwater harmful algal blooms*. Washington, D.C.: Interagency Working Group on Harmful Algal Blooms, Hypoxia, and Human Health of the Joint Subcommittee on Ocean Science and Technology. Available at: http://www.cop.noaa.gov/stressors/extremeevents/hab/habhrca/FreshwaterReport_final_2008.pdf (Accessed: 15 March 2020).

Méjean, A. *et al.* (2009) 'Evidence that Biosynthesis of the Neurotoxic Alkaloids Anatoxin-a and Homoanatoxin-a in the Cyanobacterium *Oscillatoria* PCC 6506 Occurs on a Modular Polyketide Synthase Initiated by L -Proline', *Journal of the American Chemical Society*, 131(22), pp. 7512–7513. doi: 10.1021/ja9024353.

Méjean, A. *et al.* (2014) 'Biosynthesis of anatoxin-a and analogues (anatoxins) in cyanobacteria', *Toxicon*, 91, pp. 15–22. doi: 10.1016/j.toxicon.2014.07.016.

Merel, S. *et al.* (2013) 'State of knowledge and concerns on cyanobacterial blooms and cyanotoxins', *Environment International*, 59, pp. 303–327. doi: 10.1016/j.envint.2013.06.013.

Mihali, T. K. *et al.* (2008) 'Characterization of the Gene Cluster Responsible for Cylindrospermopsin Biosynthesis', *Applied and Environmental Microbiology*, 74(3), pp. 716–722. doi: 10.1128/AEM.01988-07.

Mihali, T. K., Carmichael, W. W. and Neilan, B. A. (2011) 'A Putative Gene Cluster from a Lyngbya wollei Bloom that Encodes Paralytic Shellfish Toxin Biosynthesis', *PLoS One; San Francisco*, 6(2), p. e14657. doi: http://dx.doi.org.proxy.lib.pdx.edu/10.1371/journal.pone.0014657.

Mihali, T. K., Kellmann, R. and Neilan, B. A. (2009) 'Characterisation of the paralytic shellfish toxin biosynthesis gene clusters in Anabaena circinalis AWQC131C and Aphanizomenon sp. NH-5', *BMC Biochemistry*, 10(1), p. 8. doi: 10.1186/1471-2091-10-8.

Negri, A. P. and Jones, G. J. (1995) 'Bioaccumulation of paralytic shellfish poisoning (PSP) toxins from the cyanobacterium Anabaena circinalis by the freshwater mussel Alathyria condola', *Toxicon*, 33(5), pp. 667–678. doi: 10.1016/0041-0101(94)00180-G.

Norris, R. L. *et al.* (1999) 'Deoxycylindrospermopsin, an analog of cylindrospermopsin from Cylindrospermopsis raciborskii', *Environmental Toxicology*, 14(1), pp. 163–165. doi: 10.1002/(SICI)1522-7278(199902)14:1<163::AID-TOX21>3.0.CO;2-V.

Oh, H.-M. *et al.* (2000) 'Microcystin Production by Microcystis aeruginosa in a Phosphorus-Limited Chemostat', *Applied and Environmental Microbiology*, 66(1), pp. 176–179. doi: 10.1128/AEM.66.1.176-179.2000.

OHA (2018) 'Cyanotoxin Facts: Recreational and Drinking Water'.

OHA (2019a) '2019 Advisory Guidelines for Harmful Cyanobacterial Blooms in Recreational Waters'.

OHA (2019b) 'Facts About Oregon's Cyanotoxin Testing Rules'.

OHA (2020a) *Oregon Health Authority : Cyanobacteria Advisory Archive : Cyanobacteria Blooms : State of Oregon*. Available at: https://www.oregon.gov/oha/ph/healthyenvironments/recreation/harmfulalgaeblooms/pages/archive.aspx (Accessed: 24 February 2020).

OHA (2020b) *Oregon Health Authority : Recreational use advisory issued for Upper Klamath Lake July 19 : External Relations Division : State of Oregon*. Available at: https://www.oregon.gov/oha/ERD/Pages/Recreational-use-advisory-issued-Upper-Klamath-Lake-July-19-2019.aspx (Accessed: 24 February 2020).

O'Neil, J. M. *et al.* (2012) 'The rise of harmful cyanobacteria blooms: The potential roles of eutrophication and climate change', *Harmful Algae*, 14, pp. 313–334. doi: 10.1016/j.hal.2011.10.027.

Ongley, S. E., Pengelly, J. J. L. and Neilan, B. A. (2016) 'Elevated Na+ and pH influence the production and transport of saxitoxin in the cyanobacteria Anabaena circinalis AWQC131C and Cylindrospermopsis raciborskii T3', *Environmental Microbiology*, 18(2), pp. 427–438. doi: 10.1111/1462-2920.13048.

Orr, P. T. and Jones, G. J. (1998) 'Relationship between microcystin production and cell division rates in nitrogen-limited Microcystis aeruginosa cultures', *Limnology and oceanography*, 43(7), pp. 1604–1614.

Overman, C. C. M. (2019) 'Modeling Vertical Migration of Cyanobacteria and Zooplankton'.

Paerl, H. W. *et al.* (2016) 'Mitigating cyanobacterial harmful algal blooms in aquatic ecosystems impacted by climate change and anthropogenic nutrients', *Harmful Algae*, 54, pp. 213–222. doi: 10.1016/j.hal.2015.09.009.

Pereira, P., Dias, E. and Franca, S. (2002) 'Persistence of Paralytic Shellfish Toxins in Freshwater Environments', in. *Proceedings of the Xth International Conference on Harmful Algae, October 2002*, Steidinger, K.A., J.H. Landsberg, C.R. Tomas, and G.A. Vargo (Eds.). 2004. Harmful Algae 2002. Florida Fish and Wildlife Conservation Commission, Florida Institute of Oceanography, and Intergovernmental Oceanographic Commission of UNESCO, St. Petersburg, Florida, USA, pp. 166–168.

Pierangelini, M. *et al.* (2014) 'Photosynthetic characteristics of two C ylindrospermopsis raciborskii strains differing in their toxicity', *Journal of Phycology*, 50(2), pp. 292–302.

Pierangelini, M. *et al.* (2015) 'Constitutive Cylindrospermopsin Pool Size in Cylindrospermopsis raciborskii under Different Light and CO_2 Partial Pressure Conditions', *Applied and Environmental Microbiology*. Edited by K. E. Wommack, 81(9), pp. 3069–3076. doi: 10.1128/AEM.03556-14.

Pimentel, J. S. M. and Giani, A. (2014) 'Microcystin Production and Regulation under Nutrient Stress Conditions in Toxic Microcystis Strains', *Applied and Environmental Microbiology*, 80(18), pp. 5836–5843. doi: 10.1128/AEM.01009-14.

Polyak, Y., Zaytseva, T. and Medvedeva, N. (2013) 'Response of Toxic Cyanobacterium Microcystis aeruginosa to Environmental Pollution', *Water, air, and soil pollution*, 224(4), p. 1494. doi: http://dx.doi.org.proxy.lib.pdx.edu/10.1007/s11270-013-1494-4.

Preußel, K. *et al.* (2006) 'First report on cylindrospermopsin producing Aphanizomenon flos-aquae (Cyanobacteria) isolated from two German lakes', *Toxicon*, 47(2), pp. 156–162. doi: 10.1016/j.toxicon.2005.10.013.

Preußel, K. *et al.* (2009) 'Response of cylindrospermopsin production and release in Aphanizomenon flos-aquae (Cyanobacteria) to varying light and temperature conditions', *Harmful Algae*, 8(5), pp. 645–650. doi: 10.1016/j.hal.2008.10.009.

Preußel, K., Chorus, I. and Fastner, J. (2014) 'Nitrogen Limitation Promotes Accumulation and Suppresses Release of Cylindrospermopsins in Cells of Aphanizomenon Sp.', *Toxins; Basel*, 6(10), pp. 2932–2947. doi: http://dx.doi.org.proxy.lib.pdx.edu/10.3390/toxins6102932.

Ralston, D. K. and Moore, S. K. (2020) 'Modeling harmful algal blooms in a changing climate', *Harmful Algae*, 91, p. 101729. doi: 10.1016/j.hal.2019.101729.

Rantala-Ylinen, A. *et al.* (2011) 'Anatoxin-a Synthetase Gene Cluster of the Cyanobacterium Anabaena sp. Strain 37 and Molecular Methods To Detect Potential Producers', *Applied and Environmental Microbiology*, 77(20), pp. 7271–7278. doi: 10.1128/AEM.06022-11.

Rapala, J. *et al.* (1993) 'Anatoxin-a concentration inAnabaena andAphanizomenon under different environmental conditions and comparison of growth by toxic and non-toxicAnabaena-strains — a laboratory study', *Journal of Applied Phycology*, 5(6), pp. 581–591. doi: 10.1007/BF02184637.

Riley, G. A. (1956) 'Oceanography of Long Island Sound, 1952–1954. II. Physical oceanography', *Bulletin of the Bingham Oceanographic Collection*, 15, pp. 15–16.

Rohrlack, T. and Hyenstrand, P. (2007) 'Fate of intracellular microcystins in the cyanobacterium Microcystis aeruginosa (Chroococcales, Cyanophyceae)', *Phycologia; Abingdon*, 46(3), pp. 277–283.

Rouhiainen, L. *et al.* (2004) 'Genes Coding for Hepatotoxic Heptapeptides (Microcystins) in the Cyanobacterium Anabaena Strain 90', *Applied and Environmental Microbiology*, 70(2), pp. 686–692. doi: 10.1128/AEM.70.2.686-692.2004.

Rücker, J. *et al.* (2007) 'Concentrations of particulate and dissolved cylindrospermopsin in 21 Aphanizomenon-dominated temperate lakes', *Toxicon*, 50(6), pp. 800–809. doi: 10.1016/j.toxicon.2007.06.019.

Shan, K. *et al.* (2019) 'Analysis of environmental drivers influencing interspecific variations and associations among bloom-forming cyanobacteria in large, shallow eutrophic lakes', *Harmful algae*, 84, pp. 84–94.

Shih, P. M. *et al.* (2013) 'Improving the coverage of the cyanobacterial phylum using diversity-driven genome sequencing', *Proceedings of the National Academy of Sciences*, 110(3), pp. 1053–1058. doi: 10.1073/pnas.1217107110.

Smith, C. D. (2018) *Temporal and spatial monitoring of cyanobacterial blooms at Willow Creek Reservoir, North-Central Oregon*, *Temporal and spatial monitoring of cyanobacterial blooms at Willow Creek Reservoir, North-Central Oregon*. USGS Numbered Series 2018–5083. Reston, VA: U.S. Geological Survey, p. 36. doi: 10.3133/sir20185083.

Smith, C. and Sutton, A. (1993) 'The persistence of anatoxin-a in reservoir water', *Foundation for Water Research, UK Report No. FR0427*, p. FR0427.

Stevens, D. K. and Krieger, R. I. (1991) 'Stability studies on the cyanobacterial nicotinic alkaloid snatoxin-A', *Toxicon*, 29(2), pp. 167–179. doi: 10.1016/0041-0101(91)90101-V.

Stucken, K. *et al.* (2010) 'The Smallest Known Genomes of Multicellular and Toxic Cyanobacteria: Comparison, Minimal Gene Sets for Linked Traits and the Evolutionary Implications', *PLoS One; San Francisco*, 5(2), p. e9235. doi: http://dx.doi.org.proxy.lib.pdx.edu/10.1371/journal.pone.0009235.

Testai, E. *et al.* (2016) 'Risk to human health associated with the environmental occurrence of cyanobacterial neurotoxic alkaloids anatoxins and saxitoxins', *Critical Reviews in Toxicology*, 46(5), pp. 385–419. doi: 10.3109/10408444.2015.1137865.

Thomann, R. V. and Fitzpatrick, J. J. (1982) *Calibration and Verification of a Mathematical Model of the Eutrophication of the Potomac Estuary*. DC Department of Environmental Sciences.

Tillett, D. *et al.* (2000) 'Structural organization of microcystin biosynthesis in Microcystis aeruginosa PCC7806: an integrated peptide–polyketide synthetase system', *Chemistry & Biology*, 7(10), pp. 753–764. doi: 10.1016/S1074-5521(00)00021-1.

U.S. EPA (2014a) *Chemical Contaminants - CCL 4*, *US EPA*. Available at: https://www.epa.gov/ccl/chemical-contaminants-ccl-4 (Accessed: 24 February 2020).

U.S. EPA (2014b) 'Cyanobacteria and Cyanotoxins: Information for Drinking Water Systems'.

USBR (2021) *Tualatin Project*. Available at: https://www.usbr.gov/projects/index.php?id=411 (Accessed: 29 April 2021).

USGS (2015) *Harmful Algal Blooms and Drinking Water in Oregon*. Scientific Investigations Report.

Velzeboer, R. M. A. *et al.* (2000) 'Geographical patterns of occurrence and composition of saxitoxins in the cyanobacterial genus Anabaena (Nostocales, cyanophyta) in Australia', *Phycologia; Abingdon*, 39(5), p. 395.

Wells, S. A. (2020a) 'CE-QUAL-W2: A Two-Dimensional, Laterally Averaged, Hydrodynamic and Water Quality Model, Version 4.2.2, User Manual'.

Wells, S. A. (2020b) *CE-QUAL-W2 Hydrodynamic and Water Quality Model*. Available at: http://cee.pdx.edu/w2/ (Accessed: 4 September 2020).

Wells, S. A. and Berger, C. J. (2019) *DRAFT Henry Hagg Lake Model Development, Calibration and Proposed Reservoir Simulations*. Water Quality Research Group, Department of Civil and Environmental Engineering: Portland State University.

Wendelken, S. C. (2015) 'Method 545: Determination of Cylindrospermopsin and Anatoxin-a in Drinking Water by Liquid Chromatography Electrospray Ionization Tandem Mass Spectrometry (LC/ESI-MS/MS)'. U.S. EPA.

Wood, S. A. *et al.* (2007) ‘First report of the cyanotoxin anatoxin-a from Aphanizomenon issatschenkoi (cyanobacteria)’, *Journal of Phycology*, 43(2), pp. 356–365.

World Health Organization (ed.) (2003) *Guidelines for safe recreational water environments*. Geneva: World Health Organization.

Wunderlich, W. O. (1972) *Heat and mass transfer between a water surface and the atmosphere*. Tennessee Valley Authority, Office of Natural Resources and Economic Development, Division of Air and Water Resources, Water Systems Development Branch.

Zaffiro, A., Rosenblum, L. and Wendelken, S. C. (2016) ‘Method 546: Determination of Total Microcystins and Nodularins in Drinking Water and Ambient Water by Adda Enzyme-Linked Immunosorbent Assay’. U.S. EPA.

Appendix A: CE-QUAL-W2 Code Updates

Below are portions of the fortran90 code of the CE-QUAL-W2 W2 Modules subroutine and the Water Quality subroutine. New code additions from this study are highlighted.

W2 MODULES SUBROUTINE:

```
!**********************************************************************************************************************************
!**                                                                                                                              **
!**                                                CE-QUAL-W2                                                                    **
!**                                        A Two-dimensional, Laterally Averaged,                                                **
!**                                         Hydrodynamic and Water Quality Model                                                 **
!**                                                  for                                                                         **
!**                                        Rivers, Lakes, Reservoirs, and Estuaries                                              **
!**                                                                                                                              **
!**                                                Version 4.5                                                                   **
!**                                                                                                                              **
!**                                            Currently maintained by:                                                          **
!**                                                Scott A. Wells                                                                **
!**                                        Department of Civil and Environmental Engineering                                     **
!**                                            Portland State University                                                         **
!**                                                PO Box 751                                                                    **
!**                                            Portland, Oregon  97207-0751                                                      **
!**                                            phone number: (503) 725-4276                                                      **
!**                                            e-mail: wellss@pdx.edu                                                            **
!**                                        Major contributors to this version include                                            **
!**                                          Dr. Zhong Zhang <zz3@pdx.edu>, Portland State University                             **
!**                                                                                                                              **
!** Main contributors to CE-QUAL-W2 are shown in User Manual. Primary developer at the Corps has been                             **
!**                                            Thomas M. Cole, Retired                                                           **
!**                                            Water Quality Modeling Group                                                      **
!**                                            U.S. Army Corps of Engineers                                                      **
!**                                            Waterways Experiment Station                                                      **
!**                                            Vicksburg, Mississippi 39180                                                      **
!**                                                                                                                              **
!**                                                                                                                              **
!**********************************************************************************************************************************

!**********************************************************************************************************************************
!**                                                                                                                              **
!**                The long arm of the lawyers has found its way into the water quality modeling arena, so:                      **
!**                                                                                                                              **
!** This model was developed by the U.S. Army Engineer Waterways Experiment Station, Vicksburg, MS and is maintained by          **
!** Portland State University.  Portland State University and the US government and its components are not responsible            **
!** for any damages,including incidental or consequential damages, arising                                                       **
!** from use or misuse of this model, or from results achieved or conclusions drawn by others.  Distribution of this model is    **
!** restricted by the Export Administration Act of 1969,  50 app. USC subsections 2401-2420, as amended, and other applicable    **
!** laws or regulations.                                                                                                         **
!**                                                                                                                              **
!**********************************************************************************************************************************

!**********************************************************************************************************************************
!**                                          Module Declaration                                                                  **
!**********************************************************************************************************************************

[portion of code omitted]

    MODULE ALGAE_TOXINS
    USE PREC
    INTEGER, PARAMETER                          :: NUMATOXINS=4
    INTEGER                                     :: NATS, NATE, ATOXIN_DEBUG_FN=2501
    LOGICAL                                     :: ALGAE_TOXIN
    REAL, ALLOCATABLE, DIMENSION (:,:)          :: CTP,CTB
    REAL, DIMENSION (:)                         :: CTREL(NUMATOXINS),CTD(NUMATOXINS)
    REAL(R8),POINTER,           DIMENSION(:,:,:)  :: EX_TOXIN, CTESS
    REAL(R8),ALLOCATABLE, DIMENSION(:,:,:)      :: IN_TOXIN
    CHARACTER(2)                                :: ATOX, ATOX_DEBUG
    END MODULE ALGAE_TOXINS

[portion of code omitted]
```

WATER QUALITY SUBROUTINE:

```
!**********************************************************************************************************************************
!**                              S U B R O U T I N E   K I N E T I C S                                                           **
!**********************************************************************************************************************************
```

```
SUBROUTINE KINETICS
  USE SCREENC; USE GLOBAL; USE KINETIC; USE GEOMC; USE TVDC; USE LOGICC; USE SURFHE
  USE MACROPHYTEC; USE ZOOPLANKTONC; USE MAIN, ONLY:NPBALC, EPIPHYTON_CALC, BOD_CALC, &
      ALG_CALC, BOD_CALCN, BOD_CALCP, PO4_CALC, N_CALC, DSI_CALC, STANDING_BIOMASS_DECAY, NH3_DER, &
      CDWBC,KF_NH4_SR,KF_NH4_SD,KF_PO4_SR,KF_PO4_SD,NLDOM, NRDOM, NLPOM, NRPOM, NDGP, ORGC_CALC, CO2_DER, HCO3_DER, CO3_DER,  &
      CBODU_DER,TOTSS_DER,O2DG_DER,TURB_DER,SECCHI_DER, CHLA_DER
  USE ALGAE_TOXINS
  Use CEMAVars

[portion of code omitted]

ALGAE_TOXIN=.FALSE.
INQUIRE(FILE='Algae_Toxin.csv',EXIST=ALGAE_TOXIN)
 IF(ALGAE_TOXIN)THEN
    OPEN(2450,FILE='Algae_Toxin.csv',STATUS='OLD')
    READ(2450,*)  ! SKIP HEADER
    READ(2450,*)ATOX,ATOX_DEBUG     ! '(A2)'
    IF(ATOX == 'ON')THEN
    ALLOCATE(CTP(NUMATOXINS,NAL),CTB(NUMATOXINS,NAL),IN_TOXIN(KMX,IMX,NUMATOXINS))

    READ(2450,*)
    READ(2450,*)(CTP(1,JA),JA=1,NAL)
    READ(2450,*)(CTB(1,JA),JA=1,NAL)
    READ(2450,*) CTREL(1)      !(CTL(1,JA),JA=1,NAL)
    !READ(2450,*) CTDI(1)     !(CTDI(1,JA),JA=1,NAL)
    !READ(2450,*) CTA(1)      !(CTA(1,JA),JA=1,NAL)
    READ(2450,*) CTD(1)     !(CTDE(1,JA),JA=1,NAL)
    READ(2450,*)
    READ(2450,*)(CTP(2,JA),JA=1,NAL)
    READ(2450,*)(CTB(2,JA),JA=1,NAL)
    READ(2450,*) CTREL(2)     !(CTL(2,JA),JA=1,NAL)
    !READ(2450,*) CTDI(2)     !(CTDI(2,JA),JA=1,NAL)
    !READ(2450,*) CTA(2)      !(CTA(2,JA),JA=1,NAL)
    READ(2450,*) CTD(2)     !(CTDE(2,JA),JA=1,NAL)
    READ(2450,*)
    READ(2450,*)(CTP(3,JA),JA=1,NAL)
    READ(2450,*)(CTB(3,JA),JA=1,NAL)
    READ(2450,*) CTREL(3)     !(CTL(3,JA),JA=1,NAL)
    !READ(2450,*) CTDI(3)     !(CTDI(3,JA),JA=1,NAL)
    !READ(2450,*) CTA(3)      !(CTA(3,JA),JA=1,NAL)
    READ(2450,*) CTD(3)     !(CTDE(3,JA),JA=1,NAL)
    READ(2450,*)
    READ(2450,*)(CTP(4,JA),JA=1,NAL)
    READ(2450,*)(CTB(4,JA),JA=1,NAL)
    READ(2450,*) CTREL(4)     !(CTL(4,JA),JA=1,NAL)
    !READ(2450,*) CTDI(4)     !(CTDI(4,JA),JA=1,NAL)
    !READ(2450,*) CTA(4)      !(CTA(4,JA),JA=1,NAL)
    READ(2450,*) CTD(4)     !(CTDE(4,JA),JA=1,NAL)

    !
    DO JJ=1,NUMATOXINS
      CTREL(JJ)=CTREL(JJ)/86400.
      CTD(JJ)=CTD(JJ)/86400.
    ENDDO

    ELSE
    ALGAE_TOXIN=.FALSE.
    ENDIF
 ENDIF

RETURN

[portion of code omitted]

!**********************************************************************************************************************************
!**                                        C Y A N O T O X I N S                                                                 **
!**********************************************************************************************************************************

ENTRY INTRACELLULAR_TOXIN (J)
IN_TOXIN(KT:KMX-1,IU:ID,J)=0.0
 DO I=IU,ID
  DO K=KT,KB(I)
   DO JA=1,NAL
    IF(ALG_CALC(JA))THEN
    IN_TOXIN(K,I,J)=IN_TOXIN(K,I,J) + CTP(J,JA)*CTB(J,JA)*ALG(K,I,JA)
    END IF
   END DO
  END DO
 END DO
RETURN


ENTRY EXTRACELLULAR_TOXIN (J)
CTESS(KT:KMX-1,IU:ID,J)=0.0
 DO I=IU,ID
  DO K=KT,KB(I)
   DO JA=1,NAL
    IF(ALG_CALC(JA))THEN
    CTESS(K,I,J) = CTESS(K,I,J) + CTP(J,JA)*CTB(J,JA)*AMR(K,I,JA)*ALG(K,I,JA)
    END IF
   END DO
```

```
      CTESS(K,I,J) = CTESS(K,I,J) + CTREL(J)*IN_TOXIN(K,I,J)-CTD(J)*EX_TOXIN(K,I,J)
    END DO
  END DO
RETURN
```

[portion of code omitted]

Appendix B: Henry Hagg Lake Profile Plots

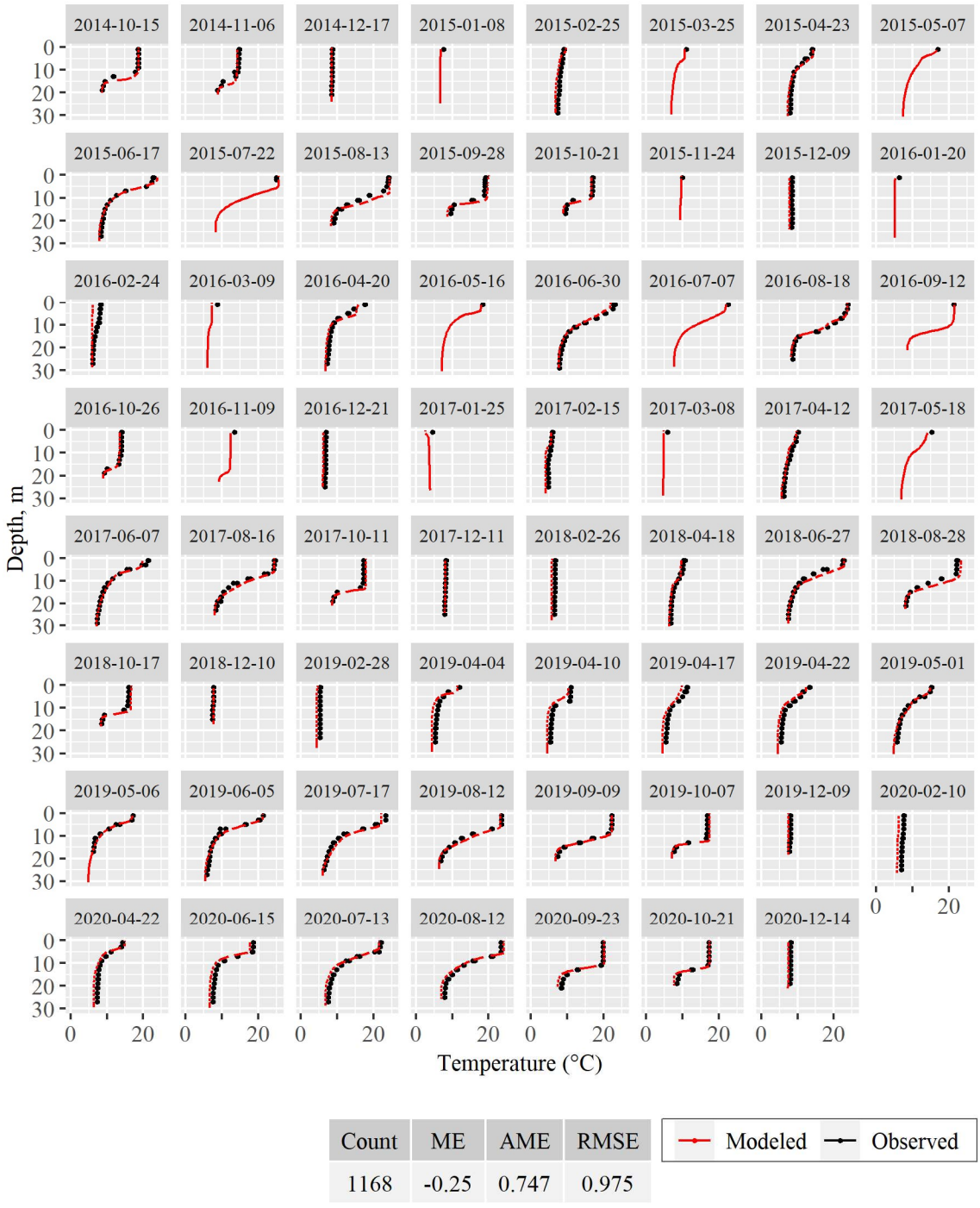

Figure B-1 Observed and predicted profiles of temperature in Henry Hagg Lake.

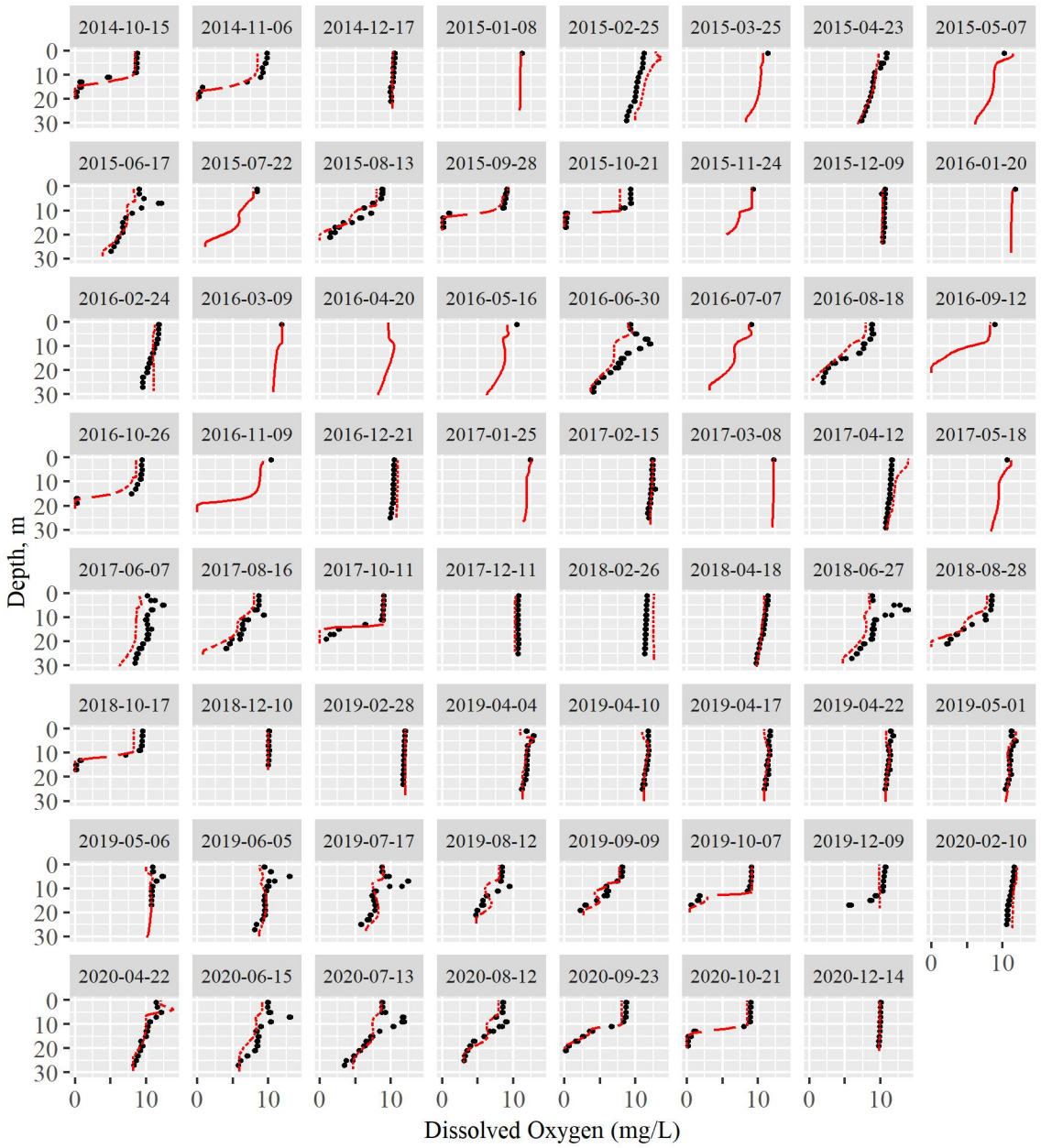

Count	ME	AME	RMSE
1136	-0.281	0.738	1.118

Figure B-2 Observed and predicted concentration profiles of dissolved oxygen in Henry Hagg Lake.

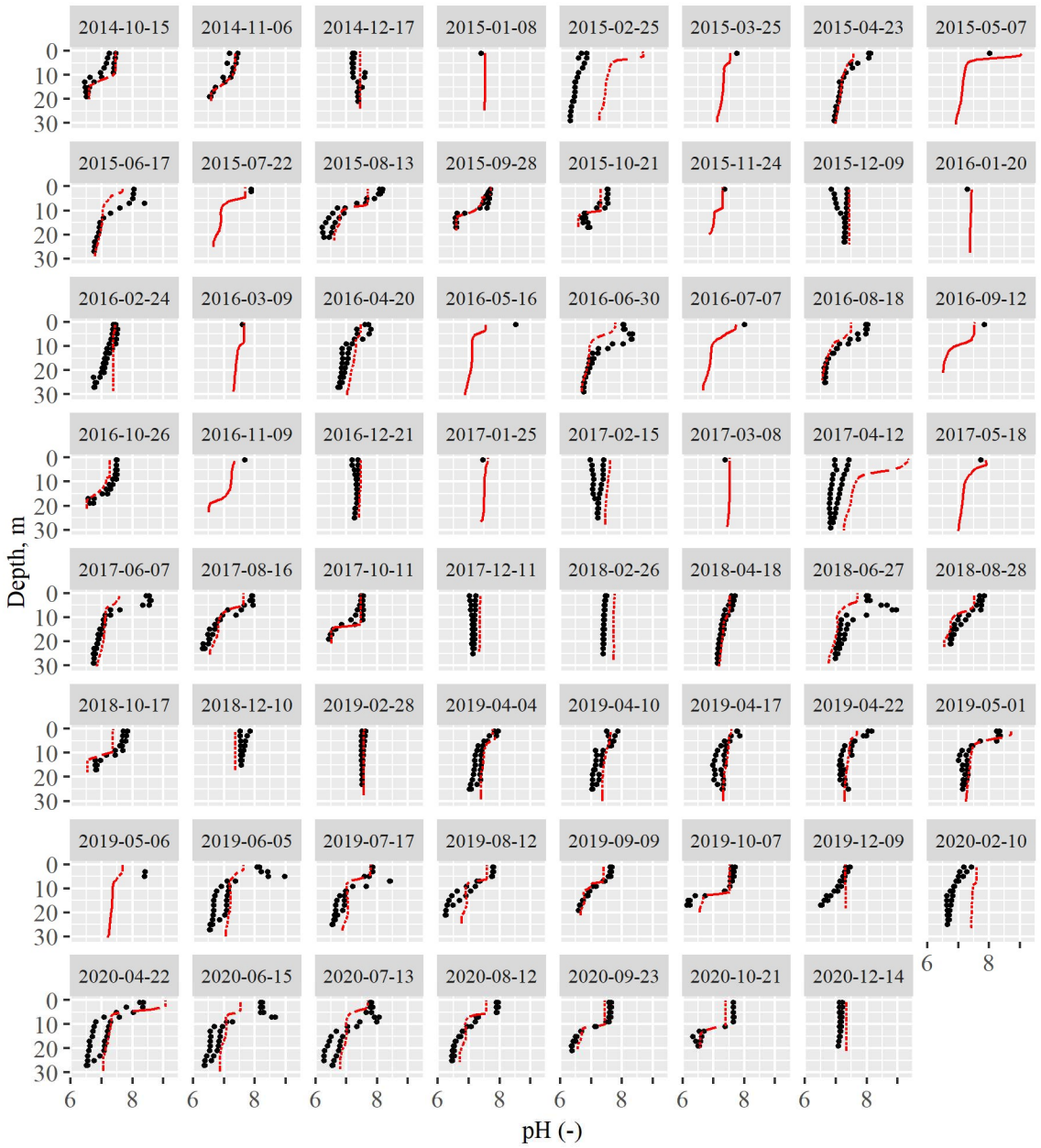

Count	ME	AME	RMSE
1152	0.081	0.28	0.404

Figure B-3 Observed and predicted profiles of pH in Henry Hagg Lake.

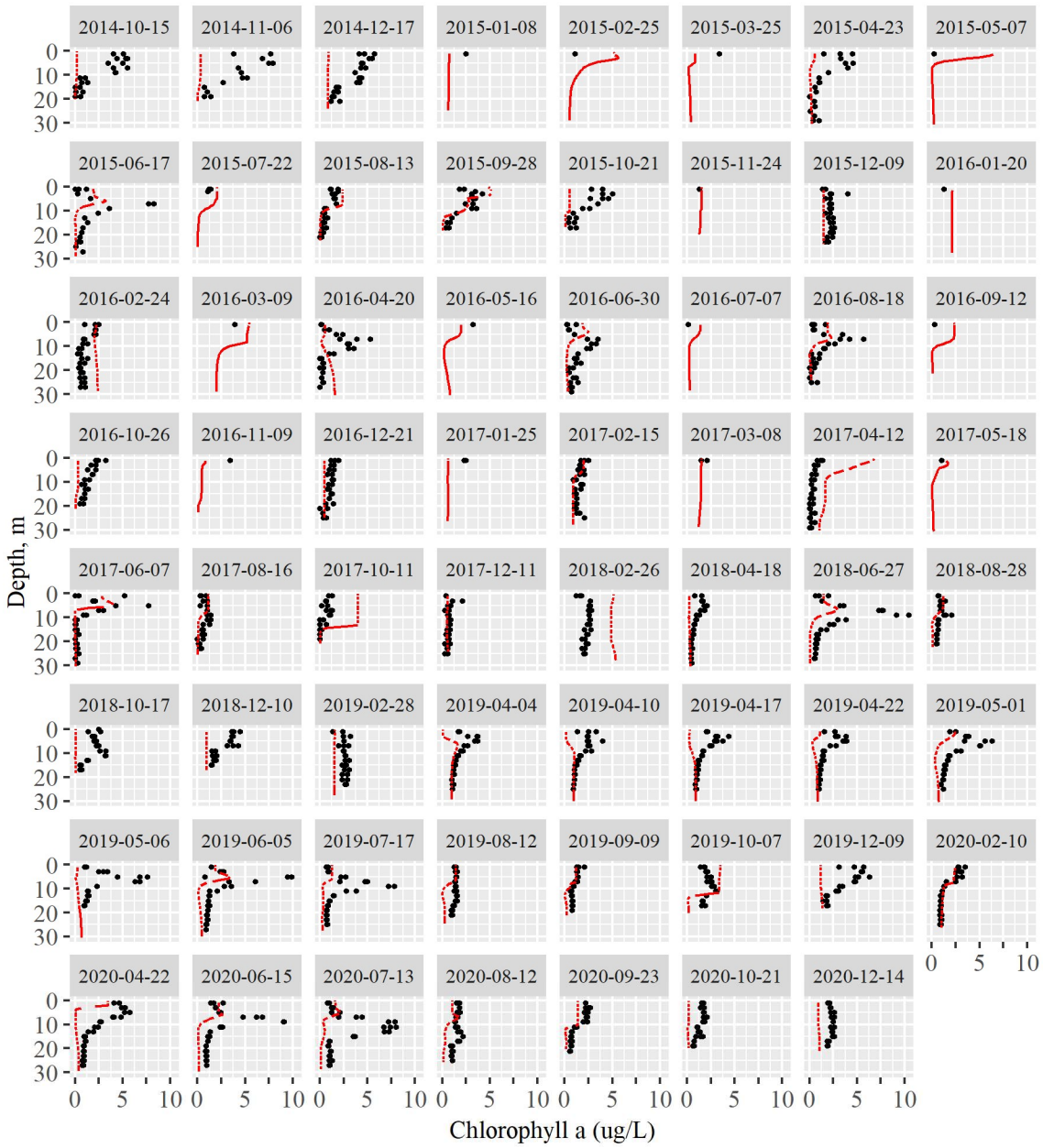

Count	ME	AME	RMSE
1222	-0.766	1.344	1.962

Figure B-4 Observed and predicted concentration profiles of chlorophyll a in Henry Hagg Lake.

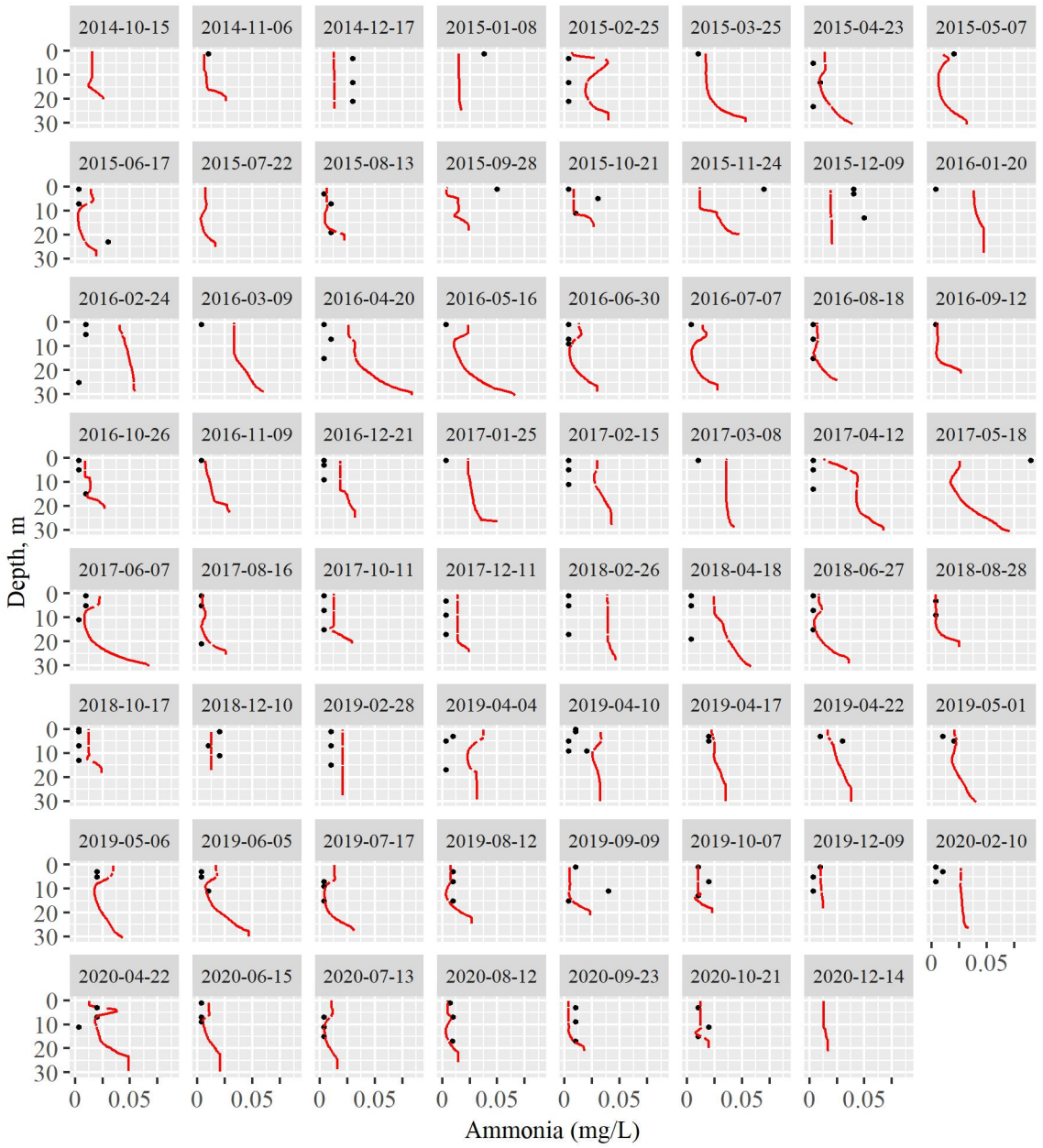

Figure B-5 Observed and predicted concentration profiles of ammonia in Henry Hagg Lake.

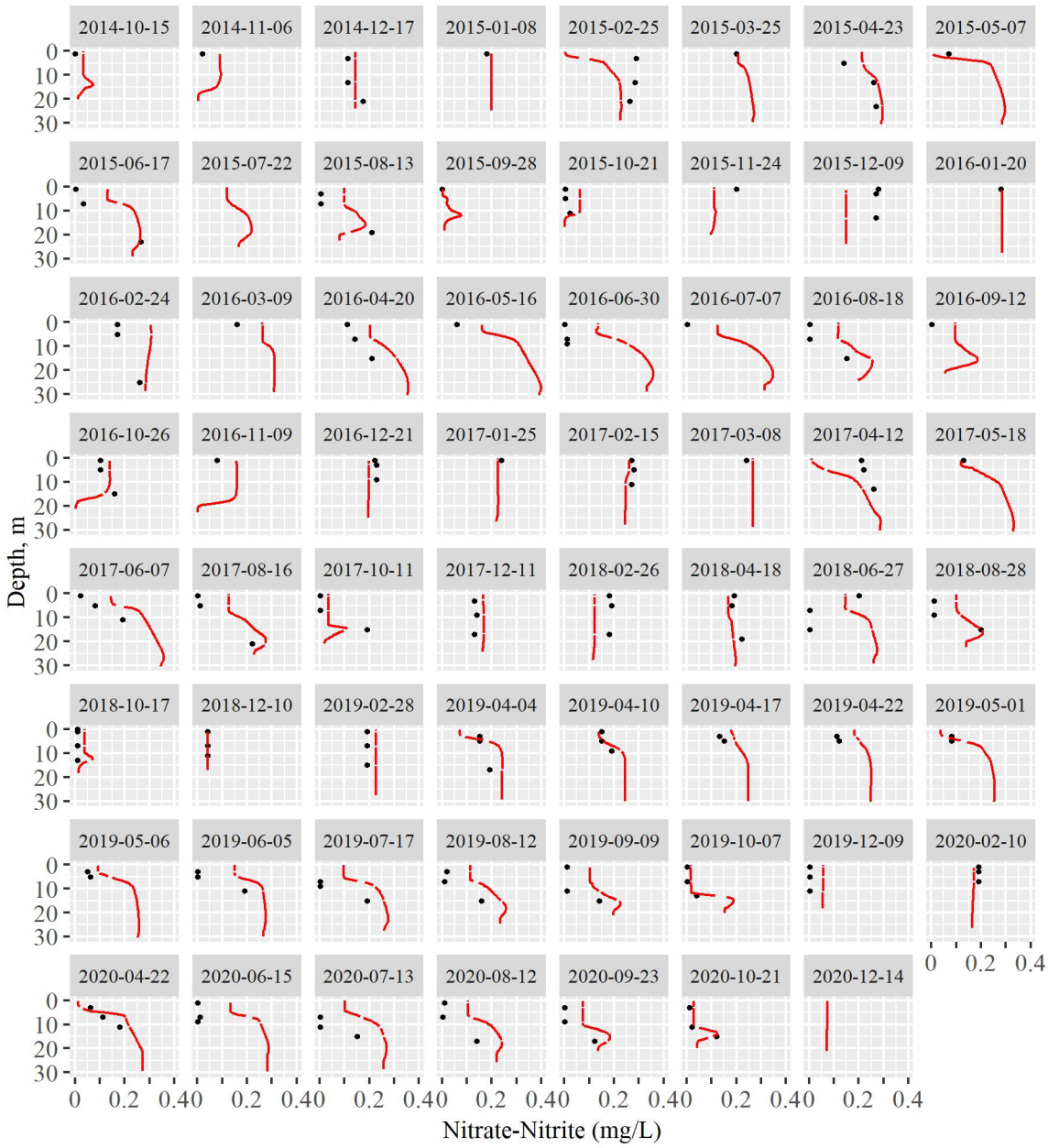

Figure B-6 Observed and predicted concentration profiles of nitrate-nitrite in Henry Hagg Lake.

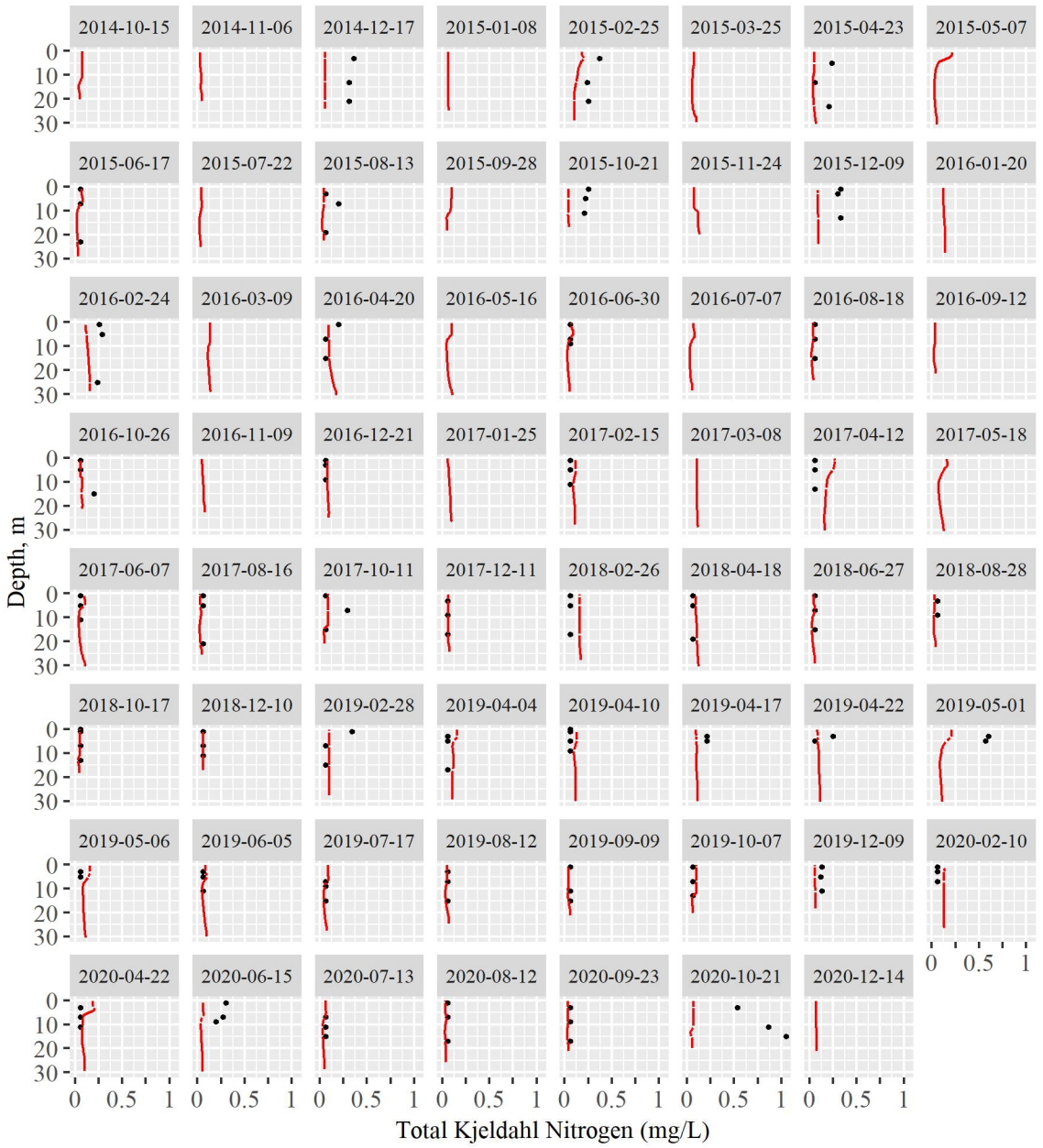

Figure B-7 Observed and predicted concentration profiles of total Kjeldahl nitrogen in Henry Hagg Lake.

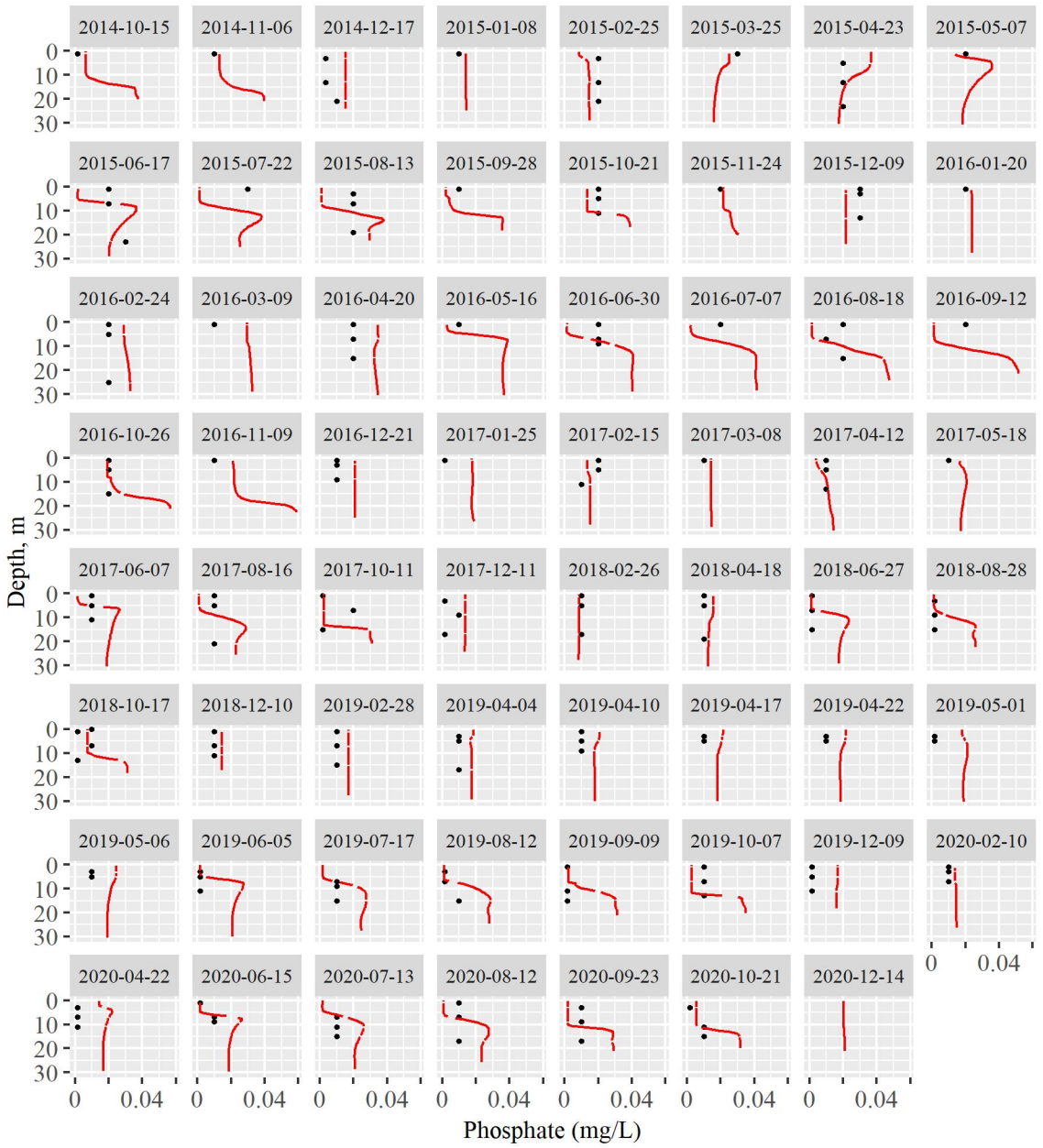

Figure B-8 Observed and predicted concentration profiles of phosphate in Henry Hagg Lake.

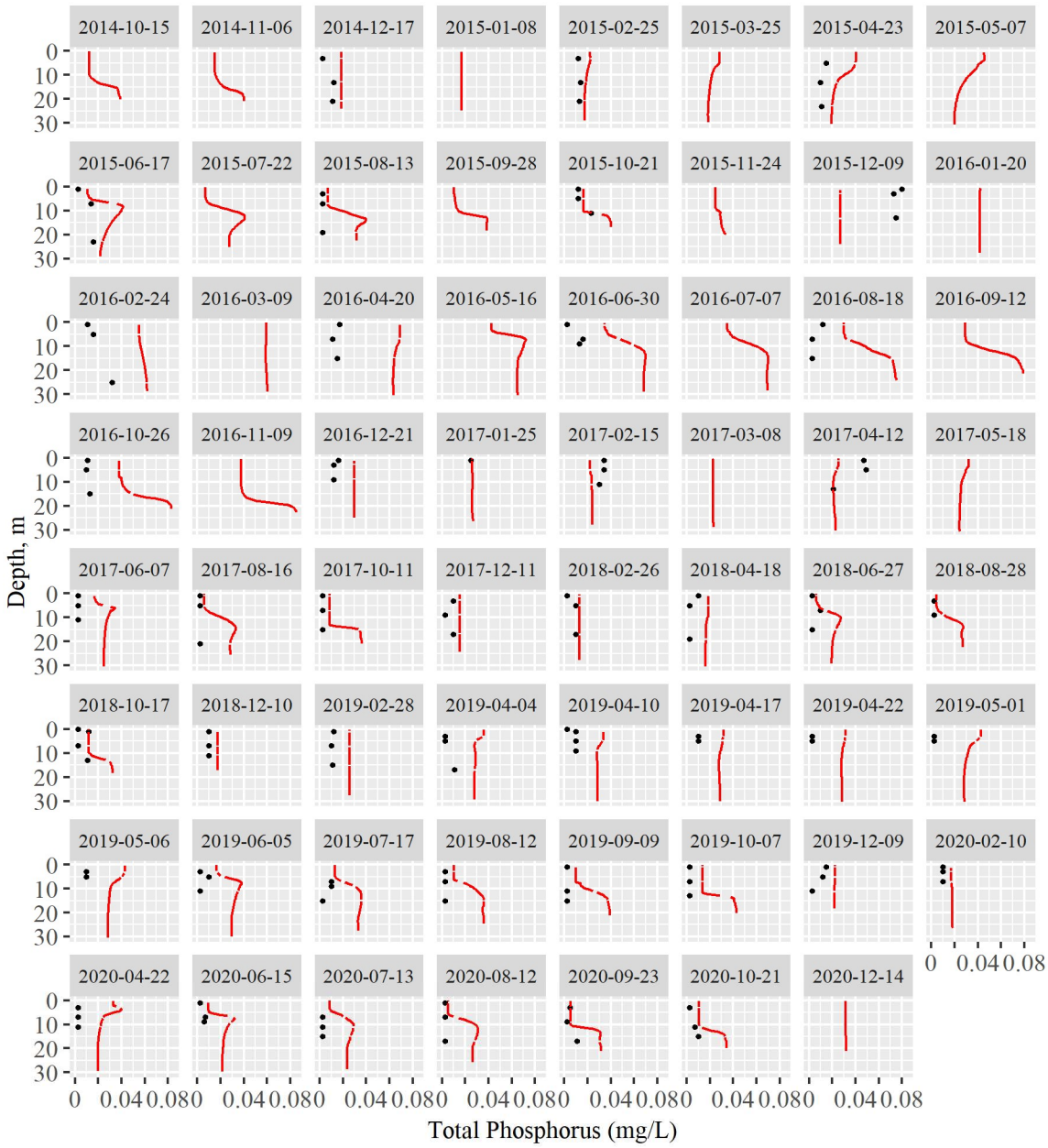

Figure B-9 Observed and predicted concentration profiles of total phosphorus in Henry Hagg Lake.

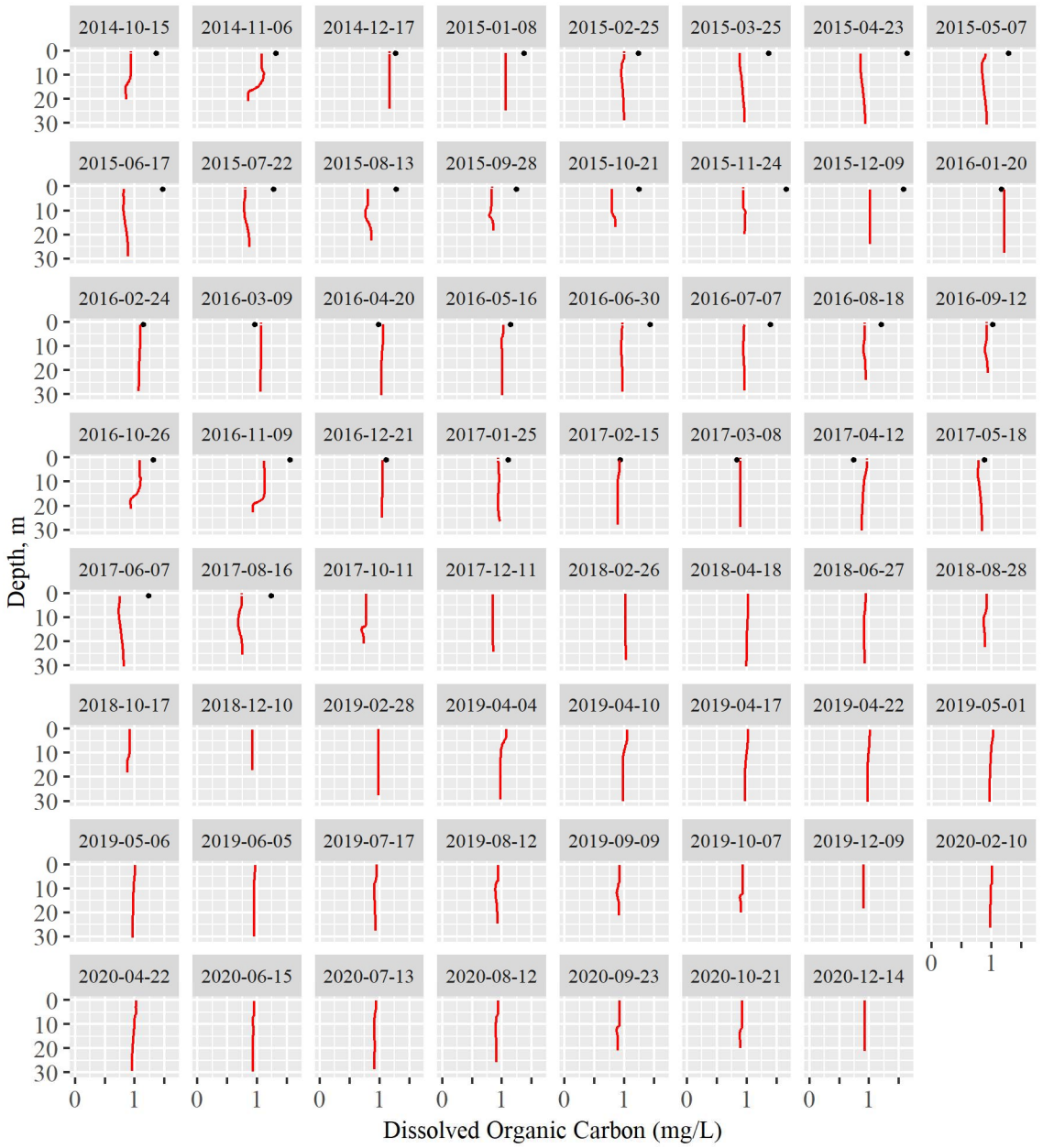

Figure B-10 Observed and predicted concentration profiles of dissolved organic carbon in Henry Hagg Lake.

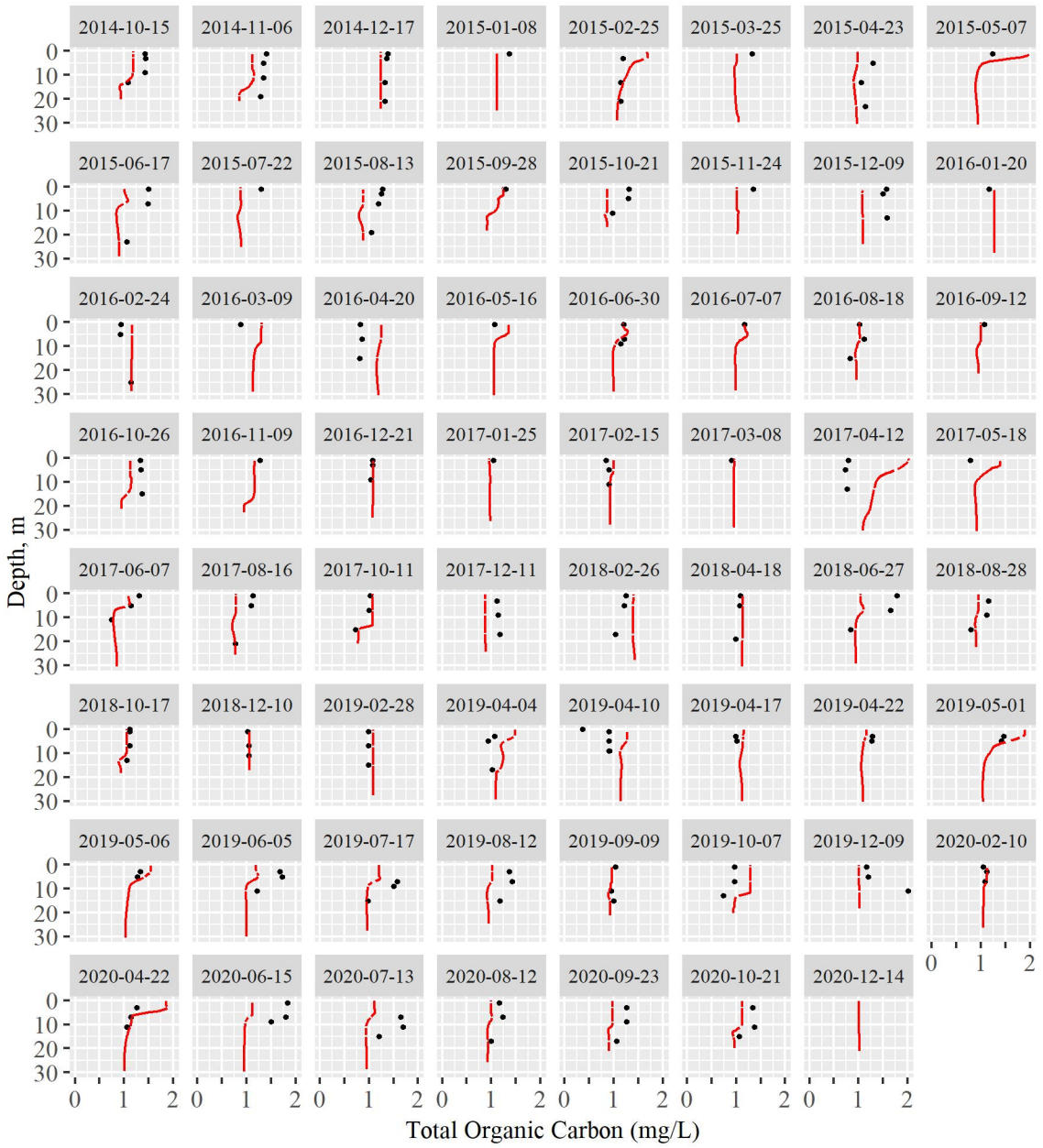

Figure B-11 Observed and predicted concentration profiles of total organic carbon in Henry Hagg Lake.

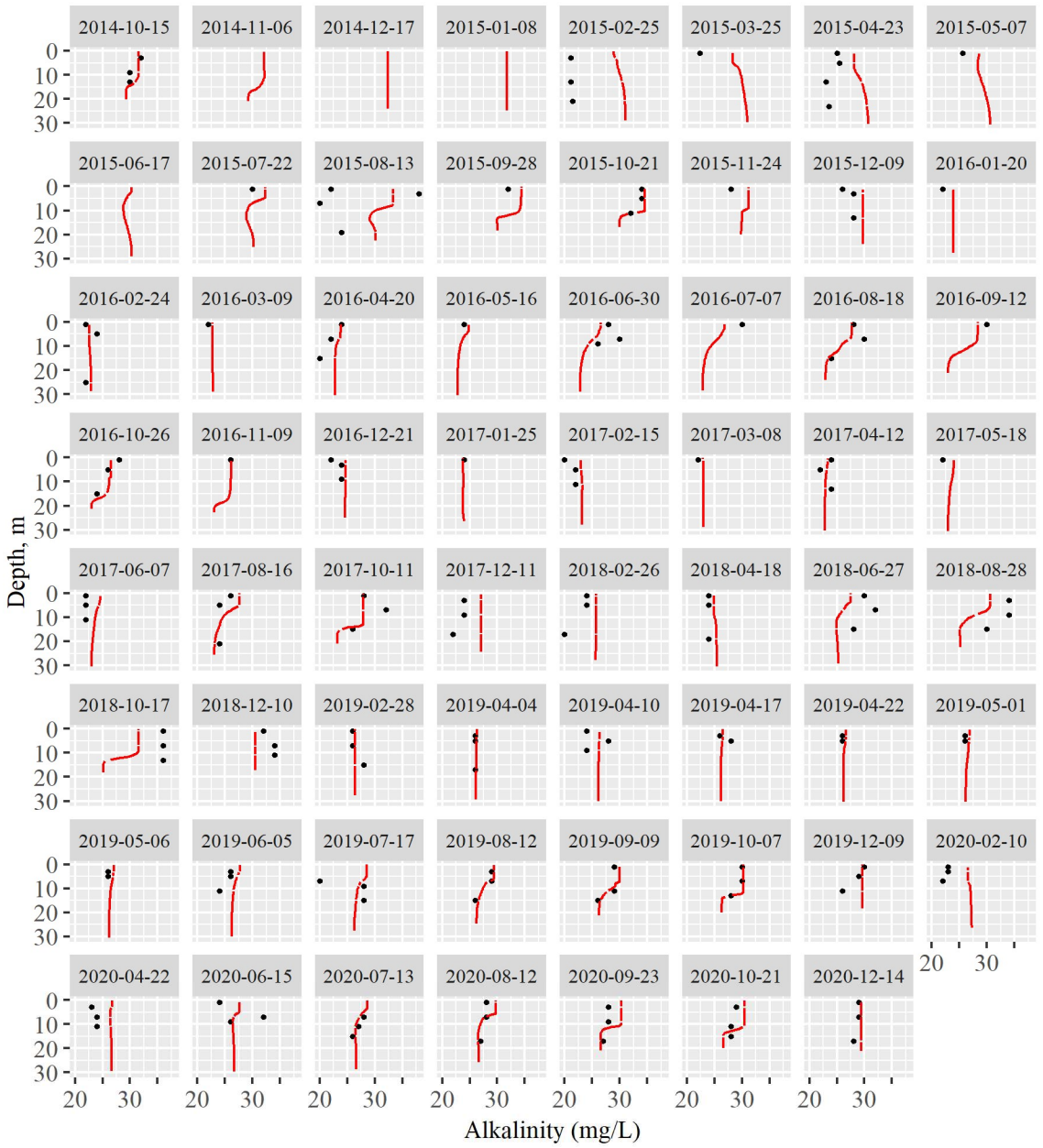

Figure B-12 Observed and predicted concentration profiles of alkalinity in Henry Hagg Lake.

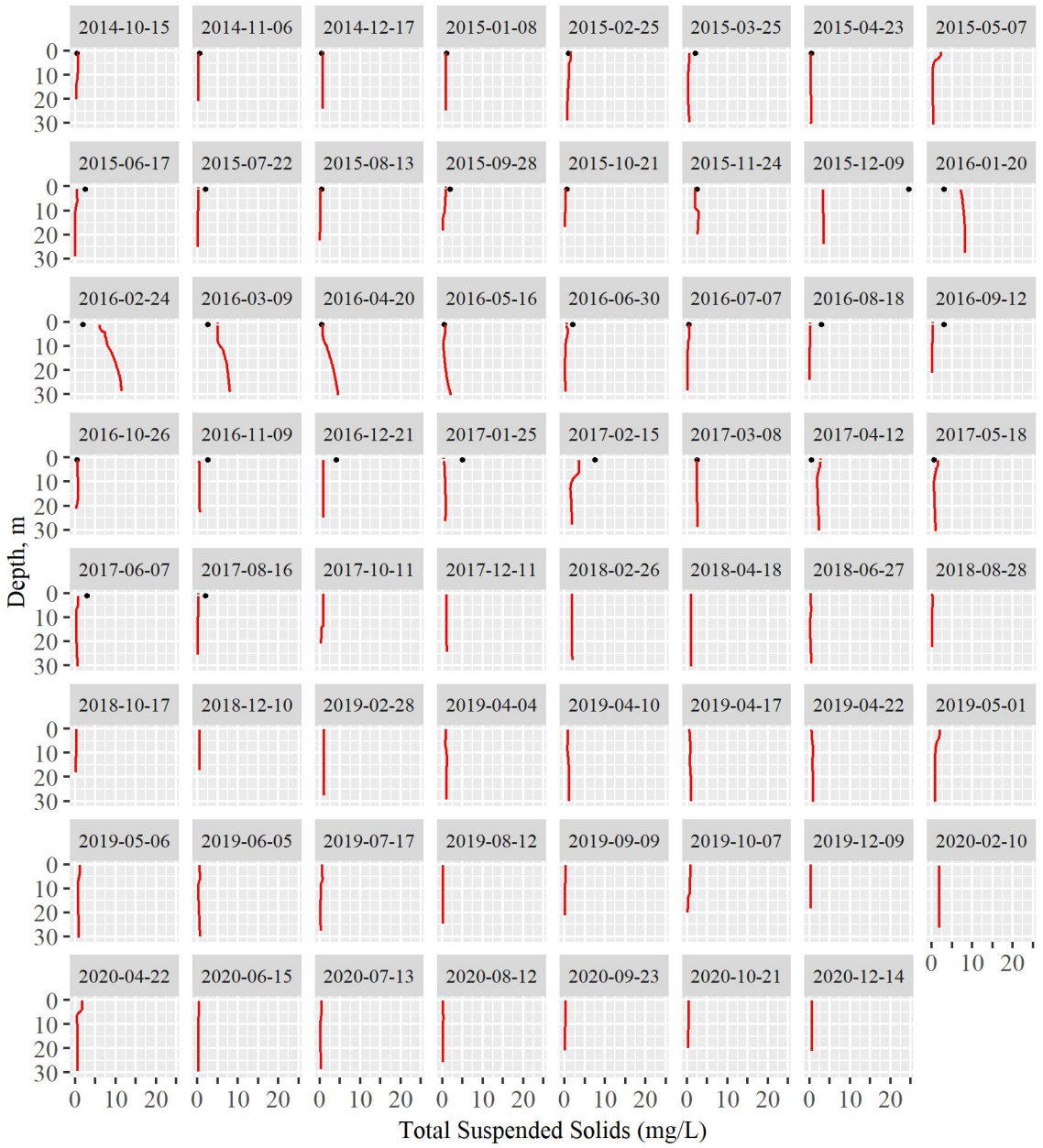

Figure B-13 Observed and predicted concentration profiles of total suspended solids in Henry Hagg Lake.

Appendix C: Henry Hagg Lake Outflow Plots

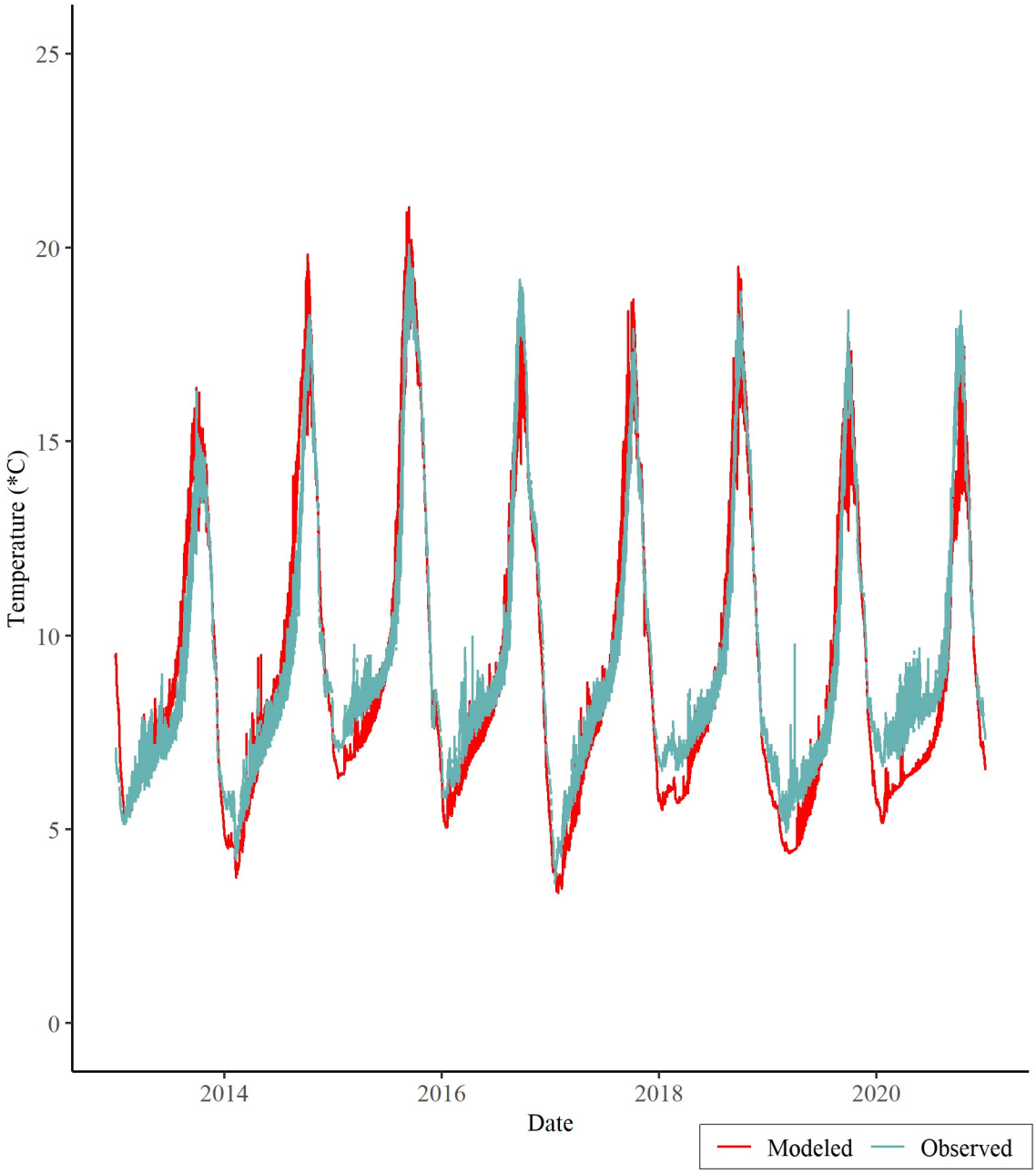

Count	ME	MAE	RMSE
139739	-0.226	0.806	1.032

Figure C-1 Observed and predicted outflow values of temperature from Henry Hagg Lake.

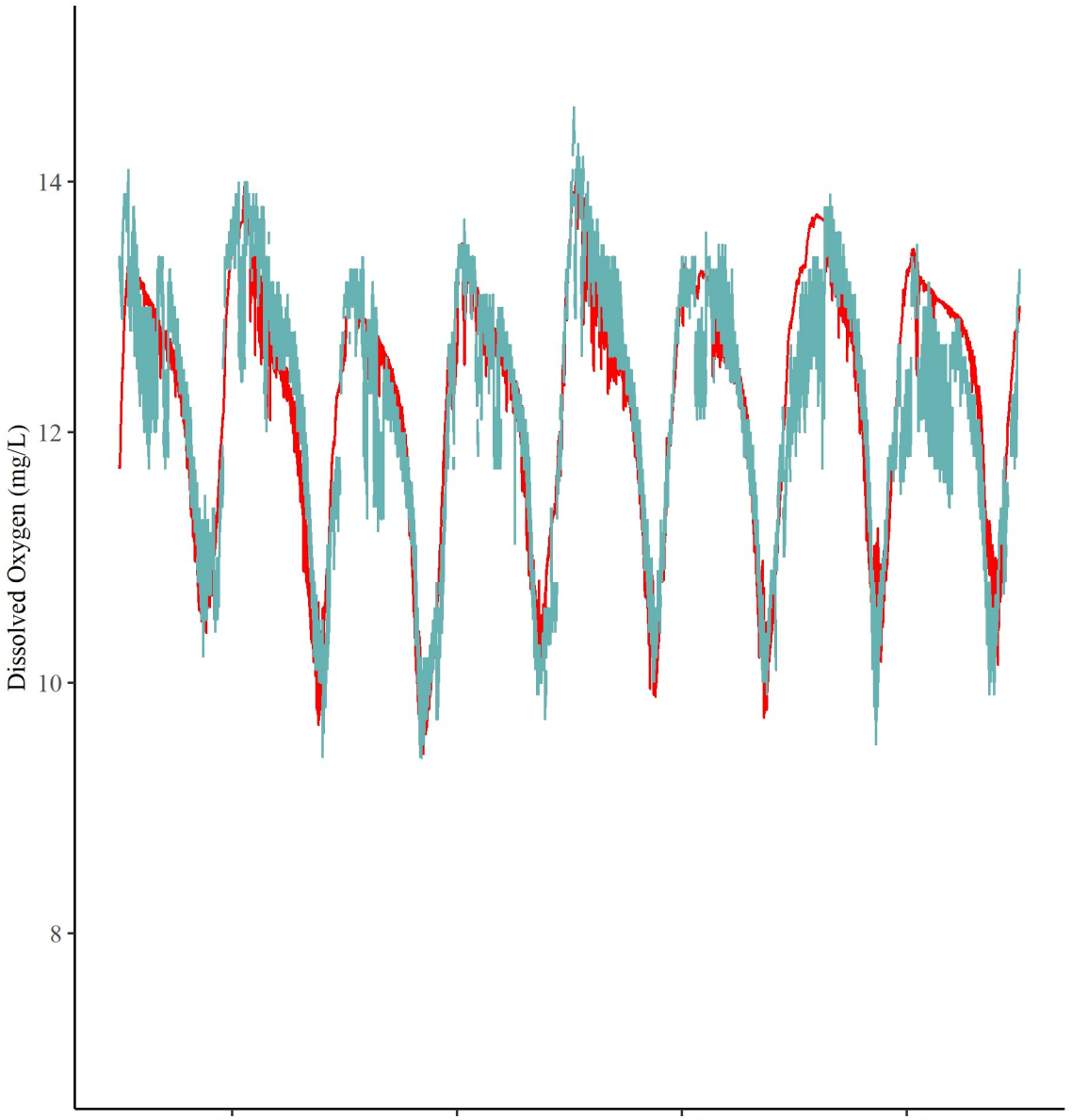

Count	ME	MAE	RMSE
139709	0.132	0.372	0.499

Figure C-2 Observed and predicted outflow values of dissolved oxygen from Henry Hagg Lake.

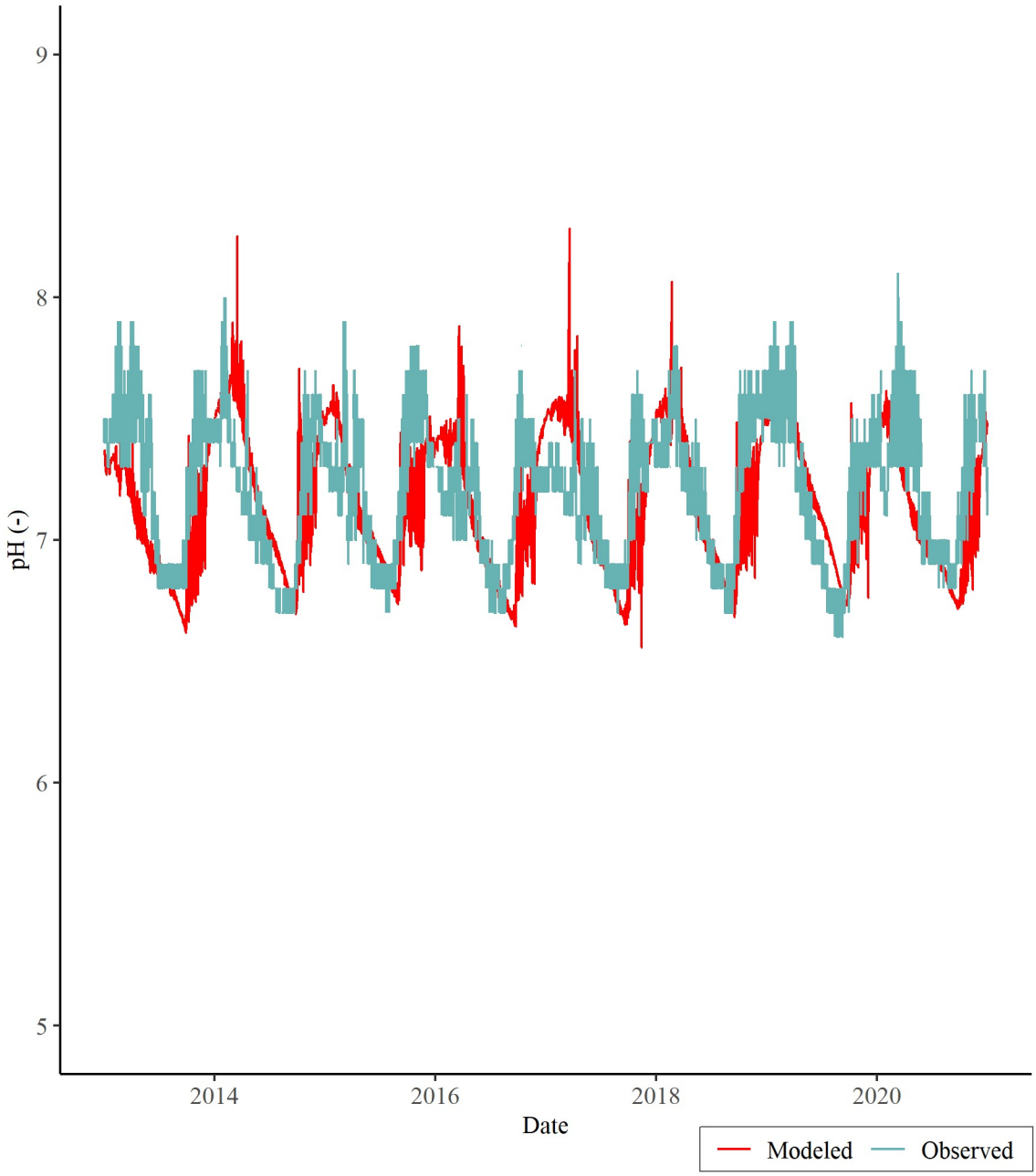

Count	ME	MAE	RMSE
139644	-0.033	0.171	0.325

Figure C-3 Observed and predicted outflow values of pH from Henry Hagg Lake.

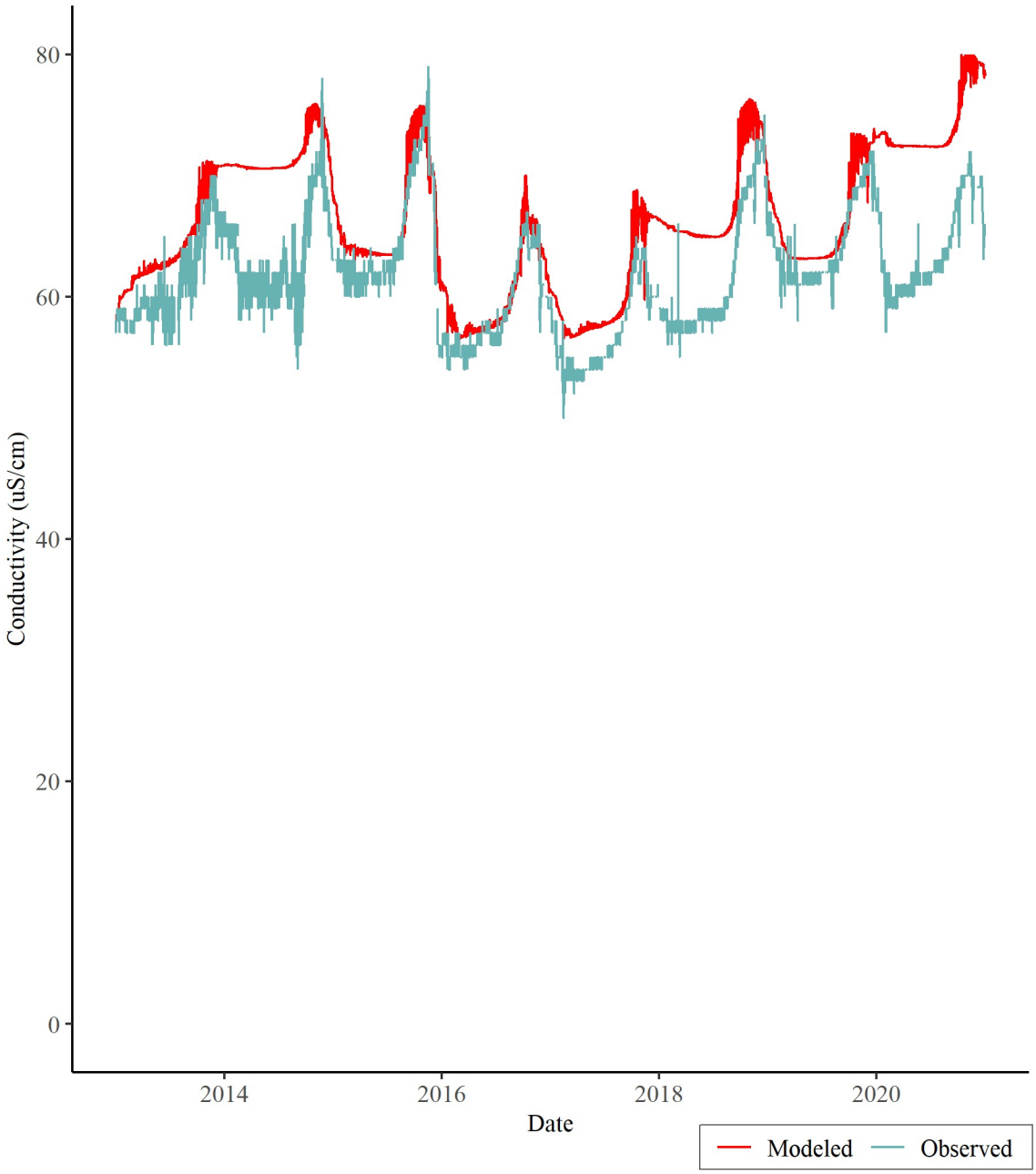

Count	ME	MAE	RMSE
135337	4.622	4.673	5.863

Figure C-4 Observed and predicted outflow values of conductivity from Henry Hagg Lake.